DANMARKS OG GRØNLANDS GEOLOGISKE UNDERSØGELSE **RAPPORT 2024/24**

Geophysical mapping of seabed substrates and habitats (JAMBAY WP1)

Lars Ø. Hansen, Mikkel S. Andersen, Niels Nørgaard-Pedersen, Nicklas Christensen, Zyad Al-Hamdani & Verner B. Ernstsen (eds.)

GEOLOGICAL SURVEY OF DENMARK AND GREENLAND
DANISH MINISTRY OF CLIMATE, ENERGY AND UTILITIES

G E U S

DANMARKS OG GRØNLANDS GEOLOGISKE UNDERSØGELSE **RAPPORT 2024/24**

Geophysical mapping of seabed substrates and habitats (JAMBAY WP1)

Lars Ø. Hansen, Mikkel S. Andersen, Niels Nørgaard-Pedersen,
Nicklas Christensen, Zyad Al-Hamdani & Verner B. Ernstsen (eds.)

GEOLOGICAL SURVEY OF DENMARK AND GREENLAND
DANISH MINISTRY OF CLIMATE, ENERGY AND UTILITIES

G E U S

Colophon

Title:	Geophysical mapping of seabed substrates and habitats (JAMBAY WP1)
Authors:	Lars Ø. Hansen, Mikkel S. Andersen, Niels Nørgaard-Pedersen, Nicklas Christensen, Zyad Al-Hamdani, Verner B. Ernstsen (task leads and editors) Henrik I. Petersen, Isak R. Larsen, Jacob R. Jørgensen, Jørgen O. Leth, Lars-Georg Rödel, Pernille Stockmarr, Peter Sandersen, Sigurd B. Andersen, Silas Clausen & Sofie Kousted (contributing authors in alphabetical order)
GEUS Report no.:	2024/24
Year:	September 2024
Reference:	Hansen, L.Ø., Andersen, M.S., Nørgaard-Pedersen, N., Christensen, N., Al-Hamdani, Z., Ernstsen, V.B. (eds.) (2024). Geophysical mapping of seabed substrates and habitats (JAMBAY WP1). GEUS Report no. 2024/24. Geological survey of Denmark and Greenland, 101 pp.
Quality assurance:	Internal review and quality assurance

Preface

The project “Mapping of seabed habitats and impacts of beam trawling and other demersal fisheries for spatial ecosystem-based management of the Jammer Bay (JAMBAY)” (Grant Agreement No 33113-B-23-189) was funded by the European Maritime and Fisheries Fund (EMFF) and the Ministry of Food, Agriculture and Fisheries of Denmark.

This Work Package 1 Report is one of four detailed work package reports. This report presents the results of “Geophysical mapping of seabed substrates and habitats (JAMBAY WP1)”. These results are summarised in the Executive Report of the JAMBAY project, where also the results of Work Package 5 are presented (DTU Aqua Report no. 445-2024).

This project had a short timeframe to conduct its work, given the magnitude and complexity of the work involved. It started in March 2023 and ended in December 2023. The initial application was accepted and awarded 12 million Danish kr., and in September was expanded to include additional work and an added 14 million Danish kr., to a total of 26 million Danish kr. More than 100 scientists and consultants from several research institutes and private companies were directly involved. Furthermore, the project indirectly involved several stakeholders.

The data collected, newly developed methods and models generated during this project have been reported upon. Part of the work has been disseminated nationally and internationally, but further work is needed to integrate the data and information across the professional fields. Follow up projects have been initiated towards this end. The outputs will inform and provide the opportunity for cross-sectorial, ecosystem-based management.

Copenhagen, February 2024

Verner B. Ernstsen
Senior Researcher

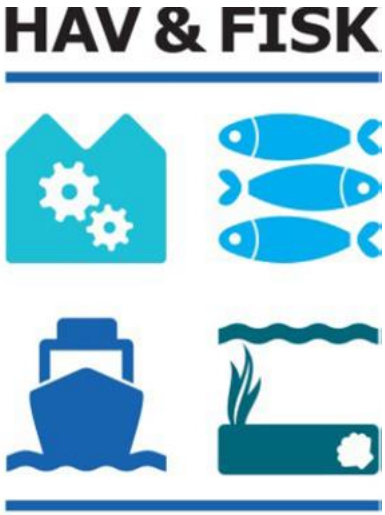

Content

English summary

Seabed geology, morphology and substrate constitute the overall components of seabed geodiversity and form seabed habitats and foundation for benthic flora and fauna.

The aims in WP1 were I) to map the seabed within the Jammer Bay Focus area – in the central part of the Jammer Bay – in high spatial resolution and precision, and with full spatial data coverage, in order to create a foundation for analysing the impact of various types of bottom trawling on the seabed surface; and II) to map the seabed within the Jammer Bay Screening area – covering the area between Hanstholm and Hirtshals from the 10 m depth curve to the EEZ border – in high spatial resolution and precision along the survey lines, with data gaps between survey lines, in order to assess the spatial distribution of seabed substrates and habitats within the Jammer Bay Screening area. The work in WP1 was organized in 11 tasks (Tasks 1.1-1.11).

In Task 1.1, a geophysical survey using vessel borne multibeam echosounder (MBES), side scan sonar (SSS) and sub-bottom profiler (SBP) systems was planned and conducted. SSS and MBES data provide information on the substrate and the morphology of the seabed surface, and SBP data provide information on the shallow subsurface. In total, 3,255 line-km of geophysical data were acquired, including instrument test and calibration lines, transit lines, turns, and revisited line-segments.

In Task 1.2, the geophysical data were processed and prepared for interpretation and generation of maps and models (Tasks 1.3-1.8). The acquired geophysical data in combination with data acquired in the context of other projects in the Jammer Bay area provide a unique dataset combining detailed surface and shallow subsurface information over a large area.

In Task 1.3, a geological model of Jammer Bay was developed based on shallow subsurface and seabed surface data. Five units were identified (Unit A-E from youngest to oldest) in the available SBP and Sparker seismic data. Unit A (Mid-Late Holocene marine deposits), C (Late Glacial glaciomarine deposits) and D (Late Quaternary glacial deposits) are present across the whole area. Unit B (Early-Late Holocene marine deposits) is confined to the northern and deeper part of Jammer Bay and close to Hanstholm. Unit E (Pre-Quaternary deposits) was only identified in the southern parts of Jammer Bay due to the limited seismic penetration.

In Task 1.4, seabed sediment thickness maps were generated based on SBP data. Detailed and reliable thickness maps of unit A (Mid-Late Holocene marine deposits) and C (Late Glacial glaciomarine deposits) were generated in the Focus area where the line spacing was 200 m. The depths and thickness maps are less detailed and with higher uncertainties outside the Focus area due to larger line spacing.

In Task 1.5, bathymetric maps were generated based on MBES data. Bathymetric models, or Digital Elevation Models (DEMs), provide information on depth. DEMs were produced with a grid cell size of 1 m x 1 m in both the Focus area and the Screening area. Furthermore, DEMs with 10 m grid cell resolution were produced as support for the delineation of sandbanks (Task 1.8). The large dataset of bathymetric data provides a baseline for high resolution

morphodynamic analyses in the shallower areas and for broad scale morphodynamic analyses in the deeper areas.

In Task 1.6, seabed morphometric and morphological maps were generated from the bathymetric models based on MBES data and supported by SSS and SBP data. The models of bathymetry, morphometry, and morphology serve as direct support for the seabed substrate and habitat interpretations and mapping (Task 1.7 and Task 1.8).

In Task 1.7, seabed substrate maps were generated based on SSS data, supported by MBES and SBP data, and in combination with knowledge from existing data. Seabed substrates were classified according to the classification system of the Danish Environmental Protection Agency (DEPA) (Miljøstyrelsens substrattyper in Danish). The maps show that the seabed in the Jammer Bay consists of a diverse distribution of substrates, with complex patterns of hard and soft substrate types. The most dominant substrate types are 1b (sand) covering 354 km^2 (62% of the mapped area), and 2a (sand, gravel and pebbles) covering 135 km^2 (24% of the mapped area). Substrate types 4, 3 and 2b (all containing stones larger than 10 cm), cover 67 km^2 in total, corresponding to 12% of the mapped area. In addition, trawl marks and other signs of human activities were also mapped. Trawl marks were mostly found in the northern part of Jammer Bay. Moreover, five wrecks were observed, and traces from pipelines were observed.

In Task 1.8, seabed habitat maps were generated based on an integration of seabed substrate and morphology that was derived in previous tasks from MBES, SSS, and SBP data. Seabed habitats were classified according to the EU Habitats Directive (Habitatdirektivets naturtyper in Danish). The specific seabed habitats that were mapped and spatially delineated were sandbank habitats (habitat code 1110) and stone reef habitats (habitat code 1170).

In Task 1.9, a second geophysical survey using vessel borne MBES, SSS and SBP systems was planned and conducted in the area along the EEZ border and in a nearshore area. In total, ~690 line-km of geophysical data were acquired, including instrument test and calibration lines, transit lines, turns, and revisited line-segments.

In Task 1.10, a topobathymetric airborne laser scanning (ALS) survey was planned and conducted in the shallow water coastal zone. ALS data were recorded from the coastline towards the 10 m water depth curve in the southern part of the Jammer Bay. Simultaneously, high-resolution RGB-images were recorded. The topobathymetric ALS data were processed to deliver fully processed and classified point clouds as well as digital surface models (DSM) of the water surface and the seabed and digital terrain models (DTM) of the seabed.

In Task 1.11, sediment and carbon analyses were performed to determine seabed surface sediment and carbon composition. HAPS cores were collected at 71 locations by WSP. Subsamples were taken from the upper 2 cm and analyzed to determine water content, organic matter content and grain size distributions. Furthermore, 60 sediment samples collected by a grab sampler by DTU Aqua were analyzed to determine organic matter content and grain size distributions. The 60 sediment samples as well as the 71 sediment samples were analyzed to determine total carbon (TC) and total sulphur (TS) as well as total organic carbon (TOC). The carbon analyses will be a first step towards a large-scale estimation of carbon content in seabed surface sediments across different substrate types, water depths and other environmental conditions in Danish waters.

In summary, the acquired and collated data and the processing and analyses as described above have generated new information and knowledge on the shallow subsurface geology and the seabed surface morphology, substrates, and habitats in Jammer Bay, forming a unique foundation for analysing the impact of various types of bottom trawling on the seabed surface.

Dansk resume

Havbundens geologi, morfologi og substrater udgør de overordnede komponenter af havbundens geodiversitet og former havbundshabitater og -fundament for bentisk flora og fauna.

Målene i WP1 var I) at kortlægge havbunden i Jammerbugt Fokusområde – i den centrale del af Jammerbugt – med høj rumlig opløsning og præcision, og med fuld dækning, med henblik på at skabe et fundament for at analysere påvirkningen af forskellige typer af bundtrawl på havbundens overflade; og II) at kortlægge havbunden i Jammerbugt Screeningsområde – som dækker området mellem Hanstholm og Hirtshals fra 10 m dybdekurven til EEZ-grænsen – med høj rumlig opløsning og præcision langs sejllinjerne, og med datahuller mellem sejllinjerne, med henblik på at vurdere den rumlige fordeling af havbundens substrater (substrattyper) og habitater (naturtyper) i Jammerbugt Screeningsområde. Arbejdet i WP1 var organiseret i 11 tasks (Tasks 1.1-1.11).

I Task 1.1 blev et geofysisk togt med skibsbåren multibeam ekkolod (MBES), sidescan sonar (SSS) og sub-bottom profiler (SBP) (sedimentekkolod) planlagt og gennemført. SSS og MBES data giver informationer om havbundsoverfladens substrater og morfologi, og SBP data giver informationer om den overfladenære havbund. I alt blev der indsamlet 3.255 linje-km geofysiske data inklusive test og kalibrering af instrumenter, transit, vendinger og genbesøgte sejllinjer.

I Task 1.2 blev de geofysiske data processeret og klargjort til tolkning udfærdigelse af kort og modeller (Tasks 1.3-1.8). De indsamlede geofysiske data i kombination med data indsamlet indenfor rammerne af andre projekter i Jammerbugt udgør et unikt datasæt med en kombination af detaljerede overflade og overfladenære informationer for et stort område.

I Task 1.3 blev der udviklet en geologisk model for Jammerbugt baseret på overfladenære og overflade data. Fem geologiske enheder blev identificeret i de tilgængelige SBP og Sparker data (Enhed A-E fra yngste til ældste). Enhed A (midt-sen-holocæne marine aflejringer), C (senglaciale glaciomarine aflejringer) og D (sen-kvartære glaciale aflejringer) er i hele området. Enhed B (tidlig-sen-holocæne marine aflejringer) er begrænset til den nordlige og dybere del af Jammerbugt og tæt på Hanstholm. Enhed E (præ-kvartære aflejringer) er kun identificeret i den sydlige del af Jammerbugt som følge af begrænset seismisk nedtrængning.

I Task 1.4 blev der genereret sediment tykkelseskort baseret på SBP data. Detaljerede og pålidelige tykkelskort af enhed A (midt-sen-holocæne marine aflejringer) og C (senglaciale glaciomarine aflejringer) blev genereret for Fokusområdet, hvor linjeafstanden var 200 m. Udenfor Fokusområdet er dybde- og tykkelseskortene mindre detaljerede og med større usikkerheder på grund af større linjeafstand.

I Task 1.5 blev der genereret batymetriske kort baseret på MBES data. Betymetriske modeller, eller digitale elevationsmodeller (DEM) giver informationer om dybde. DEMer blev produceret med en gridcellestørrelse på 1 m x 1 m i både Fokusområdet og i Screeningsområdet. Derudover blev der genereret DEMer med 10 m gridcellestørrelse til understøttelse af afgrænsning af sandbanker (Task 1.8). Det omfattende datasæt med batymetriske data giver en baseline for

højopløselige morfodynamiske analyser i lavvandede områder og storskala morfodynamiske analyser i dybere områder.

I Task 1.6 blev der genereret havbundsmorfometriske og -morfologiske kort fra de batymetriske modeller baseret på MBES data og understøttet af SSS og SBP data. Modellerne for batymetri, morfometri og morfologi understøtter direkte tolkninger og kortlægninger af havbundens substrat (substrattyper) og habitater (naturtyper) (Task 1.7 og Task 1.8).

I Task 1.7 blev der genereret substrattypekort baseret på SSS data, understøttet af MBES og SBP data, og i kombination med viden fra eksisterende data. Havbundens substrattyper blev klassificeret i henhold til Miljøstyrelsens klassifikationssystem. De genererede kort viser, at havbunden i Jammerbugt består af en mangfoldig fordeling af substrattyper med komplekse mønstre af hårde og bløde substrattyper. De mest dominerende substrattyper er 1b (sand), som dækker 354 km^2 (62% af de kortlagte områder) og 2a (sand, grus og småsten), som dækker 135 km^2 (24% af de kortlagte områder). Substrattyperne 4, 3 og 2b (alle med sten > 10 cm) dækker 67 km^2 totalt, svarende til 12% af de kortlagte områder. Ydermere blev der kortlagt trawlspor og andre tegn på menneskelig påvirkning. Trawlspor blev primært fundet i den nordlige del af Jammerbugt. Derudover blev der observeret fem vrag samt spor af rørledninger.

I Task 1.8 blev der genereret naturtypekort baseret på en integration af havbundens substrater (substrattyper) og morfologi, som blev genereret i tidligere Tasks baseret på MBES, SSS og SBP data. Havbundens naturtyper blev klassificeret i henhold til EU Habitatdirektivet. De specifikke kortlagte naturtyper er sandbanker (1110) og stenrev (1170).

I Task 1.9 blev et geofysisk togt med skibsbåren MBES, SSS og SBP (sedimentekkolod) planlagt og gennemført i området langs EEZ-grænsen og i et kystnært område. I alt blev der indsamlet 690 linje-km geofysiske data inklusiv test og kalibrering af instrumenter, transit, vendinger og genbesøgte sejllinjer.

I Task 1.10 blev et topobatymetrisk flybåren laserscanning (ALS) togt planlagt og gennemført i den lavvandede kystzone. ALS data blev indsamlet fra kystlinjen og ud mod 10 m dybdekurven i den sydlige del af Jammerbugt. Højopløselige RGB-billederblev optaget samtidigt. De topobatymetriske ALS data er processeret med henblik på at levere fuldt-processerede og klassificerede punktskyer og digitale overflademodeller (DSM) af vandoverfladen og havbunden samt digitale terrænmodeller (DTM) af havbunden.

I Task 1.11 blev der udført sediment- og kulstofanalyser for at bestemme sammensætningen af havbundens overfladesediment og kulstof. HAPS-kerner blev indsamlet af WSP på 71 lokaliteter. Delprøver blev udtaget fra de øverste 2 cm og analyseret for at bestemme vandindhold, indhold af organisk materiale og kornstørrelsesfordelinger. Derudover blev der analyseret 60 delprøver fra grabprøver indsamlet af DTU Aqua for at bestemme indhold af organisk materiale og kornstørrelsesfordelinger. Alle prøver blev analyseret for at bestemme totalt kulstof (TC) og total svovl (TS) samt total organisk kulstof (TOC). Kulstofanalyserne er et først skridt mod en storskala estimering af kulstofindholdet i havbundens overfladesedimenter på tværs af forskellige substrattyper, vanddybder og andre miljøforhold i danske farvande.

Sammenfattende har de indsamlede og sammenbragte data samt processering og analyser, som er beskrevet ovenfor, genereret ny information og viden om den overfladenære geologi og

havbundens morfologi, substrater (substrattyper) og habitater (naturtyper) i Jammerbugt, hvilket er et unikt fundament til at analysere påvirkningen af forskellige typer af bundtrawl på havbunden.

1. Introduction to WP1

Seabed geology, morphology and substrate constitute the overall components of seabed geodiversity and form seabed habitats and foundation for benthic flora and fauna.

The aims in WP1 were to I) map the seabed within the Jammer Bay Focus area – in the central part of the Jammer Bay – in high spatial resolution and precision, and with full spatial data coverage, in order to create a foundation for analysing the impact of various types of bottom trawling on the seabed surface; and II) to map the seabed within the Jammer Bay Screening area – covering the area between Hanstholm and Hirtshals from the 10 m depth curve to the EEZ border – in high spatial resolution and precision along the survey lines, with data gaps between survey lines, in order to assess the spatial distribution of seabed substrates and habitats within the Jammer Bay Screening area.

2. Geophysical survey (Task 1.1)

Lars Ø. Hansen, Mikkel S. Andersen, Lars-Georg Rödel, Sigurd B. Andersen, Isak R. Larsen, Silas Clausen, Zyad Al-Hamdani, Verner B. Ernstsen

2.1 Introduction and aim

The aim of Task 1.1 was to plan and conduct a geophysical survey using vessel borne multibeam echosounder (MBES), side scan sonar (SSS) and sub-bottom profiler (SBP) systems.

New geophysical data were acquired in the Jammer Bay in context of the JAMBAY project. Side scan sonar (SSS) and multibeam echosounder (MBES) data provide information on the substrate and the morphology of the seabed surface, and sub-bottom profiler (SBP) data provides information on the shallow subsurface.

The aims of the geophysical survey were 1) to map the seabed within the Jammer Bay Focus area (304 km^2, see Figure 2.1) – in the central part of Jammer Bay – in high spatial resolution and precision, and with full spatial data coverage, in order to create a foundation for analysing the impact of various types of bottom trawling on the seabed surface; and 2) to map the seabed within the Jammer Bay Screening area (5,230 km^2, see Figure 2.1 for spatial extent) – covering the area between Hanstholm and Hirtshals from the 10 m depth curve to the EEZ border – in high spatial resolution and precision along the survey lines, with data gaps between survey lines, in order to assess the spatial distribution of seabed substrates and habitats.

2.2 Materials and methods

2.2.1 Survey

Data were collected in the period between 5 June and 21 June 2023. As described in section 2.1, the survey area was divided into two sub-areas: a Focus area (incl. Before-After Control-Impact (BACI) areas) with 200 m line spacing and a Screening area with 2,000 m line spacing, including two normal to shore parallel lines extending to the EEZ border (Figure 2.1). The planned survey lines amount to a total of 2,804 line-km.

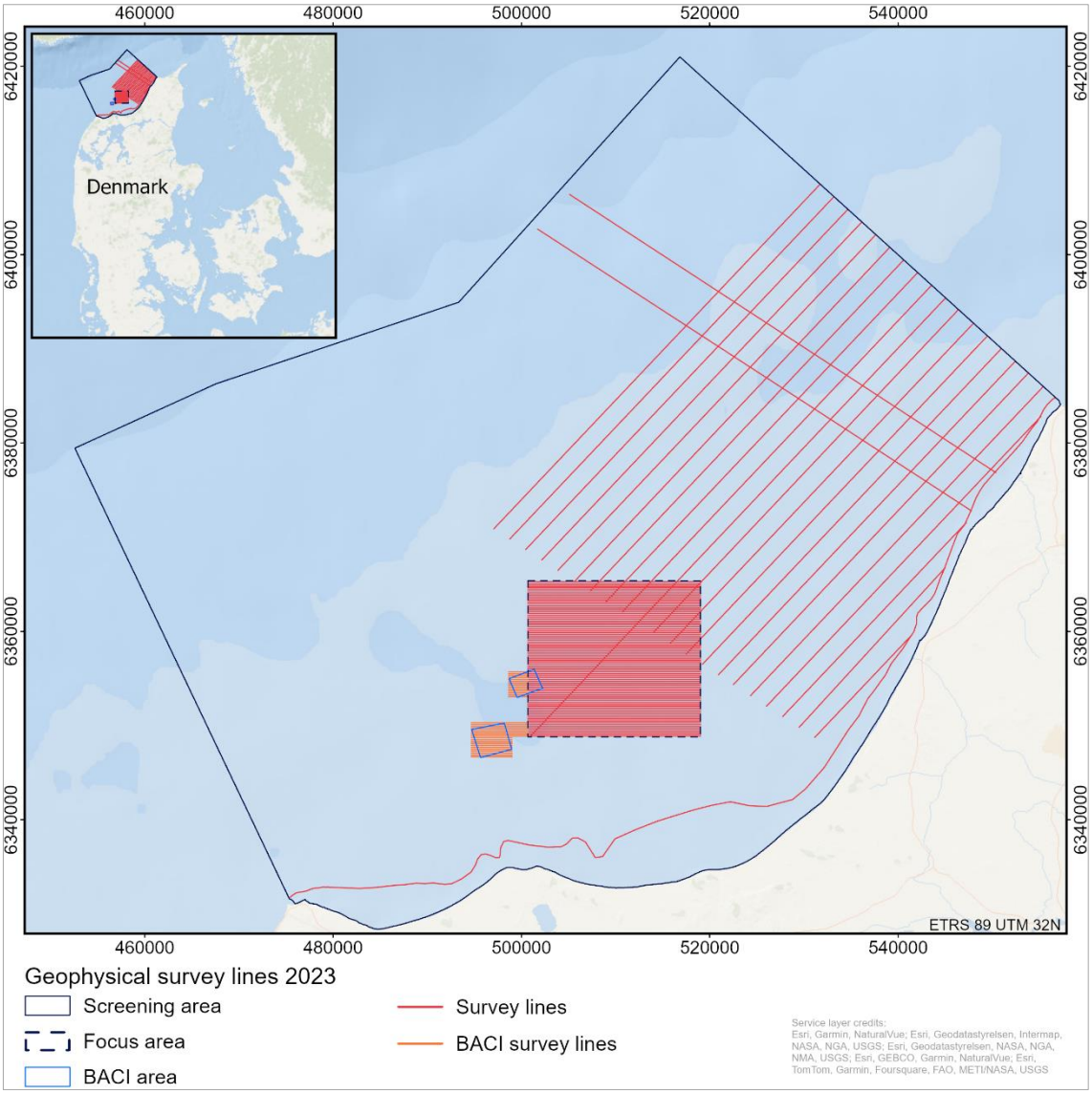

Figure 2.1: Planned geophysical survey lines.

MV Arctic Ocean was used as survey platform (Figure 2.2). The ship's length (LOA) and width (Beam) at the water line is 39.9 m and 9.45 m and the draught is 5.3 m. The ship is equipped with an A-frame and has a service speed of 10 kn and an offshore endurance of 30+ days.

The team on MV Arctic Ocean constituted the ship's crew who operated the ship, and the scientific crew who operated the geophysical instruments and did the data collection. Between two and five scientific crew members were always onboard during the survey.

Figure 2.2: MV Arctic Ocean in Hirtshals harbour on 9 June 2023. Photo: L.Ø. Hansen.

2.2.2 Instruments

The instruments used for the geophysical survey comprised a pole-mounted Edgetech 6205 combined bathymetry and side scan sonar, a towed Edgetech 4205 side scan sonar, a pole-mounted Innomar SES-2000 medium sub-bottom profiler and an R2Sonic 2024 multibeam echosounder. Primary position and motion were delivered by an SBG Navisight Ekinox GNSS/INS system with an Applanix POSMV Wave Master as backup. Motion input for the sub-bottom profiler was delivered by an SMC IMU-108. Sound velocity profiles were initially measured with a Valeport miniCTD, which was later replaced by a Valeport SWIFT SVP (Table 2.1).

Table 2.1: Instruments applied in the geophysical survey.

Instrument type	Instrument model	Mounting
Side scan sonar	Edgetech 4205	Towed
Combined bathymetry and side scan sonar	Edgetech 6205	Pole-mounted starboard
Sub-bottom profiler	Innomar SES-2000 medium	Pole-mounted port
Multibeam echosounder	R2Sonic 2024	Pole-mounted port
Sound velocity probe	Valeport MiniCTD Valeport SWIFT SVP	Hand-held Hand-held
GNSS/INS	SBG Systems Navsight Ekinox	GNSS antennas on the ship INS pole-mounted port
IMU	SMC IMU-108	Pole-mounted port

The R2Sonic multibeam echosounder was mounted on the port side pole on a custom-made bracket and the SBG IMU was mounted on the MBES. The sub-bottom profiler was mounted on the same bracket in a displaced position (forward and up) and the SMC IMU was mounted next to the pole on the railing. The Edgetech 6205 was mounted on the starboard side pole. The Edgetech 4205 side scan sonar was towed behind the ship in a tow cable connected to a winch. The sonar layback was accounted for using a cable counter (MacArtneys Cable Status Indicator MKII).

2.2.2.1 Positioning – SBG Navsight Ekinox

Navsight Ekinox consists of an Ekinox grade Inertial Measurement Unit connected to a Navsight processing unit embedding fusion intelligence and the GNSS receiver. Under optimal conditions the Ekinox provides accuracies as described in Table 2.2. The system delivered navigation solutions to the geophysical instruments.

Table 2.2: Navsight Ekinox Grade Marine Solution specifications (SBG Systems, 2022). *Baseline, dual antenna.

Parameter	RTK	PPK	RTK outage (30 s)	PPK outage (30 s)
Roll, Pitch	0.015°	0.01°	0.05°	0.04°
Heading* - 2 m / 4 m	0.03° / 0.02°	0.02° / 0.02°	0.12° / 0.1°	0.05° / 0.05°
Position (XY)	0.01 m + 0.5 ppm	0.01 m + 0.5 ppm	3 m	1 m
Altitude (z)	0.015 m + 1 ppm	0.015 m + 1 ppm	0.75 m	0.3 m
	Heave	**Wave period**		
Real-time heave	5 cm	Up to 20 s		
Delayed heave	2 cm	Up to 40 s		

2.2.2.2 Side scan sonar – Edgetech 6205

The primary purpose of this pole-mounted system was to provide high positional accuracy side scan sonar imagery containing acoustic information for interpretation of substrate and features on the seabed. Simultaneously, the instrument collected multiphase echosounder bathymetry as backup to the multibeam echosounder bathymetry. The sonar is a dual frequency system operating at a low frequency of 230 kHz and a high frequency of 520 kHz. The side scan sonar

recording range was 100-150 m (Table 2.3). Data was recorded using Discover acquisition software.

Table 2.3: Edgetech 6205 combined bathymetry and side scan sonar frequencies and recording range.

Edgetech 6205	Low frequency	High frequency
Centre frequency	230 kHz	520 kHz
Recording range (per side)	100 m – 150 m	100 m

2.2.2.3 Side scan sonar – Edgetech 4205

The towed Edgetech 4205 side scan sonar was used as a supplement to the pole-mounted side scan and to obtain higher resolution side scan data in the deeper parts of the survey area. The Edgetech 4205 side scan sonar was towed behind the ship in a tow cable connected to a winch. The sonar layback was accounted for using a cable counter (MacArtneys Cable Status Indicator MKII). The height of the sonar above the seabed was generally kept between 10 m and 20 m. The sonar is a dual frequency system operating at a low frequency of 230 kHz and a high frequency of 520 kHz. The side scan sonar recording range was 100-150 m (Table 2.4). Data was recorded using Discover acquisition software.

Table 2.4: Edgetech 4205 side scan sonar frequencies and recording range.

Edgetech 4205	Low frequency	High frequency
Centre frequency	230 kHz	540 kHz
Recording range (per side)	100 m – 150 m	100 m

2.2.2.4 Sub-bottom profiler – Innomar SES-2000 Medium

The sub-bottom profiler mounted on the port side pole delivered shallow sub-surface seismic data for interpretation of the shallow sub-surface sediment layers. The selected system settings are described in Table 2.5. Data were recorded in Innomar SES-Win acquisition software. The system was roll and heave compensated by the SMC IMU-108 motion sensor.

Table 2.5: Innomar SES-2000 Medium frequencies and ping rate setting.

Innomar SES-2000 Medium	Setting
Primary high frequency (PHF)	85-115 kHz
Secondary low frequency (SLF)	6-12 kHz
Ping rate	Variable – slave of R2Sonic MBES

2.2.2.5 Multibeam echosounder – R2Sonic 2024

The R2Sonic multibeam echosounder has a long range of adjustable settings to optimize data collection for any specific objective. The settings applied during this survey are listed in Table 2.6. The Ultra High Density (UHD) bottom sampling mode searches across each beam footprint for additional soundings providing up to 1024 real bottom soundings (R2Sonic, 2022). The swath width was controlled manually during the survey to ensure that outer beam outliers were reduced to a minimum, while at the same time increasing the ping rate because of decreased swath width. Swath width was typically between 100°-140°. The pulse length determines the

transmit pulse duration time. The pulse length was manually adjusted during survey to maintain optimal bottom detection resolution. Generally, the deeper the water depth the longer the pulse length must be to maintain adequate power in the water. The pulse length was typically kept between 20 - 35 µs. The power of the transmit pulse (191 - 221dB) was kept as high as possible while the receiver gain was kept as low as possible aiming to maintain a good balance between source level power and receiver gain and thus a good receive saturation curve. The ocean settings i.e., spreading loss and absorption are the main components of the Time Varied Gain (TVG). The spreading loss and absorption were determined from a calculator inside the sonar GUI which required input of frequency, mean depth, temperature, and salinity.

The MBES data were recorded using QINSY acquisition software and stored in QPS db-file format.

Table 2.6: R2Sonic MBES specifications and settings.

R2Sonic 2024	Setting
Frequency	450 kHz
Beam pattern	Equidistant - Ultra High Density (UHD)
Number of soundings	Up to 1024
Beam width (across x along)	0.45° x 0.9°
Swath width	100° - 140°
Roll stabilized beams	Yes
Pulse length	Variable
Pulse type	Shaped CW
Ping rate	Up to 60 Hz
Bandwidth	Up to 60 kHz
Bottom detect resolution	3 mm

2.2.2.6 Sound velocity profiler

The speed of sound in water depends on temperature, salinity, and pressure. Information on water column sound velocity is required to properly correct the bathymetric measurements in the MBES data.

The acquisition strategy of SVP during this survey was to take one SVP measurement every 6 hours, which for the Focus area meant that an SVP was taken at the end of every third survey line. In case of the longer screening lines, an SVP was acquired at the end of each line. Sound velocity profiles were initially measured with a Valeport miniCTD, which was later replaced by a Valeport SWIFT SVP due to malfunctioning issues.

2.3 Results

2.3.1 Survey track line

The vessel track lines exported from the MBES data (Figure 2.3), including instrument test and calibration lines, turns, and recorded transit lines sum up to a total of 3.255 line-km. Approximately half of the line-km (~1.700 km) were recorded inside the Focus area.

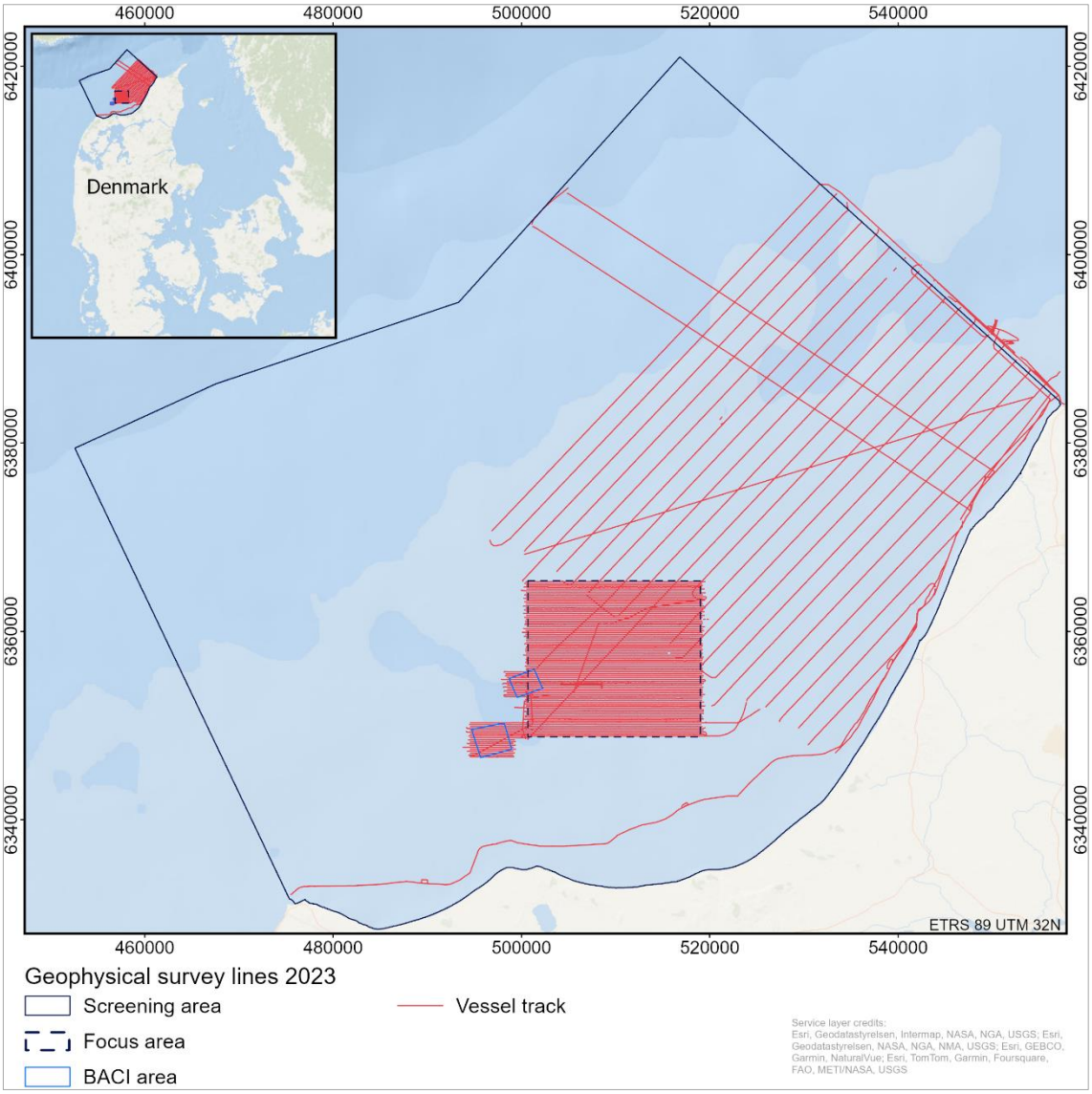

Figure 2.3: Vessel track line exported from the MBES. Screening and Focus area survey, June 2023.

2.4 Discussion and perspectives

The instrument setup with two side scan sonars, i.e. the pole-mounted Edgetech 6205 and the towed Edgetech 4205, was chosen to ensure high resolution side scan imagery on all water depths in the survey area. The pole-mounted side scan sonar provided wide coverage, high resolution and georeferenced imagery of the seabed at shallow water depths. The towed side scan sonar also produced wide coverage, high resolution side scan imagery at deeper waters as the height of the sonar above the seabed was adjustable. The positioning of the towed system was calculated from the cable layback (with reference to the tow point which was referenced to the vessel reference point) and depth of the sonar and is thus not as accurate as the pole-mounted system. Both systems were operated simultaneously during this survey. This arrangement had two advantages: 1) increasing the positioning accuracy of the data acquired with the towed system using the multibeam bathymetry along with the georeferenced side scan data from the pole-mounted system as reference; 2) data redundancy which made it possible to use the data of the

highest quality on any given segment of the seabed in relation to the interpretation of seabed substrate and features. Furthermore, in case of instrument malfunctioning a backup system was already in the water recording data which made the survey more robust and flexible.

Based on the experiences gained during this survey, it is recommended to consider a similar instrument setup for future surveys in the context of seabed substrate and habitat mapping.

3. Processing and preparation of data (Task 1.2)

Lars Ø. Hansen, Mikkel S. Andersen, Zyad Al-Hamdani, Niels Nørgaard-Pedersen, Nicklas Christensen, Jørgen O. Leth, Sofie Kousted, Isak R. Larsen, Silas Clausen, Jacob R. Jørgensen, Verner B. Ernstsen

3.1 Introduction and aim

The aim of Task 1.2 was to process and prepare the geophysical data for interpretation and generation of maps and models as described in tasks 1.3-1.8.

The instruments used for the geophysical survey comprised a pole-mounted Edgetech 6205 combined bathymetry and side scan sonar, a towed Edgetech 4205 side scan sonar, a pole-mounted Innomar SES-2000 medium sub-bottom profiler and, a R2Sonic 2024 multibeam echo-sounder. Primary position and motion were delivered by a SBG Navisight Ekinox GNSS/INS system with an Applanix POSMV Wave Master as backup. Motion input to the sub-bottom profiler was delivered by a SMC IMU-108. Sound velocity profiles were initially measured with a Valeport miniCTD, which was later replaced by a Valeport SWIFT SVP.

Data were collected in the period between 5 June and 21 June 2023. As described in 2.1, the survey area was divided into two sub-areas: a Focus area (incl. BACI areas) with 200 m line spacing and a Screening area with 2,000 m line spacing, including two normal to shore parallel lines extending to the EEZ border (Figure 2.1).

In total, ~2800 line-km of geophysical data acquisition were acquired excluding patch test lines, transit lines, turns, and revisited line-segments.

3.2 Materials and methods

3.2.1 Side scan sonar data

Two side scan systems were acquiring data simultaneously during the survey, one was pole-mounted (mostly useful in shallow area), and the other was towed behind the survey vessel (essentially used for deep water area) as mentioned in section 3.1. This setup has its advantage when e.g. one of the side scan systems is not producing optimal side scan images (e.g. due to noise in the water column or in the system).

The high and low frequency side scan datasets were loaded to and analysed by the SonarWiz V7 software. The towed side scan data was first corrected for the layback using the build in algorithm in the software and the cable-out data registered during acquisition. Then the side scan imagery positions were fine-tuned and adjusted using data obtained from the multibeam system, which produces accurately positioned data, for the same survey line. Seabed features' position that appears on the multibeam dataset was compared with the same features on the side scan image, if there was a discrepancy in position, the side scan image was rectified accordingly. The same positioning adjustment, if required, was performed on the data recorded by the pole-mounted side scan sonar. So, in both side scan datasets, the multibeam data were taken as a reference in obtaining an accurately positioned side scan imagery of the seabed which can

be confidently used later in finding targets for ground truth sampling and in delineating the different seabed substrates.

The side scan data were then corrected for the water column and the detection of the first seabed return signal using the “bottom track” module in SonarWiz. This action ensured that the noisy water column can be eliminated from the dataset, thereby rendering it clean and it can be processed further for reflected signal gain and intensity. The bottom tracking operation can be performed in a batch mode, but sometimes the water column is so noisy that automatic detection of the seabed first return is not possible, then manual tracing of the seabed was inevitable.

The next step was to adjust the “appearance” of the side scan image to make it as clear as possible for interpretation and delineation of the seabed substrate. The software provides different methods for adjusting the setting of the side scan imagery. It is up to the processors to choose the one that suits the job well. In this work we started with the Empirical Gain Normalisation (EGN) so the side scan image was balanced in intensity across the image swath. When that was not optimal for interpreting the stones distribution across the side scan swath, we then chose the User-define Gain Control (UGC) and changed the Time Varying Gain (TVG) setting to enhance the side scan image, which enabled us to identify stones and the different substrate types on the seabed.

3.2.2 Sub-bottom profiler data

Innomar RAW files were converted into SEG-Y format with Innomar SES Convert software to be used with post-processing software. Depending on data quality (especially wave motion influence/heave compensation), SEG-Y data with insignificant wave motion noise were imported directly to Kingdom seismic interpretation software for further analysis. More noisy data sets were processed with Geosuite Allworks software using trace equalisation, median filter, two times swell filter and time varying gain. Hereafter processed data were likewise imported to Kingdom seismic interpretation software.

3.2.3 Multibeam echosounder data

A flow chart depicting the processing steps of the multibeam sonar data from acquisition to final product is shown in Figure 3.1.

QPS Qimera 2.5.4 software was used for post-processing the bathymetric data. The project was set up in ETRS89 UTM32 N with DVR90 (DKGEOID02) as vertical reference. The .db files and associated QPD files were imported along with sound velocity profiles. The .db files contain vessel and instrument setup information. Post-processing in Qimera is based on sounding editing and a dynamic surface model that continuously updates every time an edit is applied.

Precise Point Positioning (PPP) solutions were post-processed in Qinertia software using the SBG Navsight Ekinox navigational data as input to generate SBET (Smoothed Best Estimate of Trajectory) files. The purpose was to improve the reference point (RP) GNSS positioning by replacing the Real-Time Kinematic (RTK) solution, which frequently drifted during the survey due to signal strength and coverage, with the SBET solution. SBET files were imported and matched with corresponding multibeam .db files.
In general, the SBET improved the overall positioning compared to the RTK solution, however, though fewer and with smaller deviations from the average height, the SBET solutions also

suffered from short-term outages affecting positional accuracy. In these cases, RTK was used instead of SBET, or if both solutions were off, they were disabled, and the line segment was adjusted manually to fit with neighbouring line-segments which were positioned by either RTK or PPP.

Sound velocity profiles were tied to the sounding files to correct for beam refraction. The SVPs were designated based on spatial and temporal closeness, i.e. the SVP closest in distance within a period of 360 minutes was valid in the Focus area. In the Screening area, the SVP strategy was closest in distance within a period between 480 and 720 minutes. Some nearshore lines were assigned specific SVPs. The shift between SVPs on the line segments was smoothed using a 120 second SVP cross fade algorithm.

Two patch tests were completed during the survey – one in the beginning, and one towards the end of the survey, the latter was to confirm that the offsets were still unchanged.

Outer beam noise was reduced by blocking soundings beyond +/- 65° from nadir and sometimes less. A set of automatic filters were applied followed by manual cleaning to remove outliers. The automatic filters consisted of a preset spline filter followed by a Reject outliers 3D filter. The spline filter fits a 3D spline surface through the point data and rejects all points that are too far from the surface. A Strong spline filter was applied based on parameter values approximated to IHO First Order specifications (QPS, 2023). The Reject Outliers 3D filter rejects soundings with large mean distance from its neighbours (QPS, 2023).

Furthermore, MBES backscatter mosaics were produced to support the interpretation of seabed substrates from side scan sonar data. The backscatter mosaics were generated using QPS FM Geocoder software.

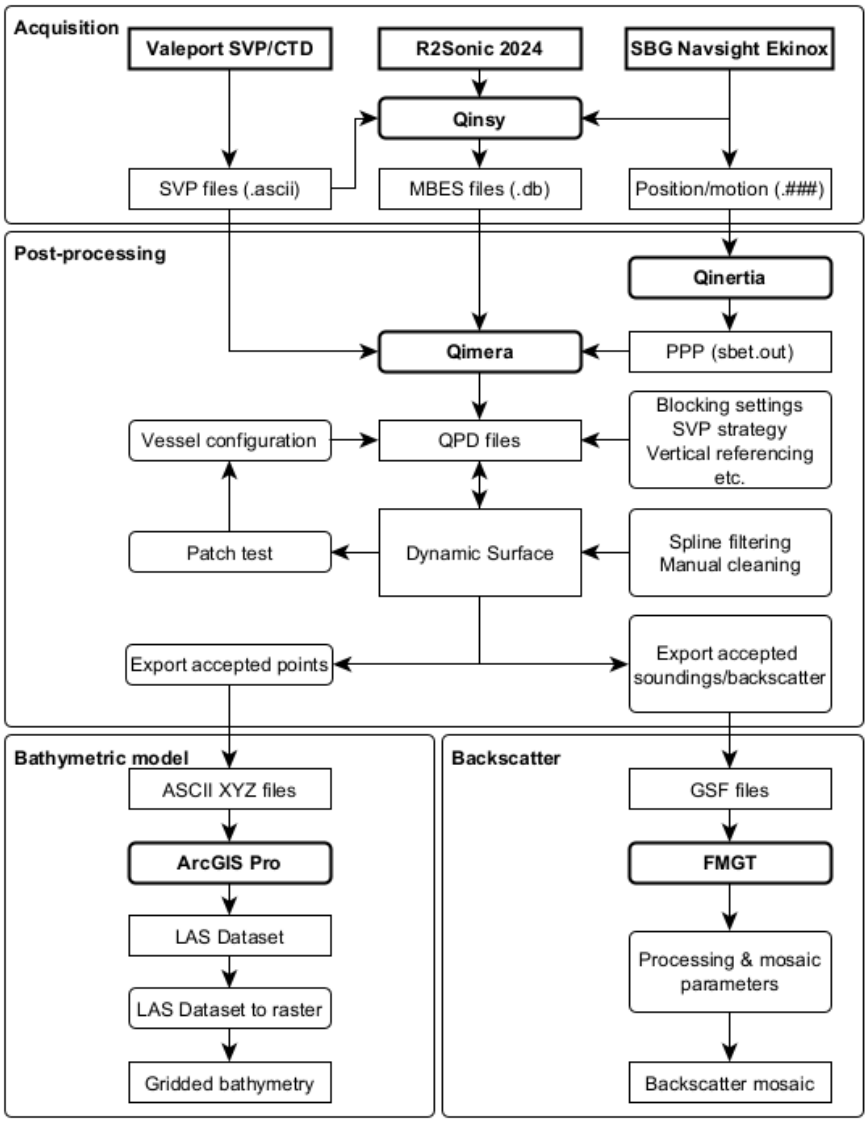

Figure 3.1: Flow chart illustrating the processing steps from acquisition to final products of the multibeam echosounder data. Intensity data stored in the MBES files enable creation of backscatter mosaics.

3.3 Results

3.3.1 Side scan sonar data

The acquired side scan .jsf files were imported to the SonarWiz software as .csf files. These files were correctly georeferenced, bottom tracked and adjusted for the gain settings to obtain the best possible image that will be utilised in the delineation of stones and substrates. The .csf files were stored in the SonarWiz project file for interpretation of substrates and human activity (Task 1.7). The processed side scan files were then exported as geotiff side scan mosaic files (georeferenced image files), to be presented and viewed on a GIS platform (see side scan mosaic from the Focus area in Figure 8.2).

3.3.2 Sub-bottom profiler data

Processed sub-bottom profiler data were imported to Kingdom seismic interpretation software. Seismic units were traced by marking interpreted seismic unit boundaries including the seabed. Unit thicknesses were calculated from two-way travel time data (ms) assuming a constant seismic velocity of 1,600 m/s in the unconsolidated sediment sequence. Thickness data were gridded in Kingdom software and exported as grid files for GIS mapping and presentation software. The SBP SEG-Y data were also imported to the SonarWiz software to be used together with the MBES and side scan data for interpreting the seabed substrates and their spatial distribution.

3.3.3 Multibeam echosounder data

The accepted soundings were exported in ascii file format, one ascii file for each db-file, containing timestamp, x, y, and z columns. The bathymetric models were built from the ascii files, see Chapter 6.

3.4 Discussion and perspectives

A key aspect, beside data quality, in this type of mapping, where different data sources are combined in the process of interpretation, is accurate and precise data positioning. For this purpose, we used a GNSS/INS system which delivered navigation solutions to the geophysical instruments. However, in the offshore environment base station coverage (required for reception of Real Time Kinematic corrections) with respect to ship position degrades as the distance to the survey vessel increases and thus the positional accuracy decreases. Precise Point Positioning (PPP) solutions were generated to improve the positional accuracy of the data. The combination of these navigational solutions provided relatively accurate data positioning for the vessel-mounted instruments. The biggest challenge was to achieve accurate positioning of the towed side scan data. The data acquired with the towed system was manually adjusted in relation to the multibeam bathymetry and the georeferenced side scan data from the pole-mounted system. This was however only possible when distinct features on the seabed were present.

The geophysical data acquired during this project in combination with the data acquired in the context of other projects in the Jammer Bay area provide a unique dataset combining detailed surface and shallow subsurface information over a large area.

4. Geological model (Task 1.3)

Niels Nørgaard-Pedersen, Nicklas Christensen, Jørgen O. Leth, Sofie Kousted, Mikkel S. Andersen, Lars Ø. Hansen, Peter Sandersen, Zyad Al-Hamdani, Verner B. Ernstsen

4.1 Introduction and aim

The aim of Task 1.3. was to develop a geological model of the Jammer Bay based on shallow subsurface and seabed surface data.

In the context of the JAMBAY project, new sub-bottom profiler (SBP) data together with multibeam and side scan sonar data have established a high-resolution data set that enables a detailed mapping of shallow subsurface geological units in selected parts of Jammer Bay. Existing deeper penetration seismic data (Sparker and TOPAS SBP data) and sediment core data were integrated with the JAMBAY project SBP data set to develop a unified geological model for the entire Jammer Bay area. Interpretation of the seismic data supported by vibrocore ground truthing are the backbone for development of the geological model. The model explains the distribution of characteristic seismic/geological units to complement the well-established knowledge of the late quaternary geological history and related relative sea level changes in northern Denmark.

Existing knowledge of the geological development of the Jammer Bay area is mostly based on onshore studies of northern Jutland (e.g. Larsen et al. 2009; Pedersen 2006), studies of deeper seismic low-resolution data from the Jammer Bay area (Nielsen et al. 2008), and over-regional studies of Weichselian ice sheet distribution and deglaciation in the southern Scandinavia-North Sea area (Hjelstuen et al. 2018; Morén et al. 2017).

4.2 Materials and methods

GEUS archive shallow seismic data combined with new JAMBAY project sub-bottom profiler data from the Focus area and the Screening area were used (Figure 4.1). The archive seismic data and sediment cores include data collected during GEUS surveys for the Danish Environmental Protection Agency (2019-2020), the Danish Coastal Authority (2020-2023), and the Danish Energy Agency (2023).

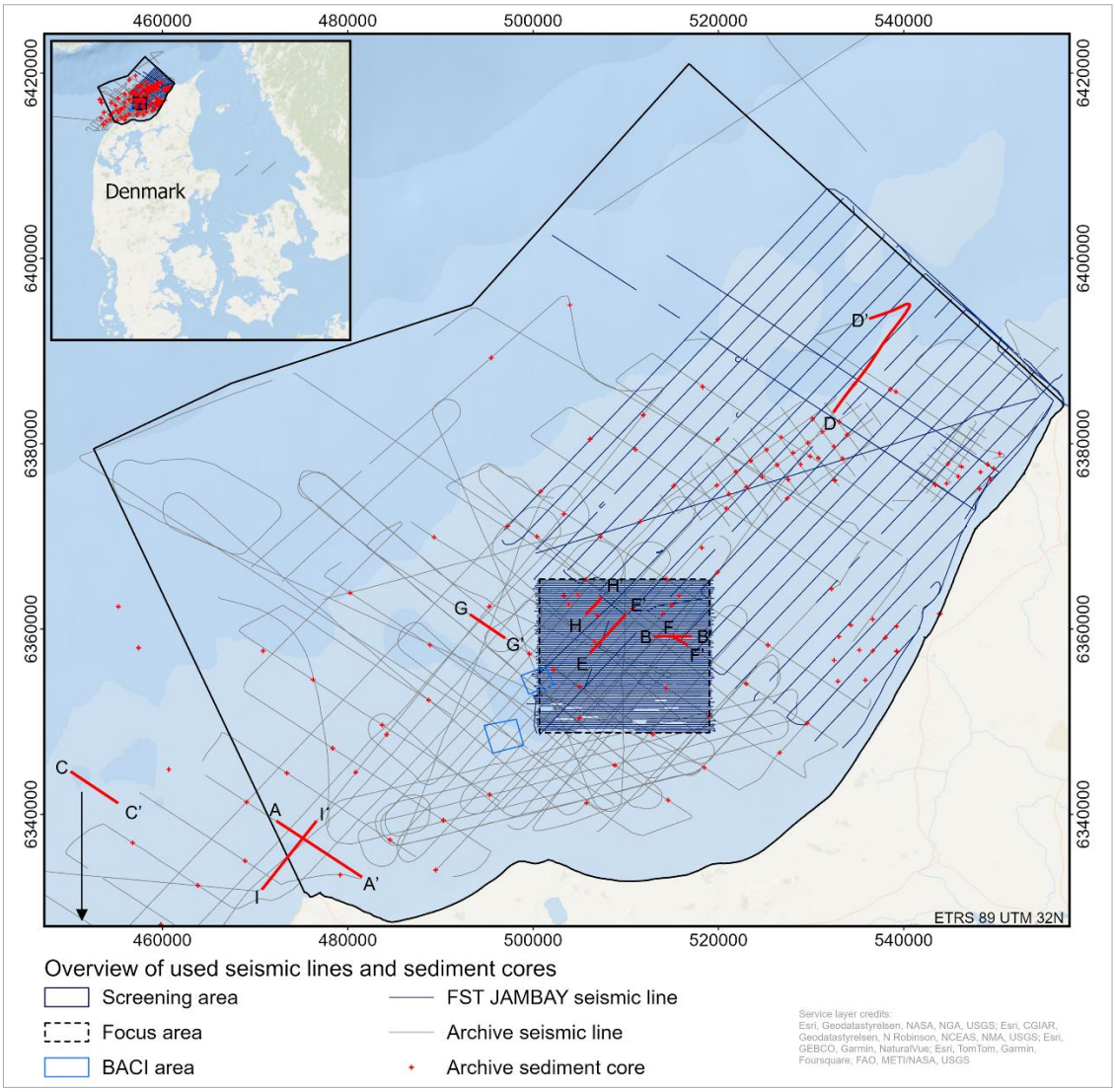

Figure 4.1: Overview of used seismic lines and sediment cores (red marking) in the Jammer Bay. The JAMBAY survey lines are marked by blue, and other archive seismic lines are marked by grey. Cross sections are marked with red lines, and letters mark initial and end point.

Most of the shallow seismic data consisted of two data types, which are parametric sub-bottom profiler (SBP) data and Sparker single channel data. The Sparker single channel data are acquired with a higher pulse and lower frequency compared to the SBP data. This means that the Sparker data have a greater penetration, but lower resolution compared to the SBP data. In Figure 4.2 are the two seismic data types compared on an identical survey line to display the limitation and advantages of both data types.

The development of the seismic model was done in the seismic interpretation software IHS Kingdom suite version 2019. The Sparker data and selected parts of the SBP data were processed with GeoSuite Allworks software to improve data quality and reduce noise. The processing included Infinite Impulse Response (IIR) bandpass filter, median filter, normalisation, trace equalisation, trace mixing, detection of seabed reflector, swell filtering and muting of water column.

After processing, Sparker data were exported in SEGY format and imported in IHS Kingdom seismic interpretation software for stratigraphic analysis. The time (depth)-axis on the seismic profiles is shown in two-way travel time (TWTT). Based on an estimated sound velocity of 1,600 m/s in the dominantly sandy upper seabed, 10 ms corresponds to approximately 8 m depth.

The seismic interpretation included identification and tracking of stratigraphic boundaries between major stratigraphic units described in the following section.

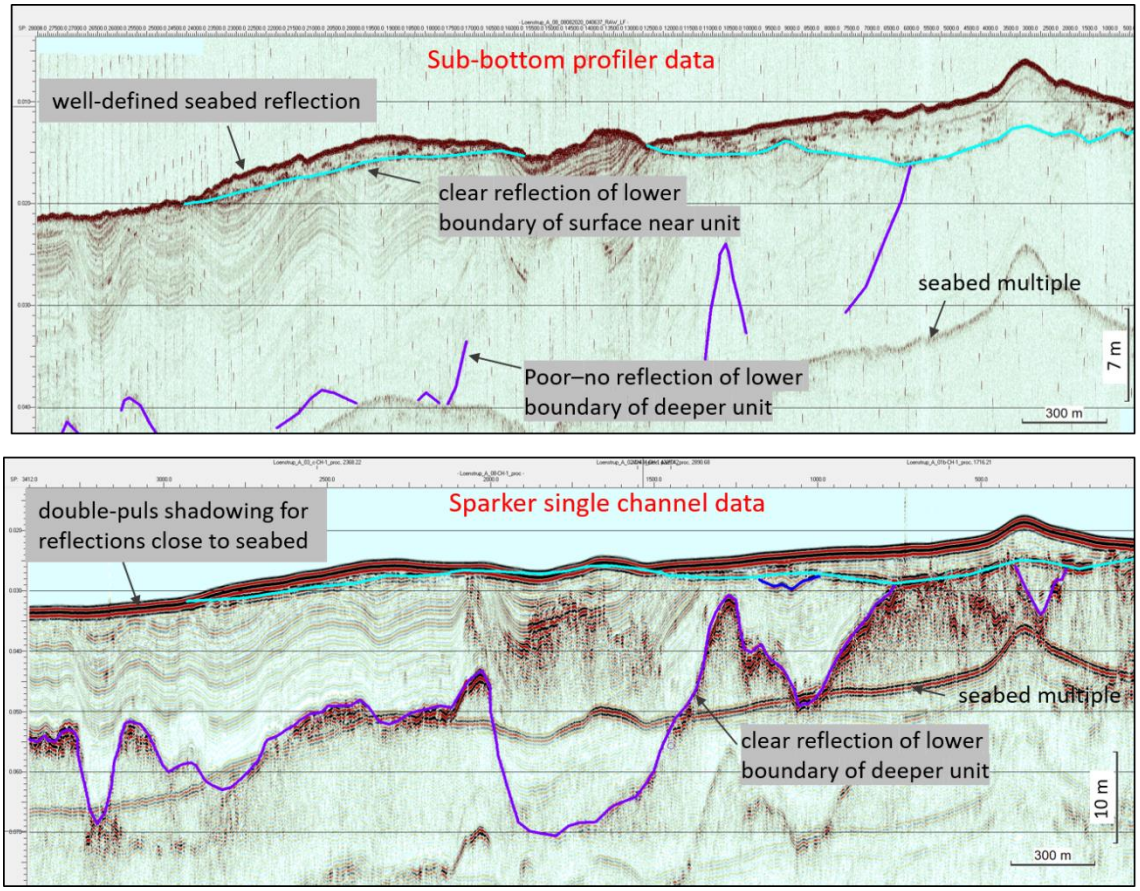

Figure 4.2: An interpreted SBP line and an equivalent Sparker line for comparison. The SBP data have lower penetration, but higher resolution compared to the Sparker single channel data.

4.3 Results

Table 4.1 shows an overview of the interpreted seismostratigraphic units in Jammer Bay. Five units were identified (Unit A-E from youngest to oldest) in the available sub-bottom profiler and Sparker seismic data. Unit A, C and D are present across the whole area. Unit B is confined to the northern and deeper part of Jammer Bay and close to Hanstholm. Unit E could only be identified in the southern parts of Jammer Bay due to the limited seismic penetration.

The geological age and depositional environment of the units were estimated based on existing knowledge from studies in the North Sea to the south of Jammer Bay (Jensen et al. 2010), onshore radiocarbon and luminescence dating (Larsen et al. 2009), and content of macrofossils in vibrocores.

Table 4.1: Overview of identified seismostratigraphic units.

Seismostratigraphic units				
Unit	**Age**	**Seismic facies**	**Depositional environment**	**Expected soil type**
A	Mid-late Holocene	Chaotic with few internal continuous reflections	Marine	Fine to medium sand with local beds of gravel.
B	Early-late Holocene	Low amplitude continuous parallel reflections	Marine	Fine grained sand with occasional laminae of silt and or clay
C	Late glacial	Dominantly Low to high amplitude parallel wavy reflections. Locally transparent.	Glaciomarine	Clay with laminae of silt. Occasional fine sand.
D	Late quaternary	Chaotic with medium to strong amplitudes. locally parallel reflections.	Glacial	Glacial till. Occasionally reworked Skærumhede Sea deposits
E	Pre-Quaternary	Inclined and folded medium to high amplitude reflections. Locally chaotic.	Marine	Cretaceous chalk/ Danian limestone

The interpreted horizons represent the seismostratigraphic unit boundaries, which is summarized in Table 4.2. The interpreted horizons are always describing the base of the individual units, except for the first (dark blue) seafloor interpretation.

Table 4.2: Overview of interpreted seismostratigraphic horizons.

Seismostratigraphic Horizons			
Horizon colour	**Description**	**Seismic signature**	**Data type**
Dark blue	Sea floor.	Strong amplitude reflection.	Sub bottom profiler and Sparker seismic data
Light blue	Base of unit A – Holocene	Erosive planar surface. Strong amplitude reflection	Sub bottom profiler and Sparker seismic data
Green	Base of unit B – Early Holocene	Medium amplitude planar reflection	Sparker seismic data
Purple	Base of unit C – Late glacial	Irregular and undulating surface.	Sub bottom profiler and Sparker seismic data
Orange	Base of unit D – Glacial and top of unit E – Pre-Quaternary.	Erosive undulating surface.	Sparker seismic data

4.3.1 Unit A – Mid-late Holocene marine deposits

Unit A, the uppermost interpreted unit, is present in most part of Jammer Bay. The unit consists of sand sheets or bars with variable thickness and with superimposed sand waves. The unit

corresponds to the so-called mobile sand layer found in many areas of the shallower Danish part of the North Sea. Large longitudinal sand bars with an extent of several tens of kilometres are found west of Hanstholm.

Internally the unit is acoustically chaotic with few continuous low amplitude reflections. Foreset structures appear frequently. The base of unit A is an erosional planar surface, which forms a strong continuous acoustic reflection (Figure 4.3, Figure 4.4). Sediment cores show a dominant lithology of fine to coarse sand with occasional thin beds of gravelly sand at the base of the unit and along internal discontinuity surfaces.

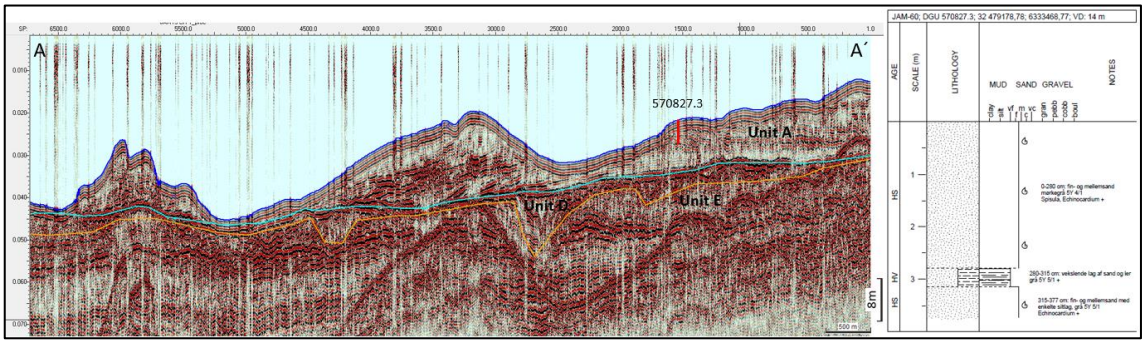

Figure 4.3: Sparker seismic profile with Unit A sand bars. Base of unit A is marked by light blue line. Vibrocore 570827.3 verifies a composition dominated by fine-medium grained sand. Location is shown on Figure 4.1.

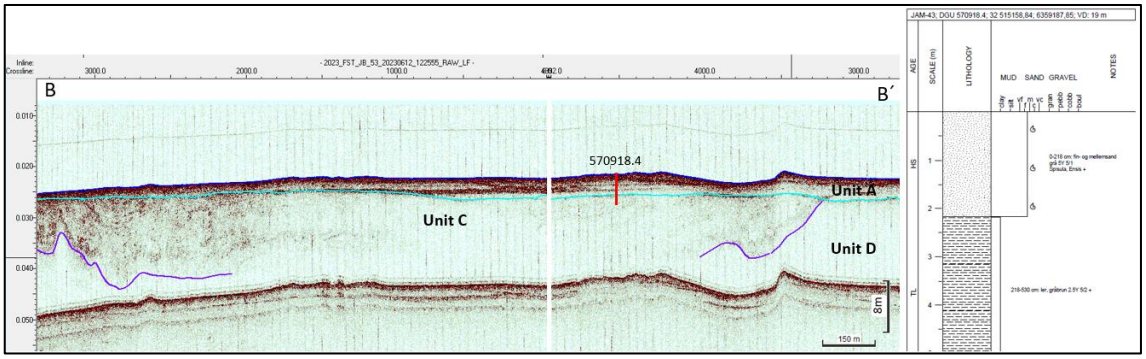

Figure 4.4: Innomar SBP with a relatively thin unit A mapped above light blue line. Vibrocore 570918.4 verifies a composition of fine-medium grained sand. The lower part of the core represents unit C clay. Location is shown on Figure 4.1.

4.3.2 Unit B – Early to late Holocene marine deposits

Unit B is present in the southwestern part of Jammer Bay west of Hanstholm and in the northern and deeper part of Jammer Bay. It is mostly superimposed by unit A, eroding into unit B. In the northern deeper part of J Jammer Bay, the unit is present directly on the seafloor. The unit is characterised by distinct subhorisontal reflections in the southern J Jammer Bay, (Figure 4.5) and by clinoform reflections forming a prograding wedge in the deeper western and northern part of Jammer Bay (Figure 4.6). Sediment cores verify that the unit is dominated by silty fine sand to more clayey and silty mud.

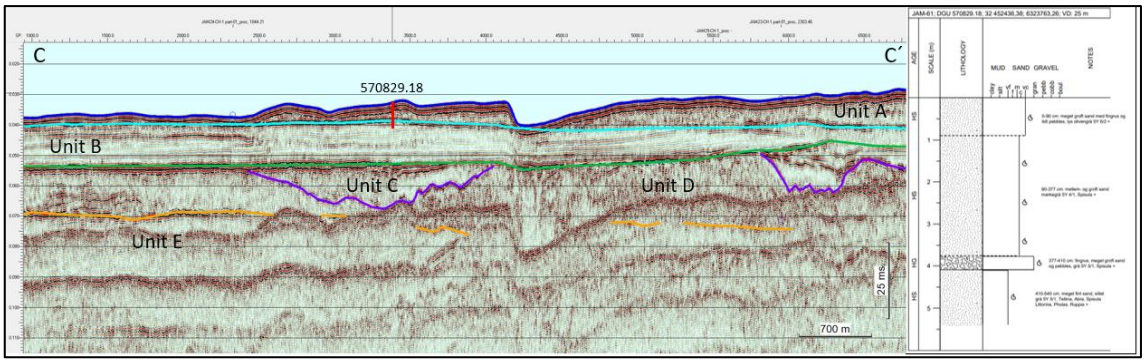

Figure 4.5: Sparker seismic example of Unit B observed in the southern part of Jammer Bay. Vibrocore 570829.18 (lower part) verify a composition of silty, very fine sand. Location is shown on Figure 4.1.

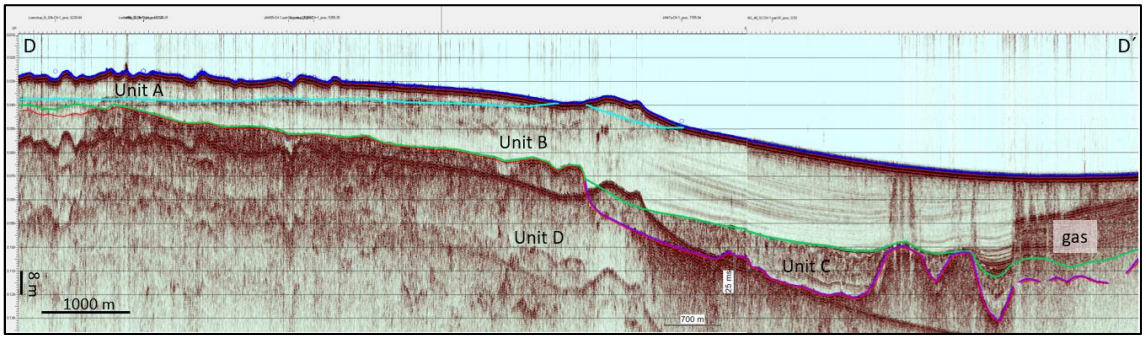

Figure 4.6: Sparker seismic section from the northern part of Jammer Bay illustrating the descending glacial surface with deposition of a prograding wedge of late glacial-holocene sediments towards deeper water. Location is shown on Figure 4.1.

4.3.3 Unit C – Late Glacial glaciomarine deposits

Unit C is present in localised areas of Jammer Bay as infill of elongated depressions in the glacial surface (Figure 4.7, Figure 4.8) and as a conformable unit on top of the descending glacial surface toward the deeper part of Jammer Bay (Figure 4.6). The glacial valley or channel infills have variable width (c. 100-5000 meters) and thickness (up to c. 20 m).

The internal seismic facies of the unit vary from low to high amplitude parallel, wavy reflectors and locally transparent. The wavy reflectors are mostly conformed with the base (purple) reflector, which corresponds to the top of the glacial unit D. In most parts of Jammer Bay, the top of the unit is eroded by the superimposed Holocene units A or B, and the unit is confined to depressions or channels in the glacial surface. In the deeper northern part of Jammer Bay, the superimposed Holocene unit B is often conformable to the late glacial unit.

Sediment cores show a dominant lithology of laminae of clay, silt, and occasionally fine-grained sand. Marine bivalve macrofossils (e.g. *Portlandia arctica*) have been found in a few cores.

Detailed 3D mapping of unit C in the Focus area (Chapter 5) reveals a large branching valley or channel system infilled mainly with conform layers.

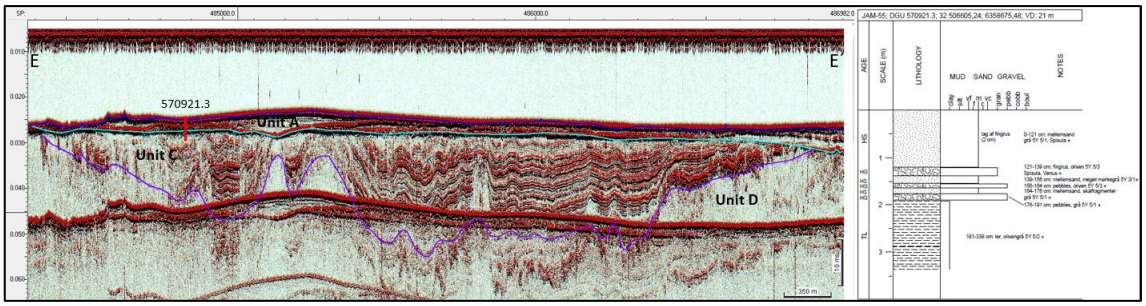

Figure 4.7: SBP profile showing late glacial Unit C with fine stratified layering deposited conformably on the glacial surface. Vibrocore 570921.3 (lower part) verifies a clayey composition. Location is shown on Figure 4.1.

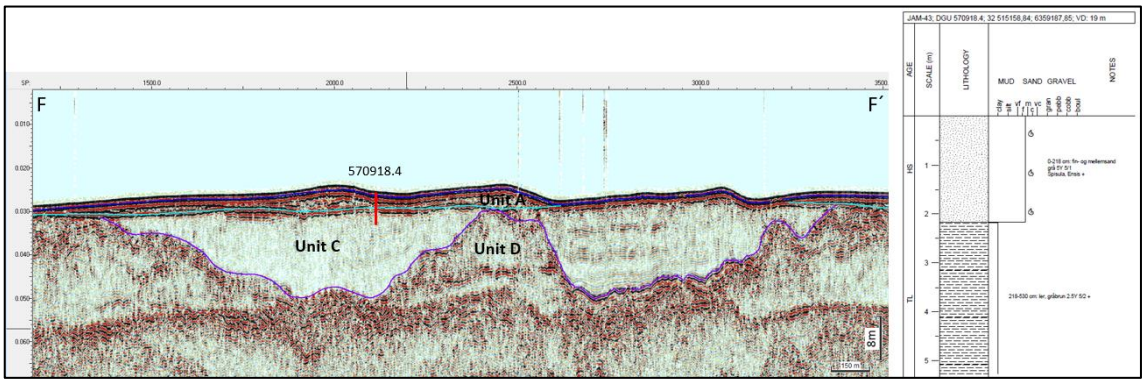

Figure 4.8: Sparker seismic example of late glacial Unit C infill in depressions in the glacial surface. Base of Unit C marked by purple. Vibrocore 570918.4 (lower part) verifies a clay composition. Location is shown on Figure 4.1.

4.3.4 Unit D – Late Quaternary glacial deposits

Unit D is present across the entire Jammer Bay, but is often superimposed by unit A, B and C. It is occasionally exposed on the seafloor, coinciding with a stony seabed substrate.

The internal seismic facies of the unit are chaotic with medium to strong amplitudes (Figure 4.9). Parallel and continuous internal reflections can be found locally. Repetitive inclined internal reflections appear in some areas (Figure 4.10). This may be indicative of glaciotectonic thrust structures.

The top of the unit is often erosionally truncated by the base of the Holocene units. Erosional structures are rarely observed at the transition to the late glacial unit.

Sediment cores show a dominant lithology of glacial till, but meltwater sand and reworked interstadial-interglacial clay or chalk thrust slices can also be expected in this unit.

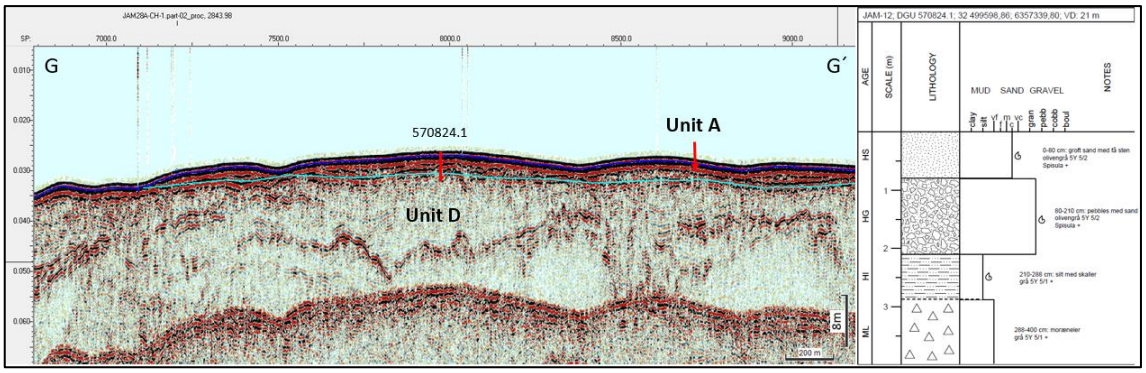

Figure 4.9: Sparker seismic example of glacial Unit D from the outer central part of Jammer Bay. Vibrocore 570824.1 (lower part) verifies a till composition. Location is shown on Figure 4.1.

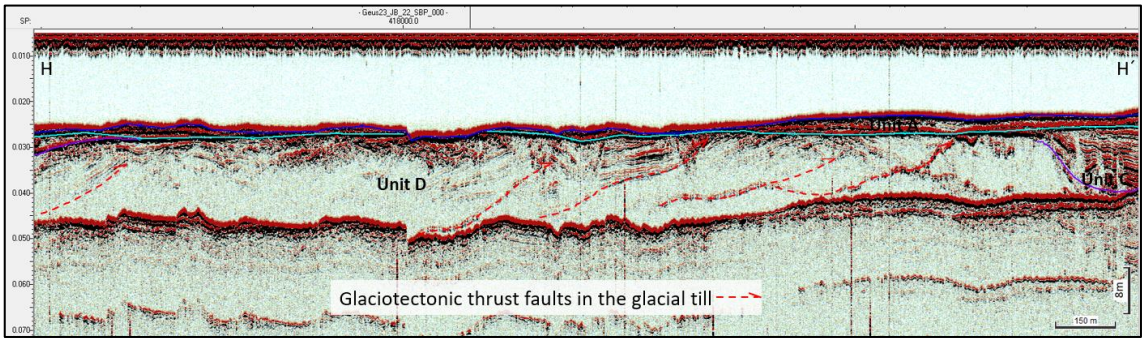

Figure 4.10: Seismic example of glacial Unit D characterised by glaciotectonic structures. Location is shown on Figure 4.1.

4.3.5 Unit E – Pre-quaternary deposits

In the southern part of Jammer Bay, a unit characterised by inclined or large scale folded layering with variable strong and weaker reflections is observed below the erosive base of glacial Unit D (Figure 4.11 and Figure 4.12). Based on deep seismic reflection data (Nielsen et al., 2008) and preliminary data from the GEUS-2023-Jammerbugt deep seismic CCS survey (Funck et al., 2023), Unit E represents pre-Quaternary deposits of Cretaceous chalk and in the southern part by Hanstholm, probably also Danian limestone.

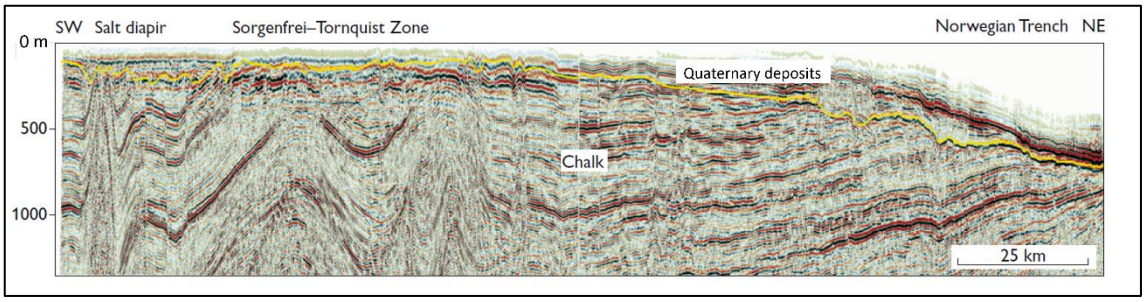

Figure 4.11: Deep-seismic profile along the outer part of Jammer Bay. The pre-Quaternary surface is marked by yellow trace (from Nielsen et al., 2008).

The unit appears relatively close to the seabed (0-10 m) in the southern part of Jammer Bay, where internal large fold structures can be observed. The fold structures are likely related to the deep-seated Sorgenfrei-Tornquist fault zone which crosses northern Jutland and the southern

Jammer Bay from SE to NW (Michelsen & Nielsen 1993; Nielsen et al. 2008). The base glacial/top pre-Quaternary surface appears less clear in the shallow seismic dataset towards the north due to increasing thickness of superimposed units and possible due to glaciotectonic modulation of the glacial/top pre-Quaternary boundary. Pedersen & Boldreel (2015) thus describes a glaciotectonic complex with thrust sheets of chalk identified on deep seismic sections in the outer part of Jammer Bay.

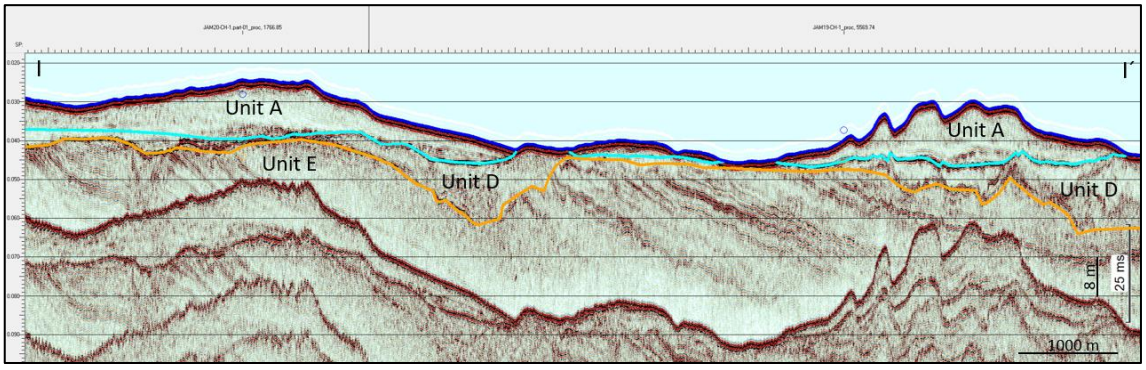

Figure 4.12: Sparker seismic section example from the southern Jammer Bay just north of Hanstholm. Inclined/folded layers of pre-Quaternary chalk/limestone are found close to the seabed. Location is shown on Figure 4.1.

4.4 Discussion and perspectives

Seismic interpretation of shallow seismic data substantiated by vibrocore ground truthing has created the backbone for development of a unifying geological model for the entire Jammer Bay area. Figure 4.13 shows a conceptual geological cross-sectional model with identified geological units A-E. The model explains the distribution of characteristic seismic/geological units in the context of existing knowledge of the late Quaternary geological history and related relative sea level changes in northern Denmark (Figure 4.14).

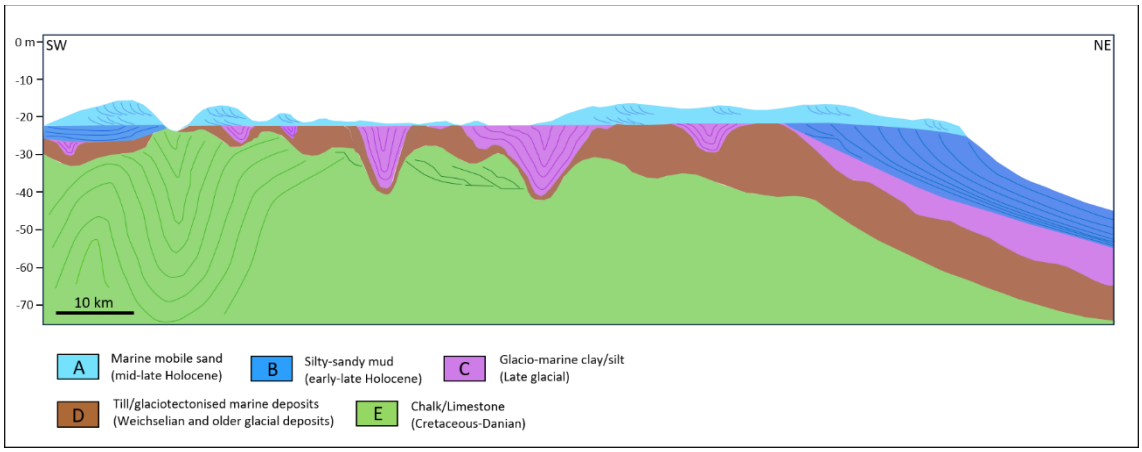

Figure 4.13: Conceptual geological cross-sectional model of Jammer Bay showing major stratigraphic units (A-E) in the upper c. 50 m below seabed.

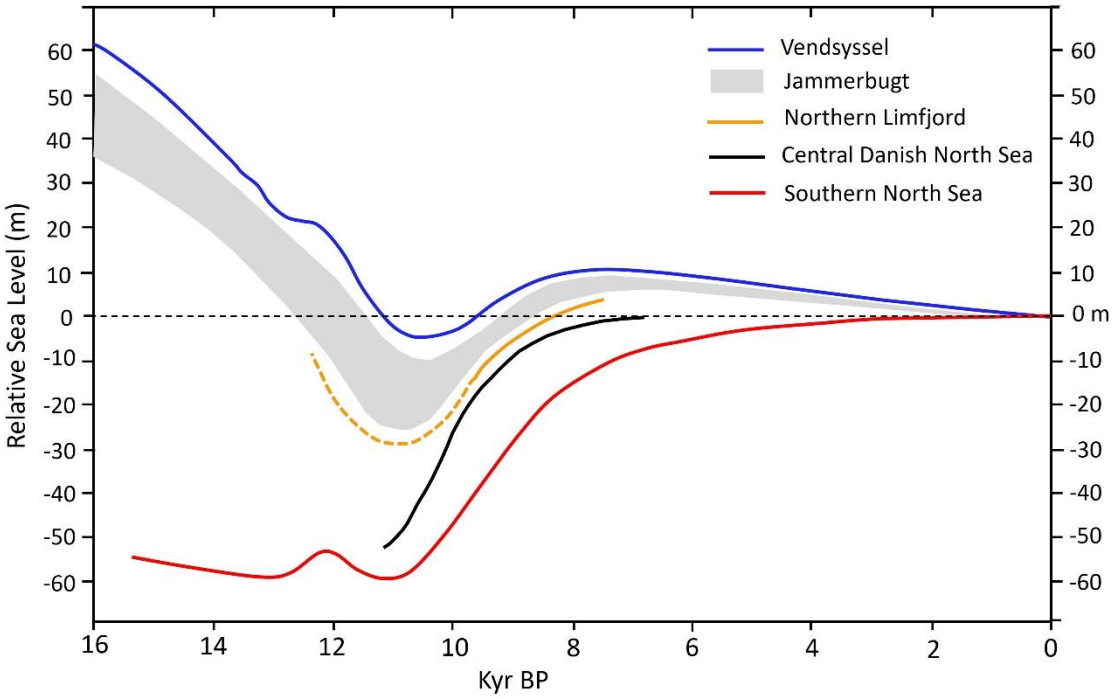

Figure 4.14: Overview of relative sea level curves (beach displacement) in different parts of the Danish North Sea over the last c. 16.000 yrs BP. from Påsse et al. (2005), Bennike et al. (2019), Astrup (2023). A tentative relative sea level interval for the Jammer Bay area is indicated.

Jammer Bay was covered by the Scandinavian ice sheet to about 18.000 BP, and earlier Weichselian ice sheet expansions and withdrawal over the area with intermittent periods dominated by glaciomarine conditions have created a complex glacial stratigraphy of unit D including both till deposits, meltwater deposits and glaciotectonised quaternary marine deposits and pre-Quaternary chalk deposits (cf. Larsen et al. 2009). As the Last Glacial Maximum ice sheet withdraw, the glacio-isostatically downpressed Jammer Bay area and the main part of North Jutland was covered by the Younger Yoldia Sea depositing late glacial Unit C consisting of a thick cover of fine grained glaciomarine sediments. The conformable nature of the late glacial fine-grained infill of depressions in the glacial surface supports that these were rapidly deposited during the earlier part of the late glacial period. Similar dated Younger Yoldia Sea marine sediments are found in the onshore Vendsyssel Formation (Larsen et al. 2009) and in the Skagerrak-Kattegat area (e.g. Morén et al. 2018).

Relative sea level estimates for northern part of Denmark suggest that the sea level initially was c. 50 m above the present level (Figure 4.13). From c. 18,000-11,500 BP (the late glacial period) glacio-isostatic rebound caused the relative sea level to fall to c. 20-25 m below the present sea level. Hereby the main shallower part of Jammer Bay became subaerially exposed in the earliest Holocene. As the Younger Yoldia Sea withdraw, local areas were likely characterized by erosion, reworking and sediment deposition confined to fluvial and lacustrine environments. Evidence of this is found in detailed studies of coastal outcrops by Nørre Lyngby between Lønstrup and Løkken (Brandes et al. 2018).

From about 10,000 BP, global eustatic sea level rise in connection to the final part of the deglaciation of the northern and southern hemisphere ice sheets overtook the local glacio-isostatic rebound in northern Denmark, and relative sea level rose c. 30 m in a few thousand years

(Littorina Sea transgression). The rapid transgression of Jammer Bay and the low-lying part of the present onshore North Jutland culminated at about 7,000 BP, c. 5-10 m above the present sea level. Marine sediments in Jammer Bay from the period 10,000-7,000 BP (Unit B) are mostly relatively fine-grained and preserved in lower troughs or along a prograding margin to the west and north of the shallower Jammer Bay area. The early Holocene unit B deposits in southern Jammer Bay likely represent distal deposits correlative to the Agger Clay unit found to the south of Jammer Bay outside and inside Nissum Bredning. As suggested for the Agger Clay deposition, it is likely that the tidal regime during that period was more pronounced. From About 7,000 BP, when relative sea level slowly began to fall again, the Jutland Current and the associated northward directed sand transport from south became much stronger (Leth 1996), due to opening of the English Channel and establishment of the present-day North Sea circulation pattern. Hereby strong erosion of underlying units and sand transport and deposition in large bar forms with superimposed smaller bed forms (Unit A) became dominant in Jammer Bay. The northward directed sand transport fed the progradation of the western and northern margin of Jammer Bay, where a large wedge of sandy and finer-grained sediment was deposited as unit B (clinoforms) and unit A (top layer sandy bedforms), increasing the area of shallower bathymetry in Jammer Bay considerable. Figure 4.15 gives an overview of the geological development of the Jammer Bay area in a stratigraphic scheme.

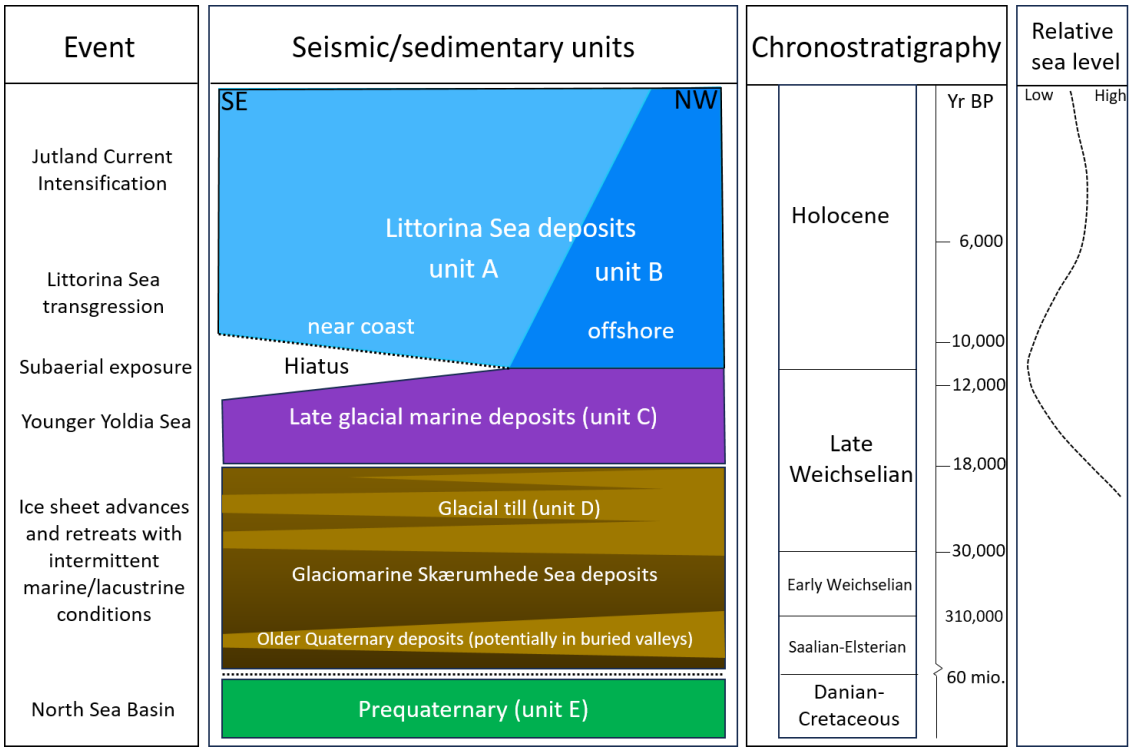

Figure 4.15. Stratigraphic scheme of the Jammer Bay area. Geological development.

Mapping of geological units and establishing a geological model create a data set that can explain major seabed surface features. E.g. where unit D till deposits become exposed, and lag gravels are found. However, the complex nature of unit D, occasionally consisting of glacially reworked older marine deposits without scattered larger stones or thrust fault units, also imply that detailed high-resolution studies are necessary to make a detailed shallow subsurface geology-seabed substrate type correlation.

This study has revealed that the shallower part of Jammer Bay has expanded considerably to the west and north, due to marine sediment transport and deposition along a growing wedge adjacent to higher-lying pre-Quaternary and glacial deposits. This explains the absence of lag gravels in a large part of the outer Jammer Bay. Only around Store Rev to the northwest, glacial and late glacial deposits become exposed at the seabed, creating a large isolated gravelly seabed, kept free of sedimentation by strong currents.

Even though that Jammer Bay and northern Jutland are still glacio-isostatically rising so that global sea level rise may have a relative smaller impact here, we know that considerable coastal erosion and retreat has taken place during historical times. The locally sourced sediment component must therefore also be taken into consideration, when bulk estimates of sediment erosion, transport, and deposition are made for the Jammer Bay area.

5. Seabed sediment thickness maps (Task 1.4)

Nicklas Christensen, Niels Nørgaard-Pedersen, Jørgen O. Leth, Sofie Kousted, Mikkel S. Andersen, Lars Ø. Hansen, Peter Sandersen, Zyad Al-Hamdani, Verner B. Ernstsen

5.1 Introduction and aim

The aim of Task 1.4 was to generate seabed sediment thickness maps based on sub-bottom profiler data.

The seabed of Jammer Bay is characterised by variable sandy, clayey and stony substrates. The substrate distribution is linked to the occurrence of subsurface glacial and late glacial units cut erosively and superimposed by a Mid-late Holocene sand layer of variable thickness (see Chapter 4). Detailed shallow seismic mapping of characteristic sediment units and coring makes it possible to map out the thickness of the different geological units in 2D and 3D.

In the following, we describe the methods used for the construction of thickness maps for the widespread occurring Mid-late Holocene sand layer unit and the late glacial unit, which typically is confined to infill of valleys or channel like features embedded in the glacial surface.

5.2 Materials and methods

Seismic data from new and existing surveys were processed and interpreted by tracing major seismic boundaries, corresponding to seismic unit tops and/or bases (see Chapter 4). The following units were identified: Pre-Quaternary, Glacial, Late Glacial, Early Holocene and Mid-late Holocene.
To determine thickness of the individual units, the first step was to grid the traced horizons (xyz data), as presented in Table 4.2. This was done in the IHS Kingdom suite with the flex gridding algorithm. The gridding parameters were set to minimum curvature and halfway smoothness. The horizon grids are dependent on data points, and since the seismic lines were spread widely across the Jammer Bay area, the data density influences the reliability of the interpolated grids. Hence, wider seismic line spacing means higher uncertainty in the interpolated grids.
The horizon grids were converted from two-way-traveltime to depth with the formula:

$$depth[m] = \left(\frac{two - way - traveltime[s]}{2}\right) * velocity[\frac{m}{s}]$$

The average velocity was estimated to be 1,600 m/s for the sediments above the glacial till. The unit thickness can readily be calculated by subtracting the lower and upper depth converted horizon grid from each other.

5.3 Results

Detailed and reliable thickness maps of unit A and C were calculated in the Focus area where the line spacing is 200 m. The depths and thickness maps are however less detailed with higher uncertainties due to a higher and more widespread line spacing outside of the Focus area. It

was not possible to calculate reliable thicknesses for these two units (A & C) in the northern part of the Screening area due to low seismic penetration and poor data coverage. It was not possible to calculate thickness maps of unit B, D or E due to the limited seismic penetration with the available Sparker and sub-bottom profiler data.

5.3.1 Unit A – Mid-late Holocene sand deposits

A 3D depth-converted surface of the lower (light blue) and upper (dark blue) horizon of the unit was created in the Focus area where the line spacing is 200 m.
Figure 5.1 shows the upper horizon that follows the seafloor, while Figure 5.2 shows the erosional planar horizon (light blue). The surface dips towards the northwest and has a few linear morphological features with a SE-NW orientation.

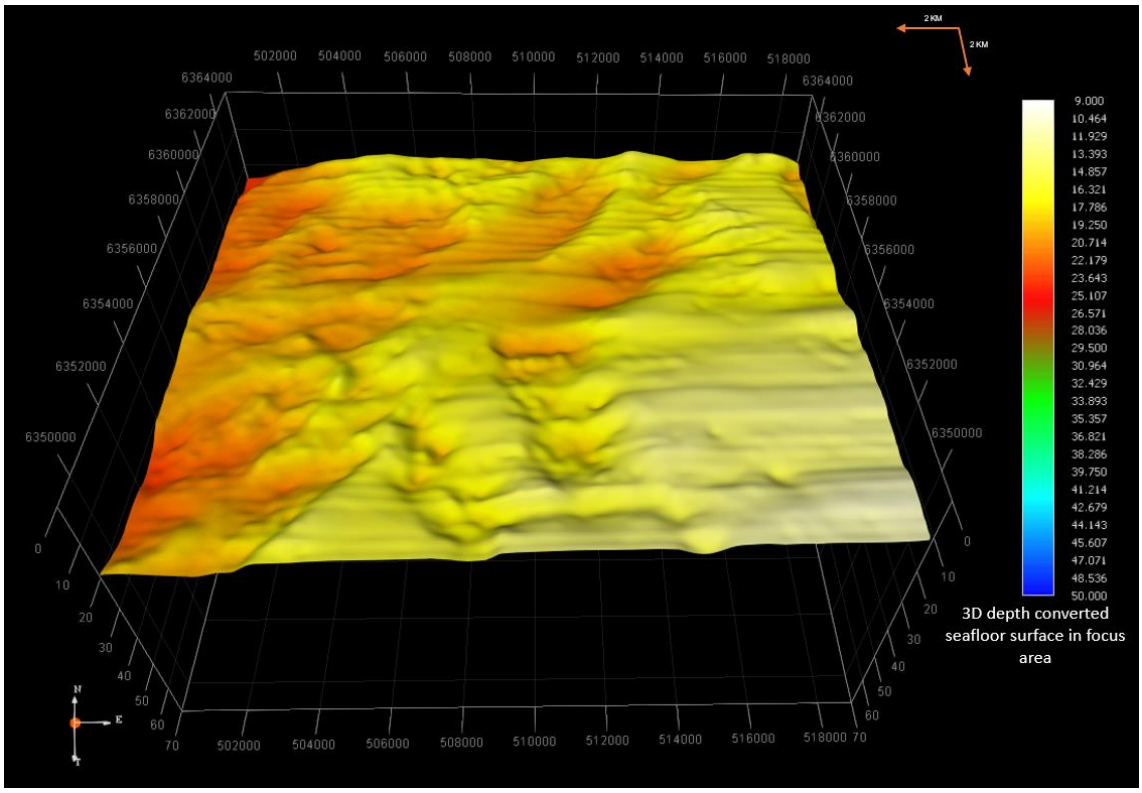

Figure 5.1: The 3D depth-converted seafloor surface in the Focus area. Z-scale is in meters.

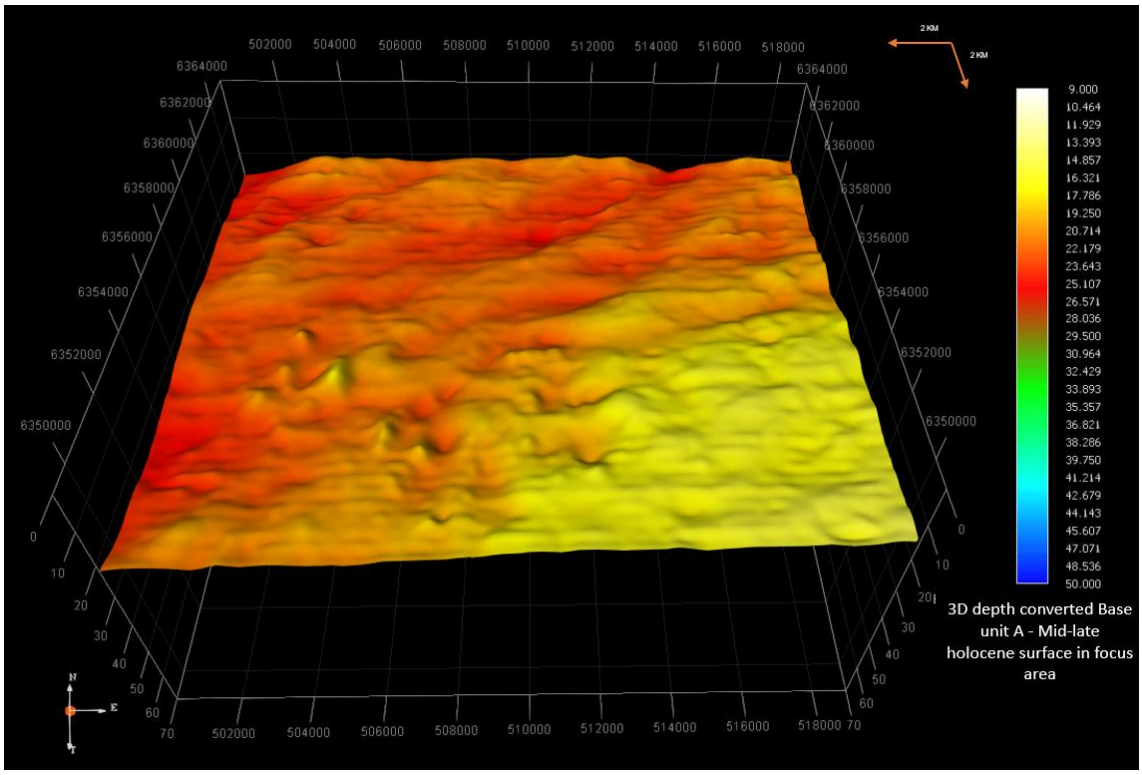

Figure 5.2: The 3D depth-converted base unit A surface. The surface has 3 linear features with a NE-SW orientation. Z-scale is in meters.

The thickness map of unit A (Figure 5.3), has a variable cell size depending on seismic data coverage. The cell size in the Focus area is down to 20 m, which gives a high resolution of the thickness variations. The cell size in the Screening area is 200 m, which gives a less detailed resolution of the thickness variations. The map shows the main depositional trends in the mid-late Holocene sand unit.

Large sand layers often covered by large bedforms are found widespread in Jammer Bay. The thickness map reveals that the sand layers are particularly thick (10-15 m) in the southern part and along the northwestern margin of Jammer Bay. Less thick sand layers (c. 5 m) occur in the shallower central part of Jammer Bay. Large parts of the intermediate depth and central part of Jammer Bay, including the Focus area, show smaller and less thick (< 5m) isolated sand layers with intervening areas, where late glacial and glacial units are found close to the seabed. To the northwest outside Lønstrup and Hanstholm a large area appears to be almost devoid of sand deposits, and the seabed is characterised by glacial and late glacial sediments exposed at the seabed, giving origin to a large concentration of gravelly lag deposits.

Unit A is not present in the few available lines north of the gridded area, and Unit B is exposed directly on the seafloor. Exceptions can be found at Store Rev in the northeastern corner of the Screening area. At Store Rev, Unit D (glacial till) is directly exposed on the seafloor (cf. Figure 5.7). The seismic line (D D´) is located at the western border to Store Rev, and the width and height of the structure increases northeast of the line.

Figure 5.4, Figure 5.5 and Figure 5.6 show three seismic lines, and the locations of these are marked on Figure 5.3.

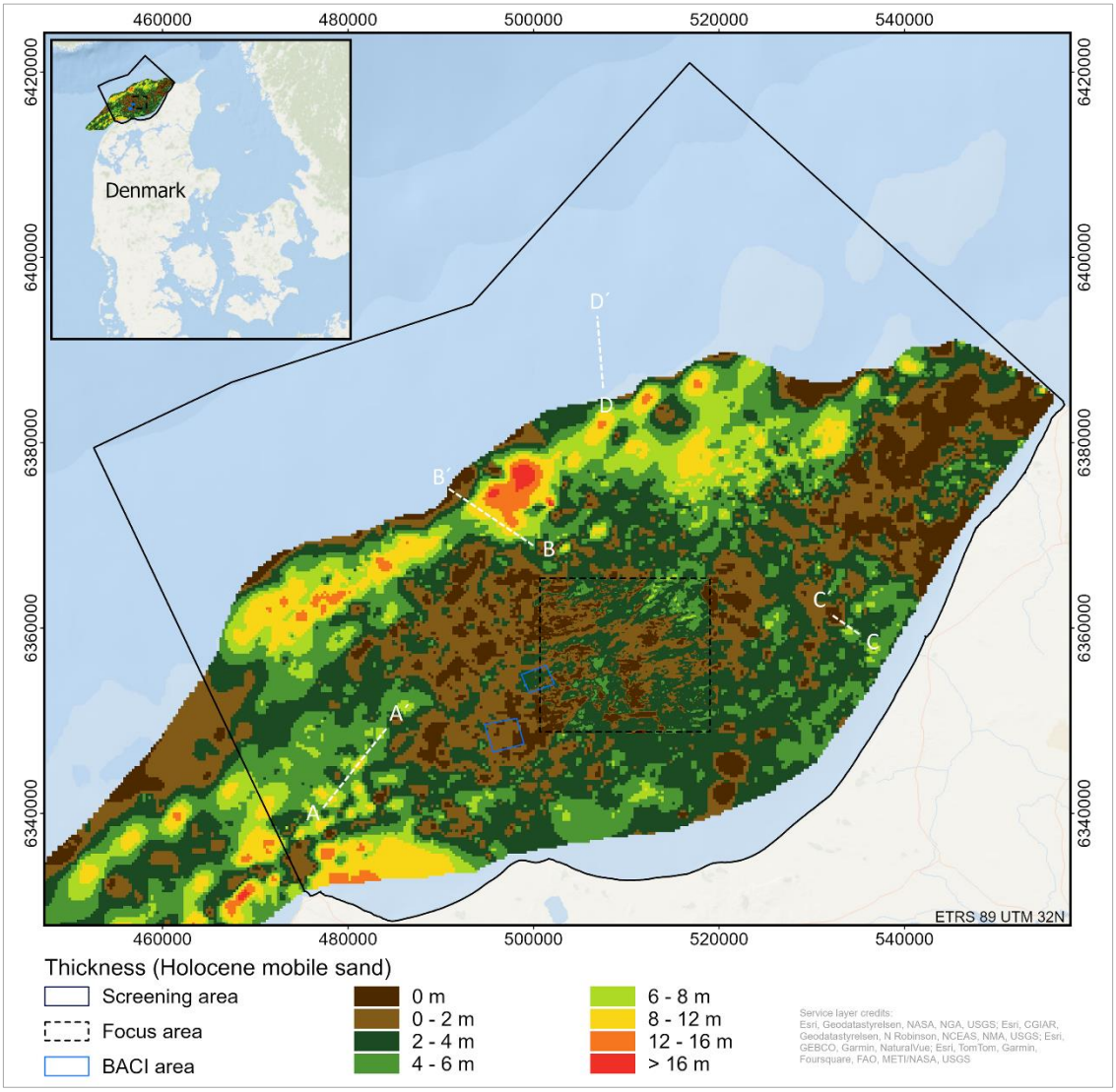

Figure 5.3: Thickness map of the mid-late Holocene sand unit A. In the Focus area is the cell size 20 m, and in the Screening area is the cell size 200 m. The location of the following 4 seismic lines (Figure 5.4, Figure 5.5, Figure 5.6 and Figure 5.7) is marked with white striped lines.

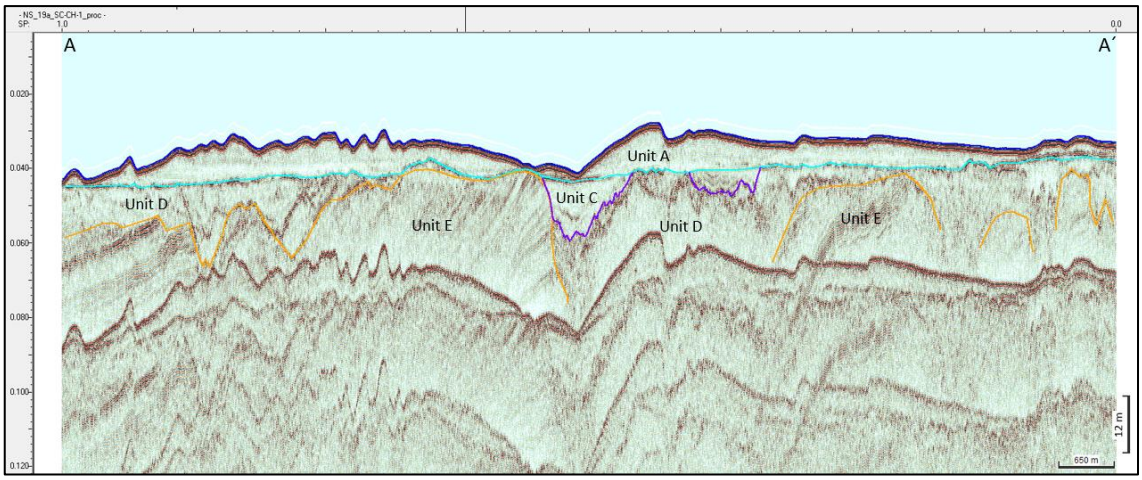

Figure 5.4: A Sparker seismic line close to Hanstholm. The sand dunes are up to 10 meter thick on the line. The line shows where the pre-quarternary (unit E) is very close to seafloor in the absence of unit A. Location is shown on Figure 5.3.

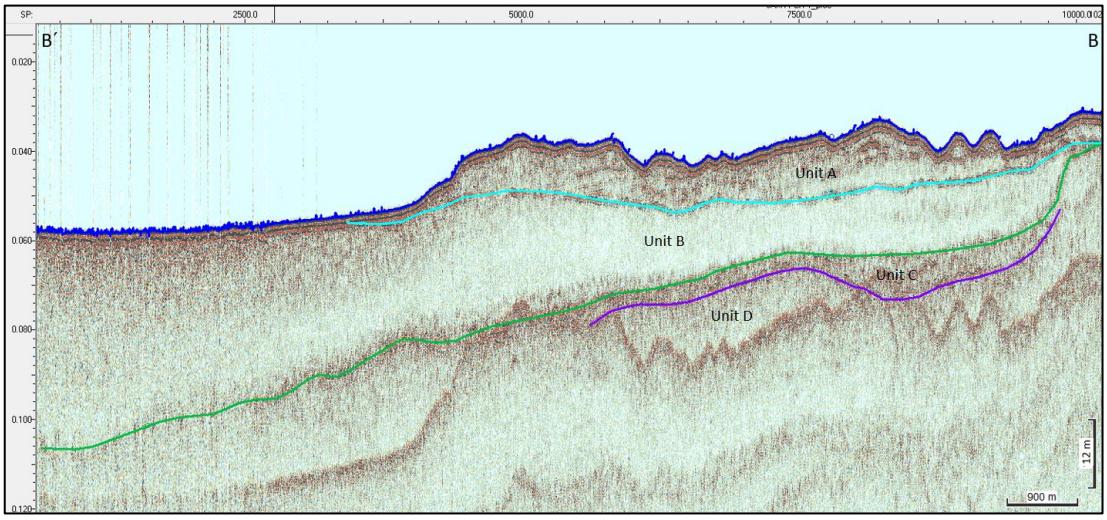

Figure 5.5: The location of the Sparker seismic line is close to the grid border, where unit A is up to 18 meter thick. The unit is not present north of the grid border, and unit B is exposed directly on the seafloor. Location is shown on Figure 5.3.

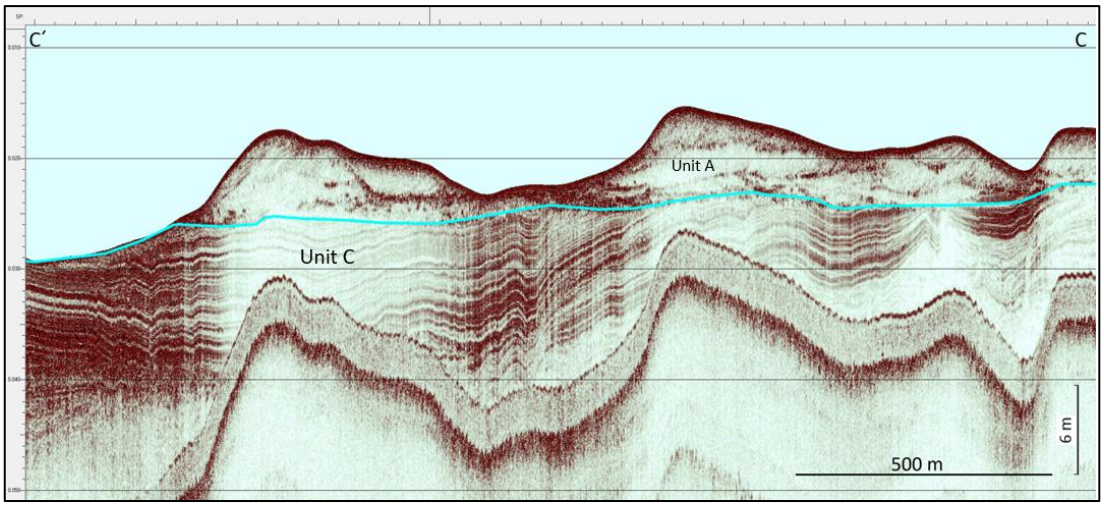

Figure 5.6: A Sub-bottom-profiler line close to Løkken. The line displays the sand dune morphology of the unit, and an example where unit C is directly exposed on the seafloor in the absence of unit A. Location is shown on Figure 5.3.

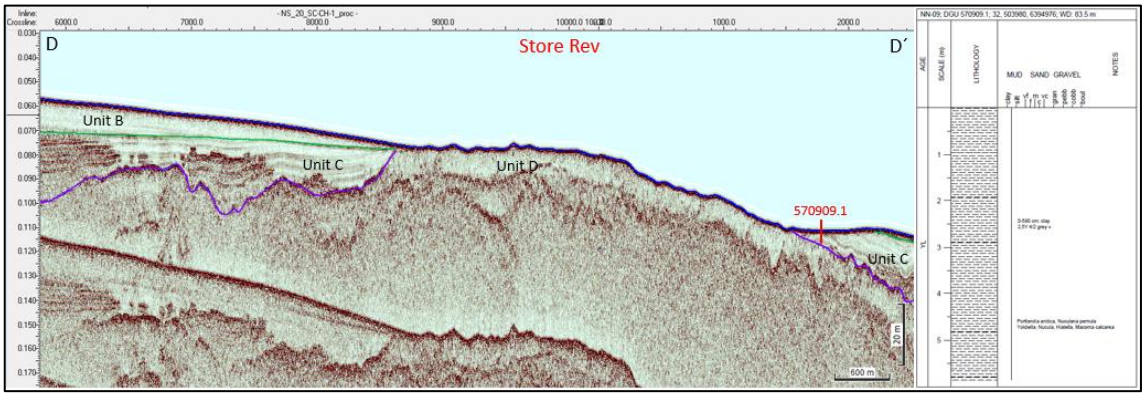

Figure 5.7: Sparker seismic line at the western border to Store Rev, location is shown on Figure 5.3. Unit D is directly exposed on the seafloor at Store Rev.

5.3.2 Unit C – Late Glacial deposits

A 3D surface of the base Late Glacial unit (purple) was created in the Focus area, where the linespacing was 200 m. The 3D surface reveals a large branching valley or channel system infilled with up to 20-30 m of glacio-marine late glacial deposits. The most prominent channel has a maximum width of 3 km and an increasing depth towards west. The orientation of the channel changes from NE-SW in east to E-W in west.

The 3D surface of the top horizon (light blue) is shown in Figure 5.2 and described in section 5.3.1. Any correlation between the two 3D surfaces is hardly visible since the top horizon is an erosional surface.

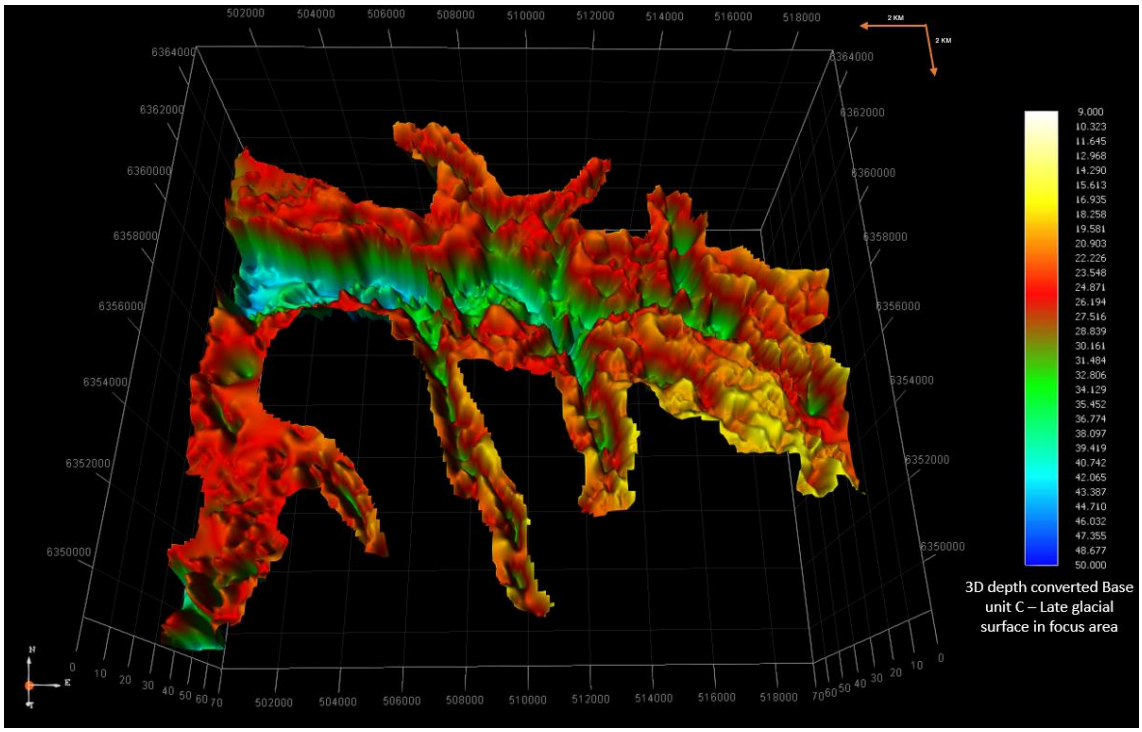

Figure 5.8: 3D surface of the base (purple) horizon of Unit C in the Focus area. The 3D surface reveals a large branching valley or channel system. The Z-scale is in meters.

The thickness map of unit C (Figure 5.9) has the same variable cell size as the thickness map of unit A (Figure 5.3), which is dependent on the available seismic lines. The cell size is 20 m in the Focus area and 200 m in the Screening area.

The spatial thickness distribution reveals the same depositional trend as the 3D surface, where the late glacial unit C is infilled in large, elongated depressions in the top glacial surface. The unit is a conform infill unit superimposed by unit B north of the grid area. It was not possible to create a satisfying thickness map north of the grid border due to a limited amount of high-quality Sparker seismic lines. On the available lines north of the grid, the unit is often not visible due to a thick unit B with shallow gas, but presence of the unit is expected.

East of the Focus area, the grid suffers from a limited amount of Sparker seismic lines. The available data consist mainly of sub-bottom profiler lines. The data have a limited penetration, as explained in Figure 4.2, and the Late glacial unit can rarely be observed if it is superimposed by 6-8 meter of Holocene mobile sand (unit A). Because of this issue, the thickness map shows the late glacial unit as deposited in isolated basins, but these might be connected.

Figure 5.10, Figure 5.11, and Figure 5.12 show three seismic lines, and the location of these are marked on Figure 5.9.

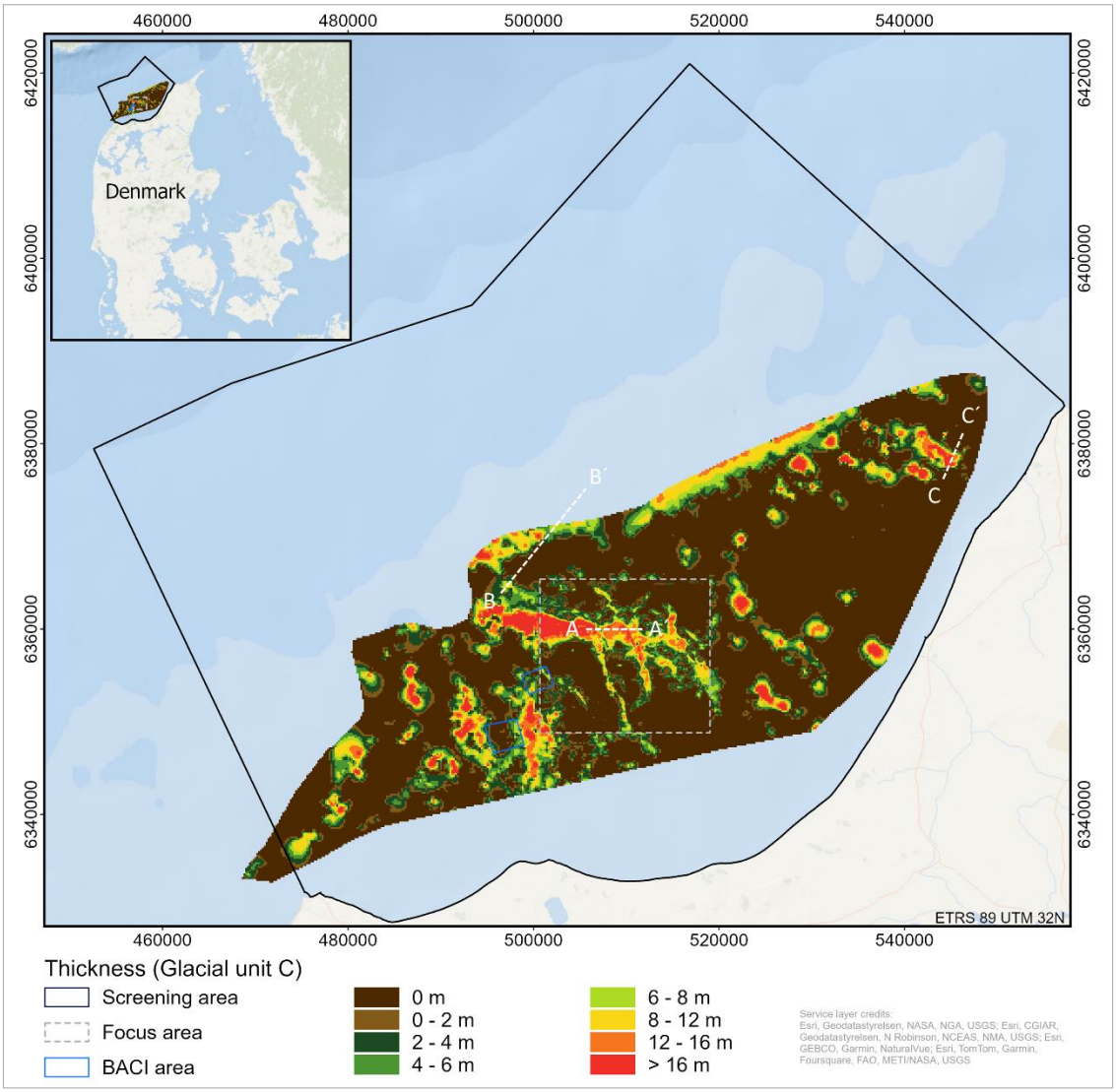

Figure 5.9: Thickness map of the glacial unit C. In the Focus area, the cell size is 20 m, and in the Screening area, the cell size is 200 m. The location of the following 3 seismic lines (Figure 5.10, Figure 5.11 and Figure 5.12) is marked with white striped lines.

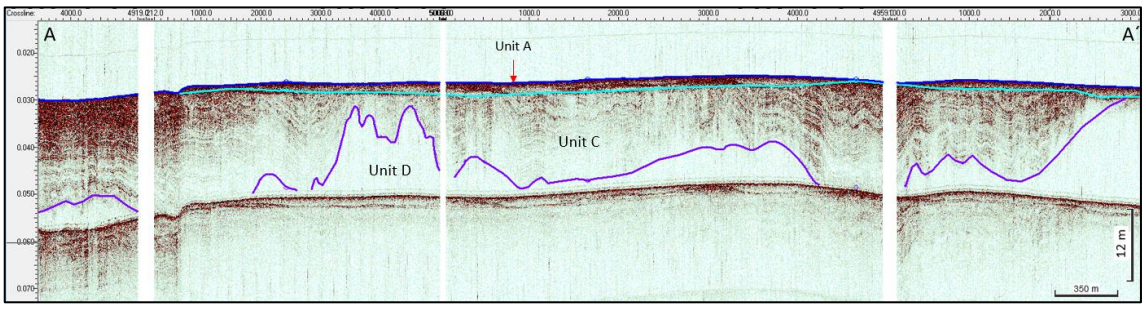

Figure 5.10: Sub-bottom profiler line from Focus area. The location is shown on Figure 5.9. The seismic line shows the conform unit with parallel low to high amplitude internal reflections.

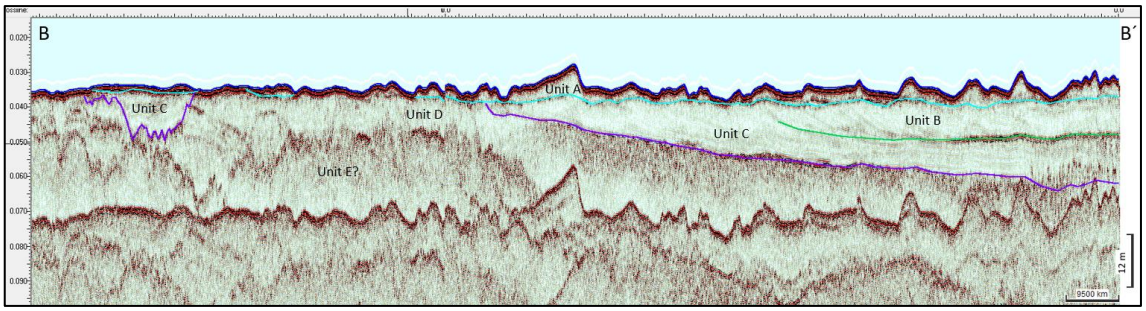

Figure 5.11: High quality Sparker seismic line at the grid border (location is shown on Figure 5.9). The bottom (purple) horizon can usually not be traced below a thick unit B with shallow gas north of the grid border.

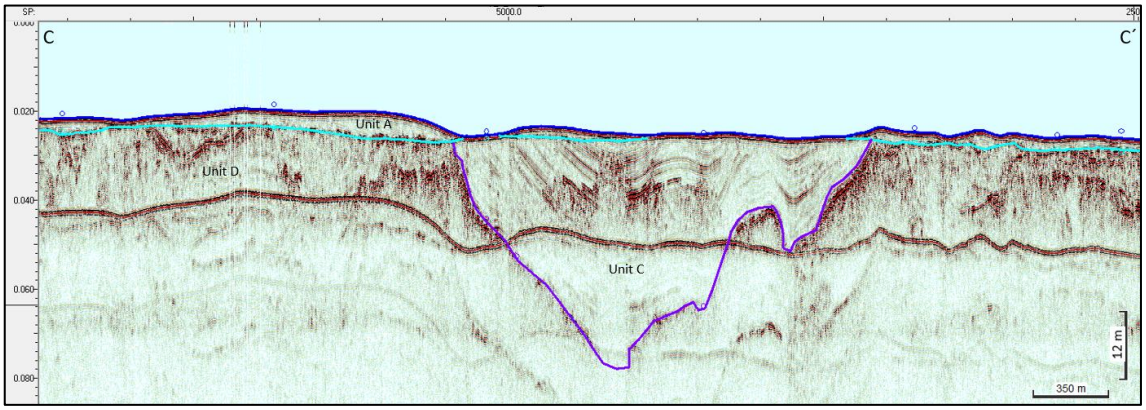

Figure 5.12: Sparker seismic line close to Hirtshals, location is shown on Figure 5.9. The line reveals a 40 meter deep valley infilled with the late glacial unit C.

5.4 Discussion and perspectives

By mapping the thickness of characteristic shallow subsurface sediment units with a different geological origin, we can better explain the formation of the units and the distribution of seabed substrates and morphological features at the seabed surface.

Mapping the thickness of late glacial typically fine-grained sediments showed that they appear to be confined to valley-like depressions in the glacial landscape. High data density in the Focus area and parts of the surrounding area made it possible to map a large late glacial infilled valley or channel with smaller bifurcations reminiscent of a fluvial drainage system. The late glacial infill is assumed to represent glaciomarine sediments deposited during relatively high sea level due to the dominant conform character of the fine stratified sediment infill in the valley system. The late glacial sediments probably once covered the whole Jammer Bay area and were later eroded during the sea level low stand in early Holocene, and only preserved in depressions in the glacial landscape. We cannot rule out that the depressions in the glacial landscape found in the Jammer Bay are so called buried glacial valleys that are formed subglacially at glacier margins by over-pressured meltwater. Such valley systems have been found in many places in the North Sea and on land (Sandersen et al. 2009; Andersen et al. 2012).

The spatial thickness distribution of the Mid-late Holocene sand (unit A) in the Jammer Bay shows large coherent areas of thick sand layers and other areas almost devoid of sand. The

spatial distribution probably reflects areas of prolonged sand deposition and other areas dominated by erosion and sediment transport and bypassing. The large and thick sand layer structures on the northwestern margin of Jammer Bay appear in the mid-late Holocene to have built out on top of the advancing wedge of clinoform structures found on the slope towards deeper water, where accommodation space was available. The large elongate sand layer structures found in the southern Jammer Bay off Hanstholm are in many aspects similar to the elongate sandbanks found in Læsø Rende. The core of the elongate sand structures may originate from earlier in Holocene when the tidal regime may have had more influence on sediment transport and deposition along the northwestern part of Jutland. Large areas in the central Jammer Bay and off Lønstrup and Hirtshals that are characterised by relatively small and thin sand layers with intervening areas of glacial till and late glacial clayey sediments right under the seabed are exposed to erosion and sediment transport and bypassing. The Jutland current transports sediment into the Jammer Bay from south, but coastal erosion along the Jammer Bay coast (2-3 m/year at Lønstrup (Brandes et al. 2018)) must also be assumed to be an important source of sediment.

6. Bathymetric maps (Task 1.5)

Lars Ø. Hansen, Mikkel S. Andersen, Zyad Al-Hamdani, Nicklas Christensen, Verner B. Ernstsen

6.1 Introduction and aim

The aim of Task 1.5 was to generate bathymetric maps based on multibeam echosounder (MBES) data. Bathymetric models, or Digital Elevation Models (DEMs), provide information on depth. From the bathymetric models, morphometric and morphological models were generated which are central in relation to e.g. substrate and habitat mapping as well as geomorphological interpretation and mapping. The models of bathymetry, morphometry, and morphology serve as direct support for the substrate and habitat interpretations and mapping as described in tasks 1.7 and 1.8.

6.2 Materials and methods

The accepted soundings exported in ascii xyz format served as input for production of raster DEMs. The Coordinate Reference System (CRS) used for the DEMs was the *European Terrestrial Reference System* (ETRS89) with the projected coordinate system *Universal Transverse Mercator* (UTM) zone 32 N. The vertical reference was the *Danish Vertical Reference 1990* (DVR90). The DEM z-values were computed as the mean of all point z-values within each raster grid cell. The actual grid cell size of the DEMs were determined from considerations of point density, along-track sounding spacing, and beam footprint size.

Point density was determined from a preliminary sounding density model (1 m x 1 m grid cell resolution) generated in QPS Qimera providing information on number of soundings/m^2.

Along-track resolution (or sounding spacing) is constrained by the inter-ping distance (i.e., only one ping is present in the water column at a time) and is a function of water depth and vessel speed (Hughes-Clarke et al. 1996). The outer beam range is thus the limiting factor of the ping rate. The ping rate is equal to *1 / two-way travel time,* where the two-way travel time is equal to *2*range* divided by the *speed of sound.*

The along-track resolution was determined as vessel speed divided by the ping rate.

The beam footprint is the beam-ensonified area on the seabed. Beam geometry causes an increase in footprint size from nadir toward the outer swath beam. For simplicity, footprint sizes of the nadir beam and outer swath beam were computed, based on equiangular beam spacing, as:

Footprint across-track and along-track at nadir:

$$\tan A = \frac{a}{b} \rightarrow a = \tan A * b$$

$$a = \tan(0.5 * A) * b * 2$$

where *a* (footprint diameter) is the opposite and *b* (depth) is the adjacent line to the angle *A* (beam width).

Outer beam across-track footprint:

$$a = b * \tan A - b * \tan A_1$$

Outer beam along-track footprint:

$$\cos A = \frac{b}{c} \rightarrow c = \frac{b}{\cos A}$$

$$a = c * \tan A$$

$$a = 2 * c * \tan(0.5 * A)$$

where *c* is the hypotenuse or the outer range of the swath.

Production of the DEMs were carried out in ArcGIS Pro following the workflow shown in Figure 3.1. The ascii files were converted to las file format (.las) using LAStools which is an add-on toolbox developed by rapidlasso GmbH. The las files were linked by creating a las dataset from which the raster DEMs were created using the *las dataset to raster* tool.

6.3 Results

The grid cell size of the DEMs were determined from considerations of point density, along-track sounding spacing, and beam footprint size. The point density statistics along the lines associated with the Focus area had a mean value of 75 soundings/m^2 with a standard deviation of 45. The along-track resolution was 0.25 m based on a swath width of 130°, a water depth of 28 m, a sound speed of 1,485 m/s, and a vessel speed of 5.5 knots. The computed beam footprint diameters along-track and across-track at nadir and at the outer beam are shown in Table 6.1.

Table 6.1: Computed beam footprint diameters at the nadir beam and at the outer beam.

	Nadir footprint diameter (m)	Outer beam footprint diameter (m)
Across-track	0.22	1.21
Along-track	0.44	1.04

Based on these results, the DEMs were produced with a grid cell size of 1 m x 1 m in both the Focus area and the Screening area. Furthermore, DEMs with 10 m grid cell resolution were produced as support for the delineation of sandbanks in task 1.8.

The entire Screening area is shown in Figure 6.1. The mapped depths span from approximately -6 m to -150 m DVR90. Zoom-in of the Focus area bathymetry is shown in Figure 6.2. The mapped depths in the Focus area are between -11 m and -29 m DVR90.

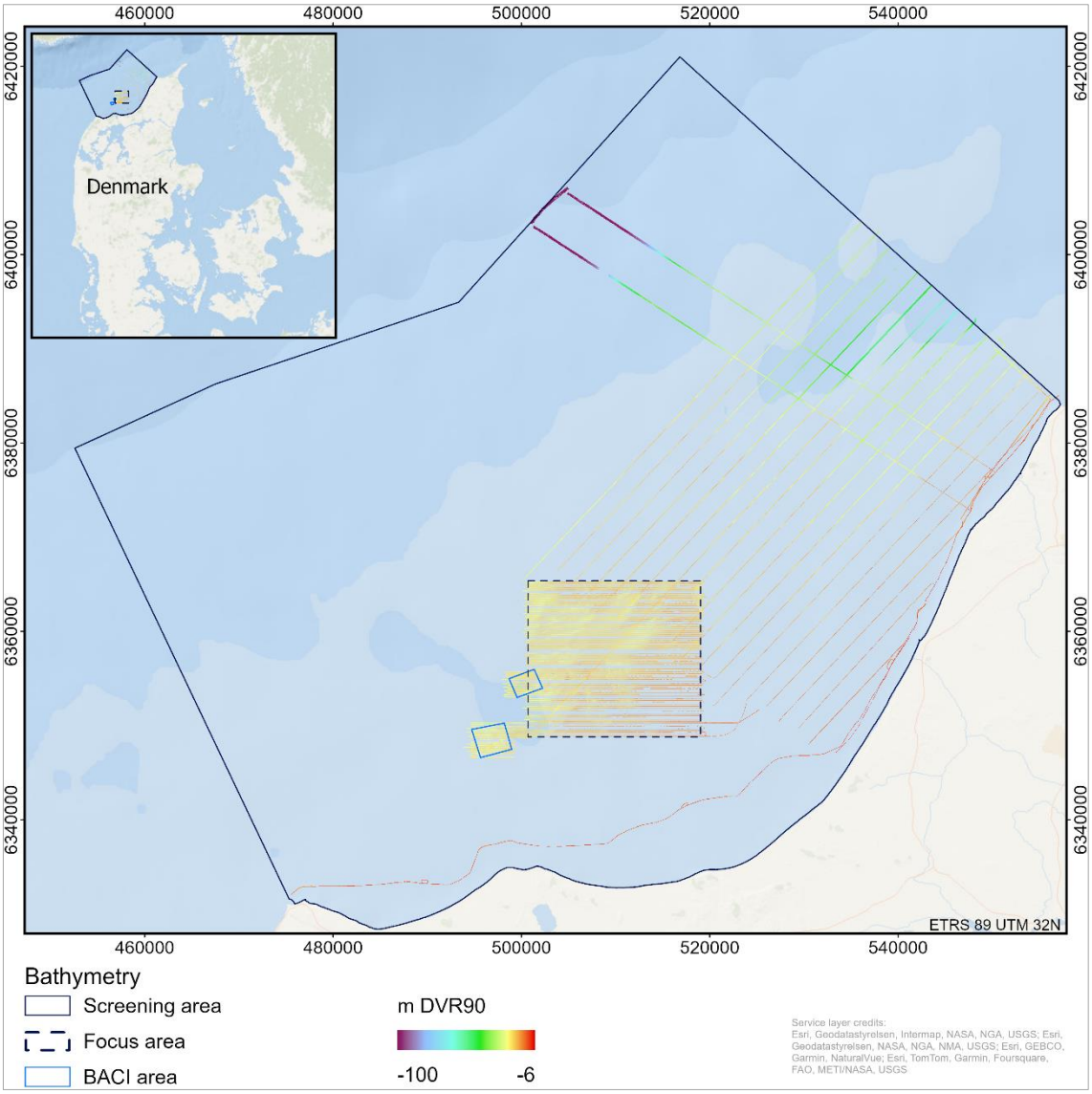

Figure 6.1: Bathymetric map of the Screening area and the Focus area (1 m x 1 m grid cell resolution).

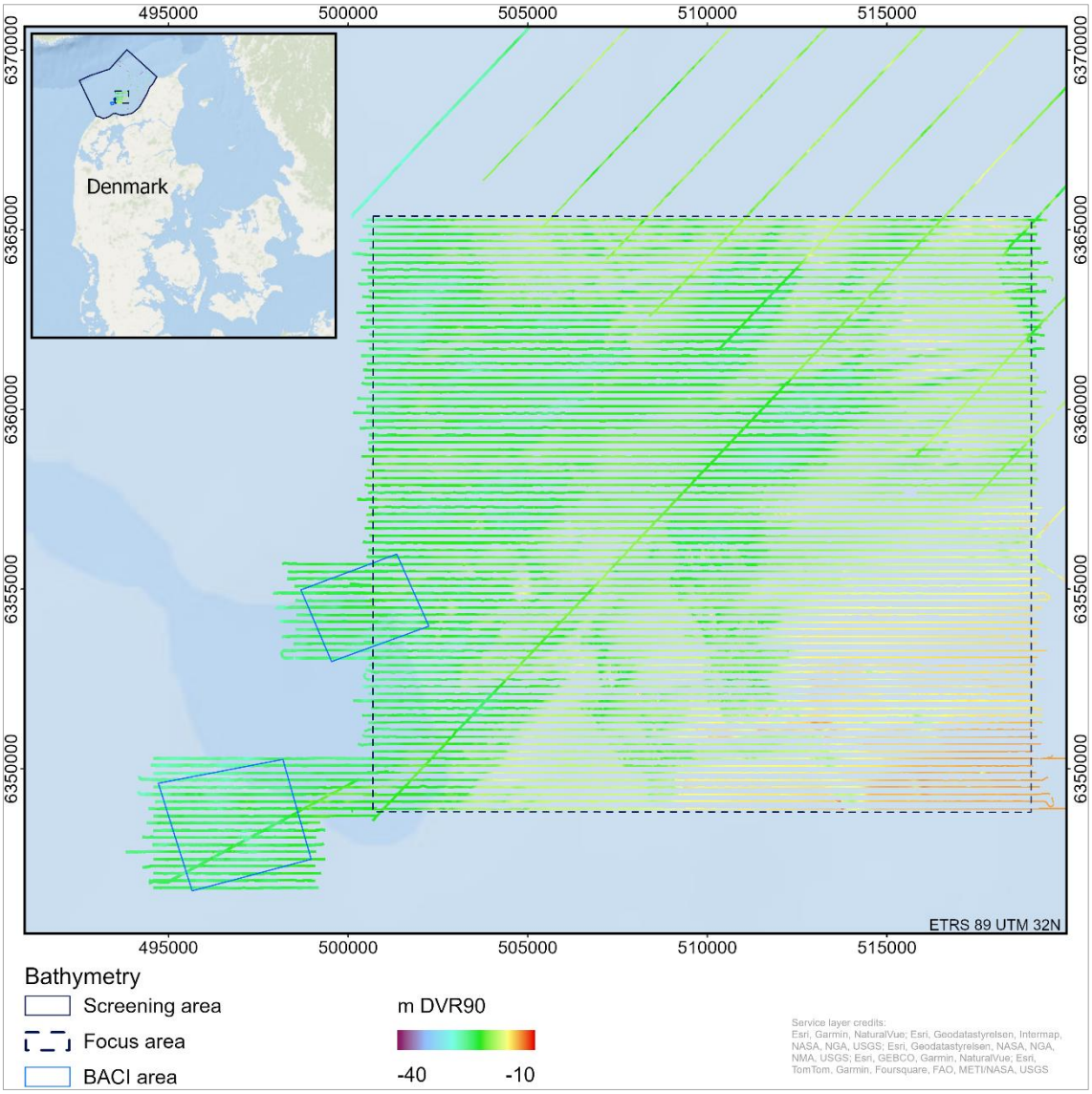

Figure 6.2: Bathymetric map of the Focus area (1 m x 1 m grid cell resolution).

6.4 Discussion and perspectives

The DEMs are derived by merging discrete swath corridors of MBES data. Surface attributes derived from these DEMs provide valuable information for analysing seabed characteristics. However, the imaging geometry of the MBES impacts the accuracy and resolution of the DEMs and needs to be considered. The imaging geometry consists of range, angle, azimuth, point density, and overlap attributes which are impacted by the sonar configuration relating to e.g. beam widths, beam spacing, vessel speed and stability. Superimposed are effects related to ancillary sensor integration and oceanographic conditions. Each of these components affect the minimum resolvable scale of morphological features (Hughes-Clarke 2018).

We estimated an appropriate DEM resolution (1 m x 1 m) based on point density, along-track resolution, and beam footprint sizes in the Focus area to preserve the finer scale morphology in the shallower parts of the DEMs. The trade-off is that the grid cell resolution in the deeper areas is higher than the imaging geometry “permits”. This is not necessarily a problem, but it means

that the minimum resolvable features do not correspond to the DEM resolution, and needs to be considered, when analysing seabed characteristics.

This large dataset of bathymetric data provides a baseline for high resolution morphodynamic analyses in the shallower parts of the DEM and for broad scale morphodynamic analyses in the deeper areas.

7. Seabed morphometric and morphological maps (Task 1.6)

Lars Ø. Hansen, Mikkel S. Andersen, Zyad Al-Hamdani, Verner B. Ernstsen

7.1 Introduction and aim

The aim of Task 1.6 was to generate seabed morphometric and morphological maps based on multibeam echosounder (MBES) data, supported by side scan sonar (SSS) and sub-bottom profiler (SBP) data to provide characterisation of seabed geometry and as support for the substrate and habitat interpretations and mapping as described in tasks 1.7 and 1.8. Geomorphometry is the quantitative study of topography. A raster DEM is often the fundamental input in a geomorphometric analysis, i.e. a system of quadratic grid cells in cartesian space each representing an approximation of a specific section of the land surface by an attributed value. Hence, the technical properties related to spatial analysis are primarily controlled by the grid cell size, i.e. the spatial resolution of the raster grid. Two distinct DEM-derived entities are surface parameters and surface objects (Pike et al. 2009). These entities can provide information for the delineation and characterization of benthic habitats (Wilson et al. 2007). A surface parameter is a measure of surface form such as slope, curvature, aspect, or roughness. Whereas a surface object is a discrete spatial feature such as a ridge or depression.

7.2 Materials and methods

DEM-derived surface parameters of slope, curvature, and aspect were produced in ArcGIS Pro using the *surface parameters* tool in the Spatial Analyst toolbox. Slope is a measure of the rate of change in elevation. Slope was computed using a quadratic surface function with a 3 x 3 cell neighbourhood. Aspect is a measure of the downslope direction with the maximum rate of change. Aspect was computed using a quadratic surface function with a 3 x 3 cell neighbourhood measuring the slope orientation in positive degrees (0° – 359.9°) clockwise from North. Curvature is referred to as the slope-of-slope and measures the convexity/concavity of the surface. Two types of curvature were computed i.e., profile curvature, which is parallel to the direction of maximum slope, describing the rate of change of slope, and the tangential curvature, which measures the curvature perpendicular to the direction of maximum slope.
Curvatures were computed using a quadratic surface function with a 3 x 3 cell neighbourhood.

Features of the seabed was mapped using a semi-automated geomorphometric approach to landform mapping i.e., Geomorphon Landforms tool in ArcGIS Pro. The geomorphon landform classification was introduced by Jasiewicz and Stepinski (2013) and applies an algorithm that combines elevation differences and visibility concepts to classify terrain into 10 different landforms, i.e. morphological features. The classification is based on the bathymetric model and requires definitions of a flat terrain angle threshold in degrees, a search distance radius of the analysis window, and optionally a skip distance radius (i.e. the distance away from the target cell to where the analysis area begins). Here we applied a flat terrain threshold angle of 1.2°, a search distance radius of 20 cells, and a skip distance, or inner radius of the annulus shaped analysis window, of 1 cell.

7.3 Results

Here we present the results of the morphometric analyses derived from the bathymetric models (1 m grid cell resolution) for the Focus area i.e., slope (Figure 7.1), aspect (Figure 7.2), profile curvature (Figure 7.3), and tangential curvature (Figure 7.4). A slope model with a 10 m x 10 m grid cell resolution was also produced. This model was used as support for delineating sand-banks in task 1.8.

The morphological feature classification with the Geomorphon Landforms method is shown in Figure 7.5.

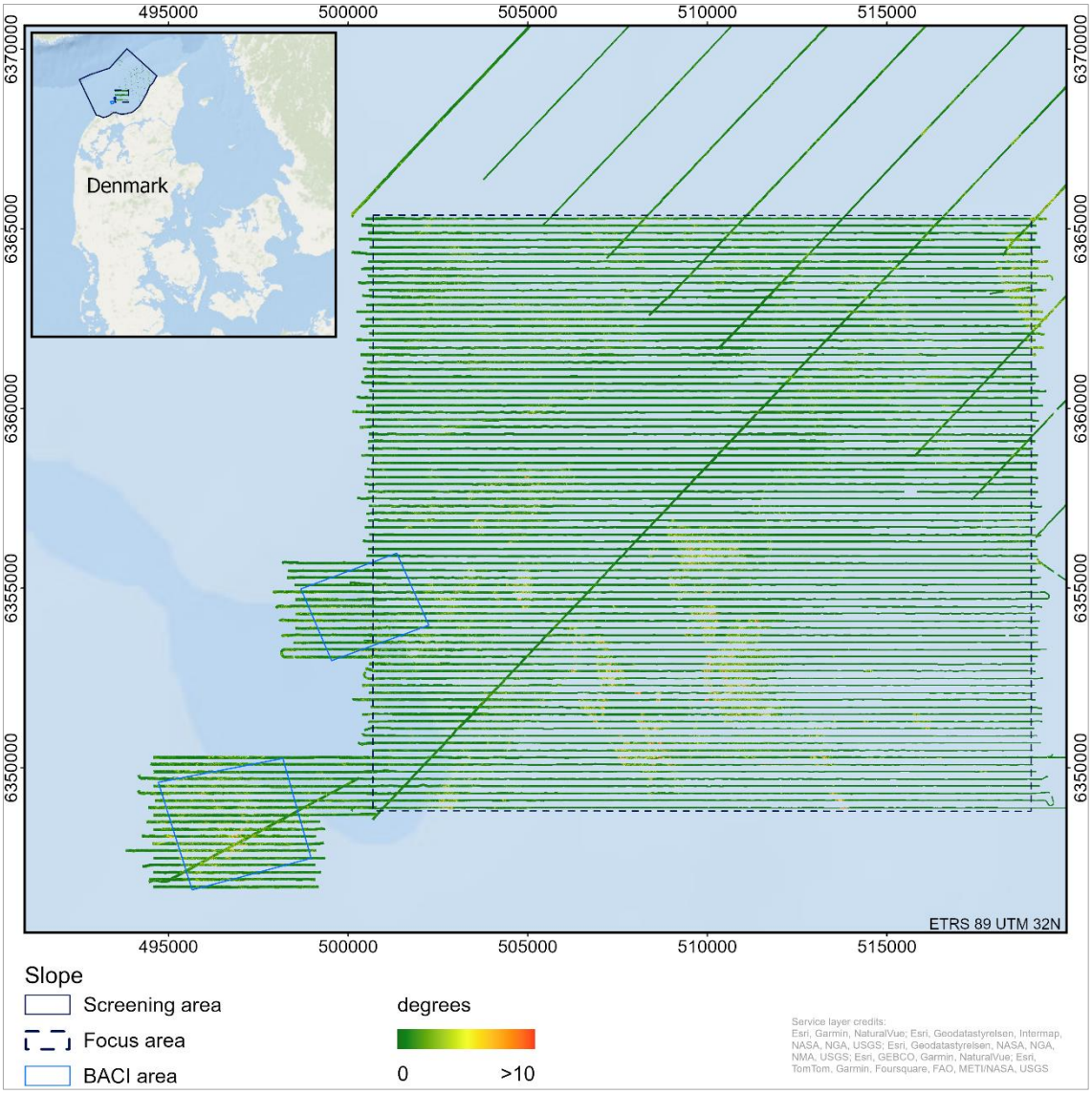

Figure 7.1: Slope map of the Focus area (1 m x 1 m grid cell resolution).

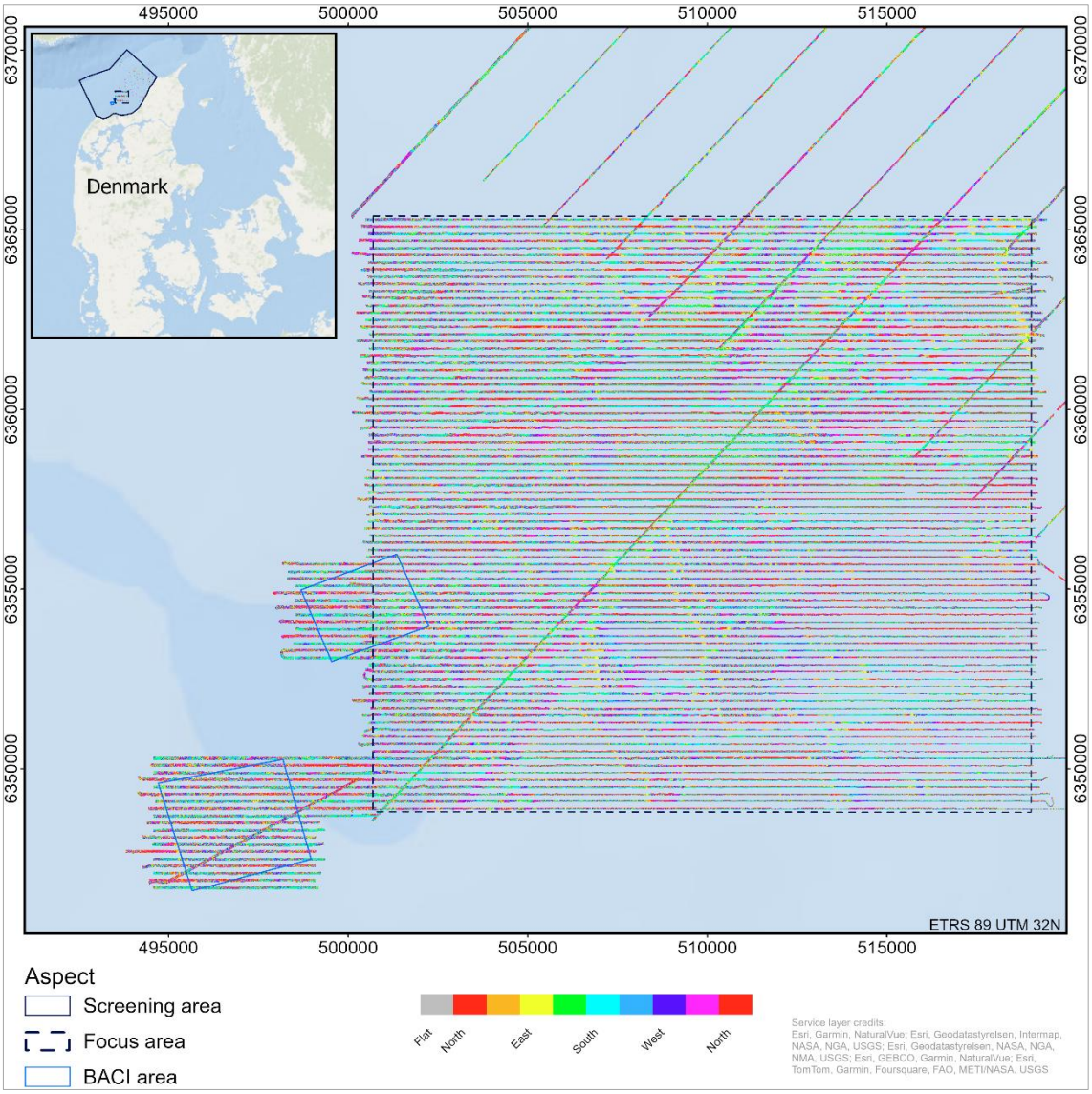

Figure 7.2: Aspect map of the Focus area (1 m x 1 m grid cell resolution).

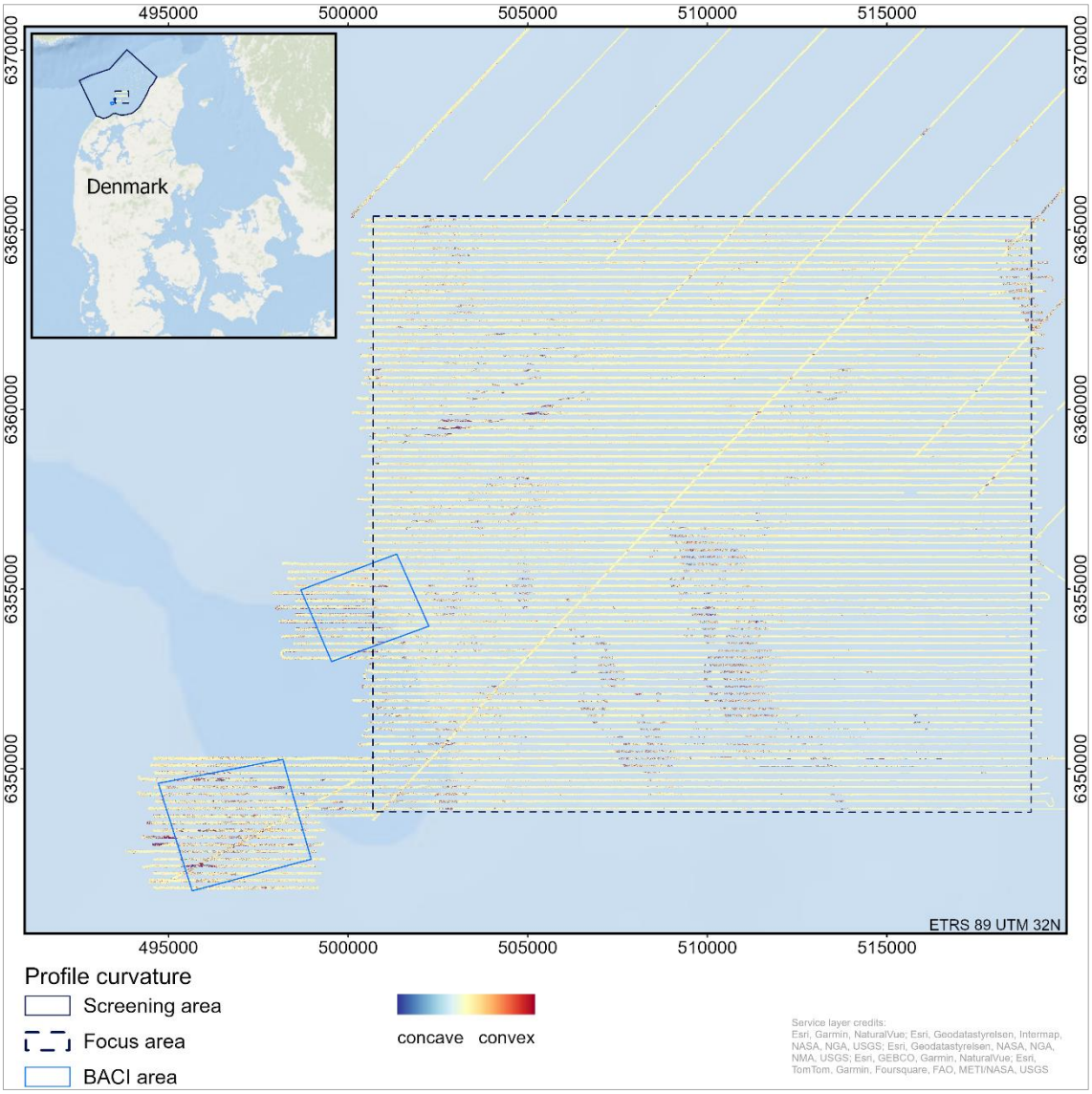

Figure 7.3: Profile curvature map of the Focus area (1 m x 1 m grid cell resolution).

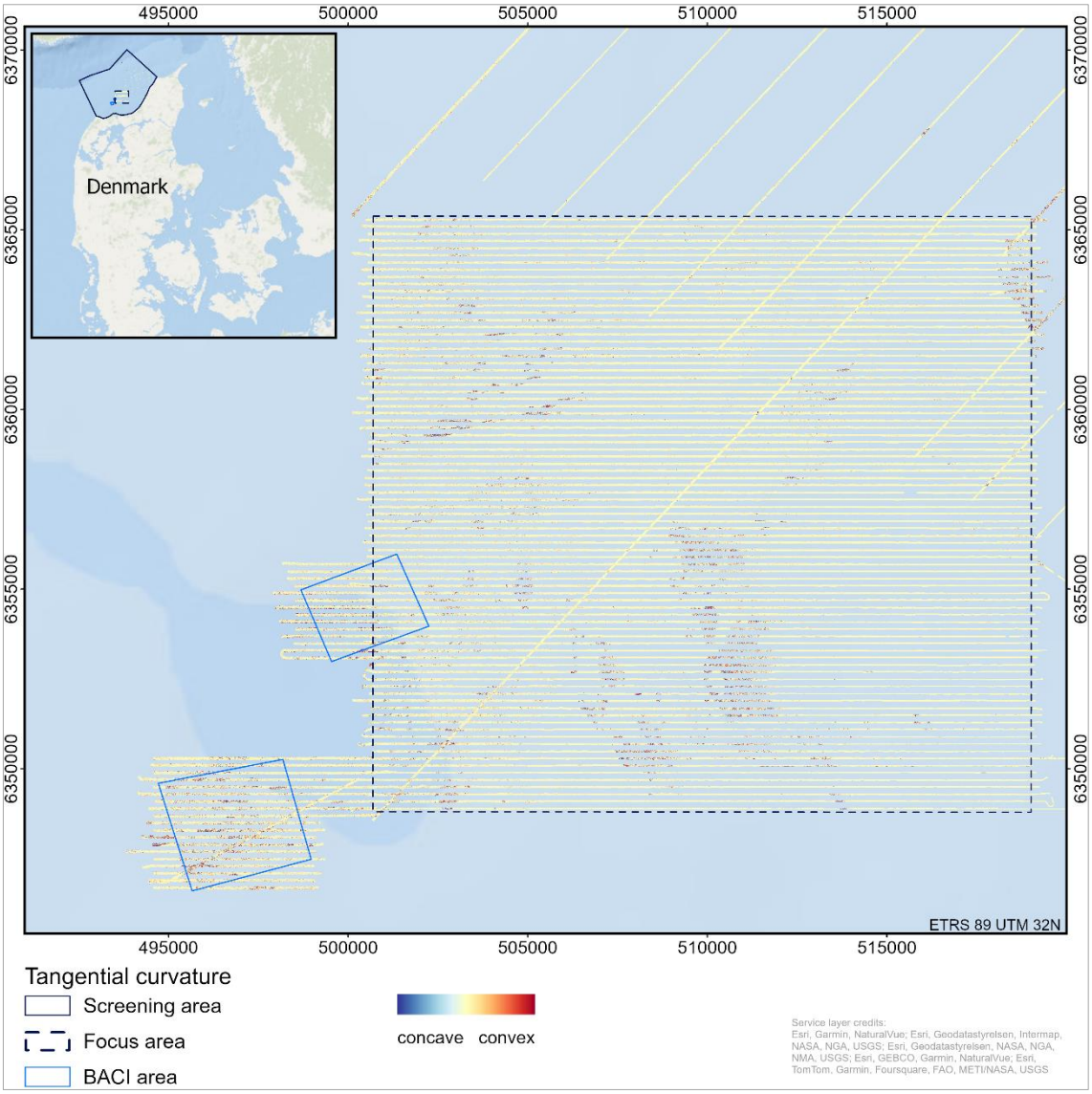

Figure 7.4: Tangential curvature map of the Focus area (1 m x 1 m grid cell resolution).

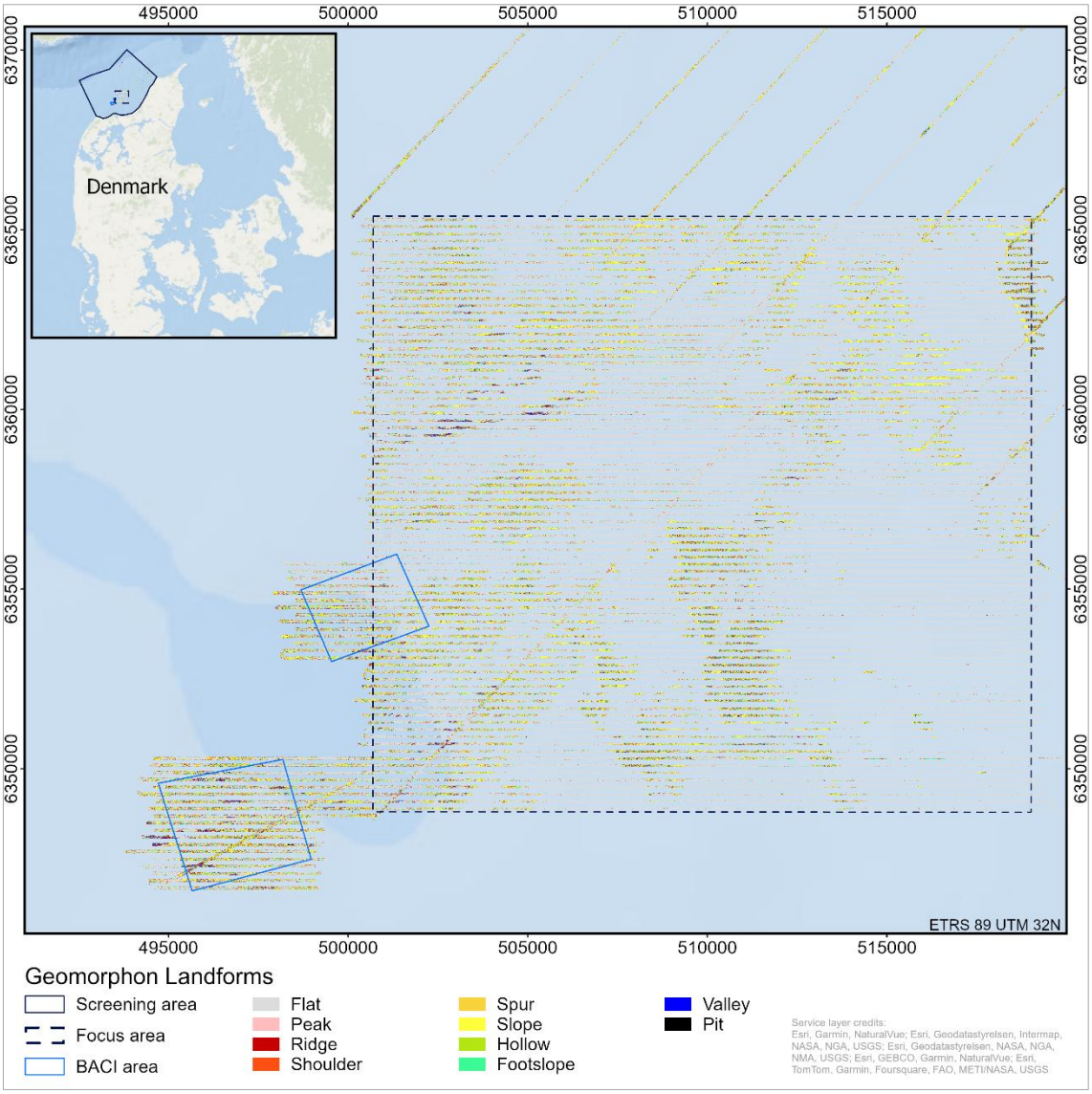

Figure 7.5: Geomorphon Landforms classification in the Focus area (1 m x 1 m grid cell resolution).

7.4 Discussion and perspectives

The concept of scale is essential in morphometric analysis as the terrain attributes depend on the scale at which they are calculated. The spatial scale of a DEM is intrinsically linked to the grid cell size of the raster grid (i.e., the spatial resolution) which governs the technical properties related to spatial analysis (Pike et al. 2009).

We chose to compute surface parameters from a high-resolution DEM (1 m resolution) to capture terrain attributes of small-scale morphologies such as stones associated with stone reefs and small-scale bedforms in the shallower regions of the study area. The trade-off was that the impact of small-scale artefacts (related to component limitations of the MBES system as discussed in section 6.4) increased. However, as the appropriate spatial resolution of a DEM is application specific, we resampled the DEMs to a 10 m resolution smoothing out signals from small-scale features and artefacts to support an improved delineation of broad-scale features such as sandbanks.

The advantage of applying the Geomorphon Landforms classification for mapping the seabed morphological features is that it provides a semi-automated, objective, and repeatable classification as a baseline for further analyses of morphodynamics.

The derived surface parameters and seabed morphology provides in combination with the substrate and shallow subsurface geology the basis for the development of a geomorphological model of the Jammer Bay area. Information on the processes acting upon and shaping the seabed features, i.e. the hydrodynamics, would provide a strong additional input for the interpretation of the geomorphology.

8. Seabed substrate maps (Task 1.7)

Mikkel S. Andersen, Zyad Al-Hamdani, Isak R. Larsen, Silas Clausen, Jakob R. Jørgensen, Lars Ø. Hansen, Niels Nørgaard-Pedersen, Nicklas Christensen, Jørgen O. Leth, Verner B. Ernstsen

8.1 Introduction and aim

The aim of Task 1.7 was to generate seabed substrate maps based on side scan sonar data, supported by multibeam bathymetry and backscatter data and sub-bottom profiler data, and in combination with knowledge from existing data.

It was also an overall aim of the project to analyse and map the impacts of all individual mobile bottom-contacting gears on seabed habitats. Hence, trawl marks and other signs of human activities were also mapped based on interpretation of the acquired side scan and multibeam data.

8.2 Materials and methods

Seabed substrates were classified according to the classification system of the Danish Environmental Protection Agency (DEPA) (Miljøstyrelsens substrattyper in Danish) (Naturstyrelsen, 2012). The 7 substrate types are shown and described in Table 8.1.

Table 8.1: Definition of substrate types used for the substrate mapping (Miljøstyrelsen, 2018). Substrate type 2a was introduced by Miljøstyrelsen (2021b).

Substrate type	Definition
1a. Mud	Homogeneous mud/silt bottom, where the bottom is not dynamically affected, and where the sediment consists of silt and silty sand or mud.
1b. Sand	Homogeneous sand bed (sand is defined as grain sizes from 0.06–2.0 mm) characterized by a certain form of dynamic with beforms etc. This type of substrate can also have varying elements of shells, gravel and silt.
1c. Hard clay	Area consisting of clay or larger relict clay blocks on a silty to sandy seabed, where the highly reflective clay gives the seabed a patterned appearance. These clay patterns can have very distinct current stripes.
2a. Sand, gravel and pebbles	Very variable substrate type, dominated by sand and coarse sand with varying amounts of gravel and pebbles. The substrate consists of a mixture of sand, coarse sand and gravel with a grain size of approx. 0.06 - 20 mm and pebbles with sizes of approx. 2 to 10 cm.
2b. Sand, gravel and pebbles with (< 10 %) stones >10 cm	Very variable substrate type, dominated by sand and coarse sand with varying amounts of gravel and pebbles and scattered large stones. The substrate consists of a mixture of sand, coarse sand and gravel with a grain size of approx. 0.06 - 20 mm and pebbles with sizes approx. 2 to 10 cm. The substrate type can also contain larger stones >10 cm, but only up to 10% coverage.
3. Sand, gravel and pebbles with (10-25 %) stones >10 cm	Area consisting of mixed substrates with sand, gravel and small stones and with a sprinkling of larger stones >10 cm. The substrate type contains stones >10 cm, with a coverage of 10% - 25%.
4. Stones > 10 cm covering >25 %	Area dominated by stones >10 cm, but also with varying elements of sand, gravel and pebbles. The stones are either scattered on the seabed or as a dense layer of stones with a coverage >25%.

The mapping of seabed substrates was based on interpretation of the geophysical data acquired as part of the JAMBAY project (Task 1.1), as well as interpretation of geophysical data acquired as part of another survey conducted by GEUS for the Danish Energy Agency (ENS). The data for the JAMBAY project were collected in June 2023, and the data for the ENS project were collected in May 2023. Both surveys were carried out using the same ship, Arctic Ocean, as described in Task 1.1.

Data collection was carried out in two sub-areas (as described in section 2.1): 1) the Focus area (incl. BACI areas) with 200 m line spacing, and 2) the Screening area with 2,000 m line spacing, including two normal to shore parallel lines extending to the EEZ border as well as a survey line parallel to the shore following the 10 m depth curve (Figure 8.1). The planned survey lines' total length was ~2,800 line-km. The additional survey lines from the ENS project, included in the interpretation for this project, were in total 795 km.

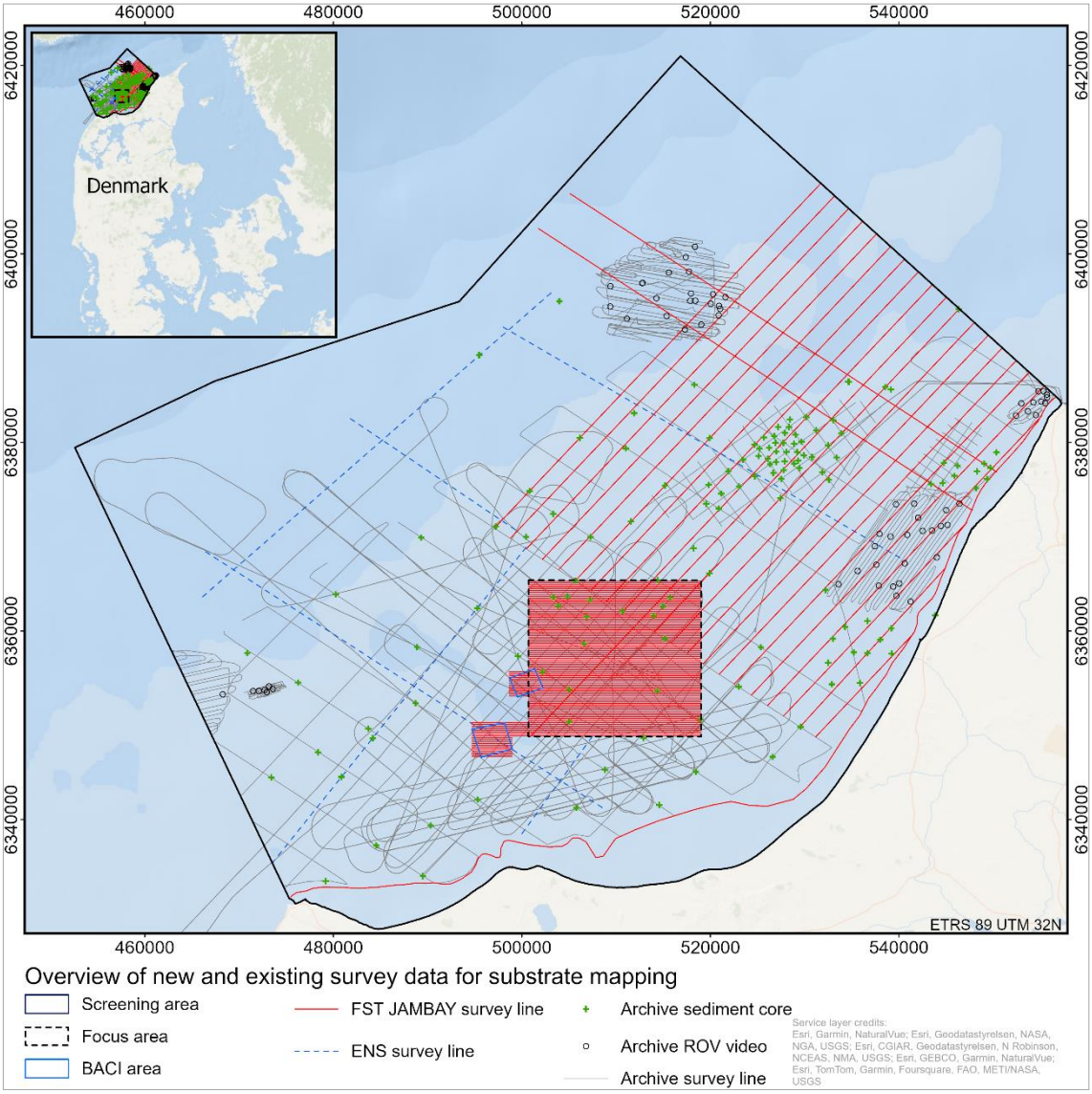

Figure 8.1: Survey lines in Jammer Bay used for the mapping of seabed substrate types and the designation of targets for ground truth sampling.

Data were used from three different types of instruments for the classification of seabed sub-strates: Side scan sonar, sub-bottom profiler and multibeam echosounder.

The primary instrument was side scan sonar. Two side scan sonar systems were operated onboard the ship, an Edgetech 6205 which was fixed (pole mounted) to the ship and an Edg-etech 4205, which was towed behind the ship. The fixed side scan sonar was used for shallow water depths (approx. < 35 m) and the towed side scan sonar was used for deeper water depths (approx. > 35 m). This depth threshold was based on knowledge from previous surveys that ensures optimal area of seabed being covered with each swath.

The sub-bottom profiler was an Innomar SES-2000 Medium and the multibeam echosounder was an R2Sonic 2024 (for more details see chapter 2). The instrument setup for the ENS

survey was similar, apart from the multibeam echosounder and the towed side scan, which were not used.

Side scan sonar data were post-processed in SonarWiz 7 software. The post-processing aimed to optimize data for use in the substrate interpretation. The towed sonar's position was calculated using the cable length input from the cable counter (MacArtney MKII) and depth information from the sonar using the layback algorithm in SonarWiz 7. The calculated sonar positions were validated and corrected by comparing the position of identifiable objects on the seabed from side scan images with the more accurate multibeam data. In addition, the signal from the water column was removed (using bottom tracking) and various visualization parameters were adjusted to obtain the optimal contrast between different objects and substrate types. See section 3.2.1 for a more detailed description of the side scan processing procedure.

Figure 8.2 shows a side scan mosaic of the processed side scan data in the Focus area.

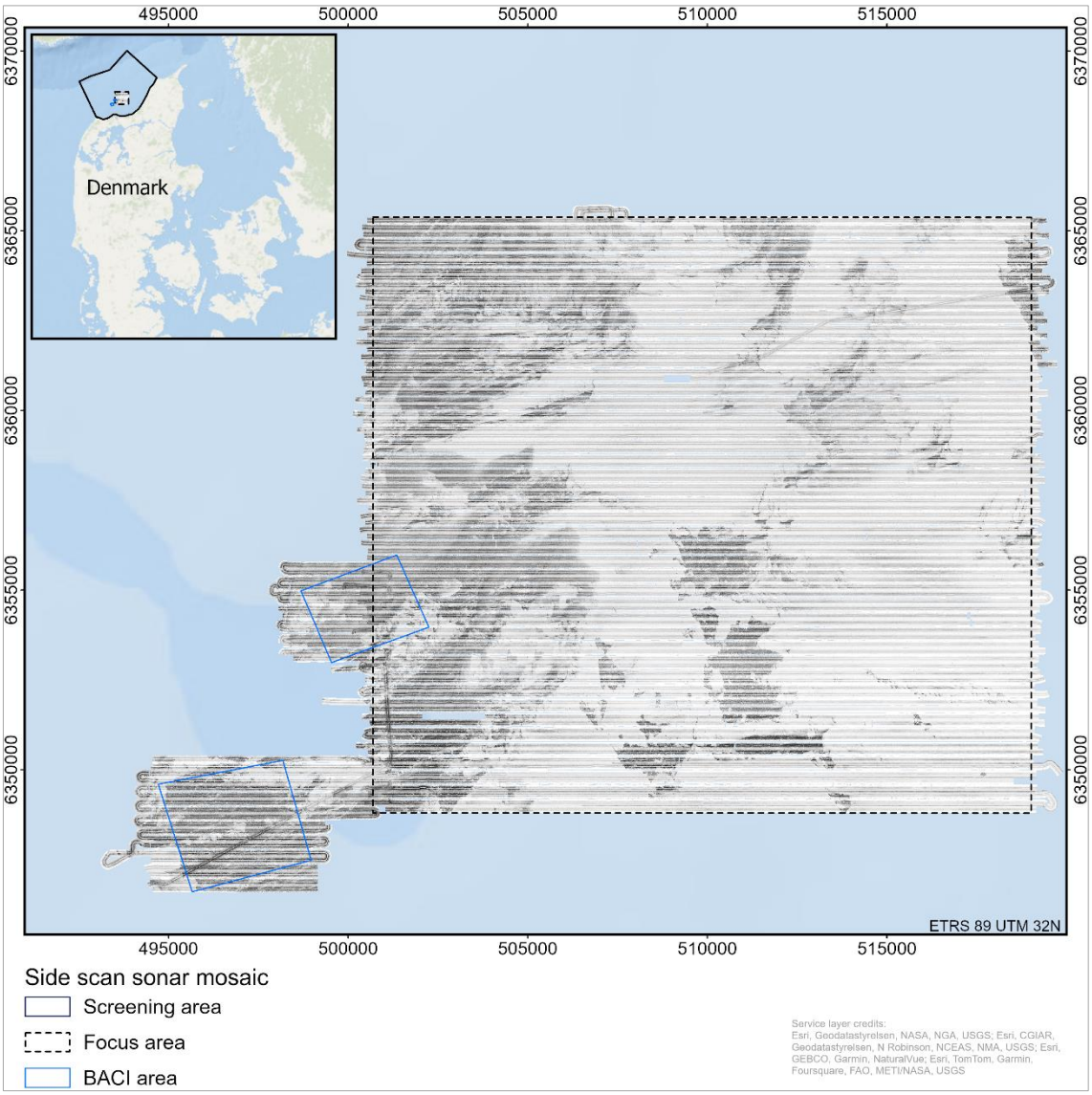

Figure 8.2: Side scan mosaic of the processed side scan data in the Focus area.

8.2.1 Interpretation of seabed substrates

The primary data for seabed substrate interpretation was the side scan data as the intensity of the reflected signal from the seabed is directly influenced by the seabed material and the sonar geometry. However, the sub-bottom profiler and multibeam bathymetry served as important supplementary data sources. The sub-bottom profiler gives information of the shallow subsurface layers of the seabed and clearly shows the different soft and hard sediment deposits on top of, and below, the seabed surface. For example, one can identify a soft sandy seabed substrate with a hard moraine layer underneath that occasionally crops out of the soft layer. The multibeam bathymetry shows the 3D surface of the seabed, which often gives an indication of the substrate type, e.g. hard substrate with large stones yields an irregular and rugged bathymetry, while sandy bedforms appears with distinct geometric shapes. Thus, the datasets produced from the three above mentioned instruments were all used for optimising the interpretation of the seabed substrates.

Furthermore, existing data were also utilised for substrate interpretation. This included ROV videos, sediment samples and sediment cores, which served as ground truth information for our interpretation (keeping in mind that the seabed is a dynamic environment with potential changes occurring between surveys).

8.2.2 Interpretation of human activity

Three types of human activity were identified in the geophysical datasets: Trawl marks, wrecks, and pipelines. The mapping of human activity was done with a manual approach by interpreting the geophysical data, particularly the side scan data in combination with the multibeam bathymetry data. The marks that are left by trawling in the seabed are often most visible in the side scan data as distinct parallel lines with distinct acoustic signature which can be interpreted as features caused by human activity. The side scan mosaic, especially in the Focus area where full coverage side scan data were collected, helped a lot in recognising and connecting the trawl marks across survey lines. The delineation of trawl marks was done by drawing polygons around the trawl marks.

8.3 Results

8.3.1 Seabed substrates

Figure 8.3 shows the spatial distribution of the mapped seabed substrates in the Screening area and Focus area. Figure 8.4 shows a zoom in on the seabed substrates in the Focus area. The areal coverage of the interpretation of different substrate types is summarised in Table 8.2. An area of 574 km^2 were interpreted and mapped into the different substrate types.

The results show a diverse spatial distribution of soft and hard seabed substrate types throughout the survey areas. The most dominant substrate types are 1b (sand) covering 354 km^2 (62% of the mapped area), and 2a (sand, gravel and pebbles) covering 135 km^2 (24% of the mapped area). Substrate types 4, 3 and 2b (all containing stones larger than 10 cm), together cover 67 km^2, corresponding to 12% of the mapped area.

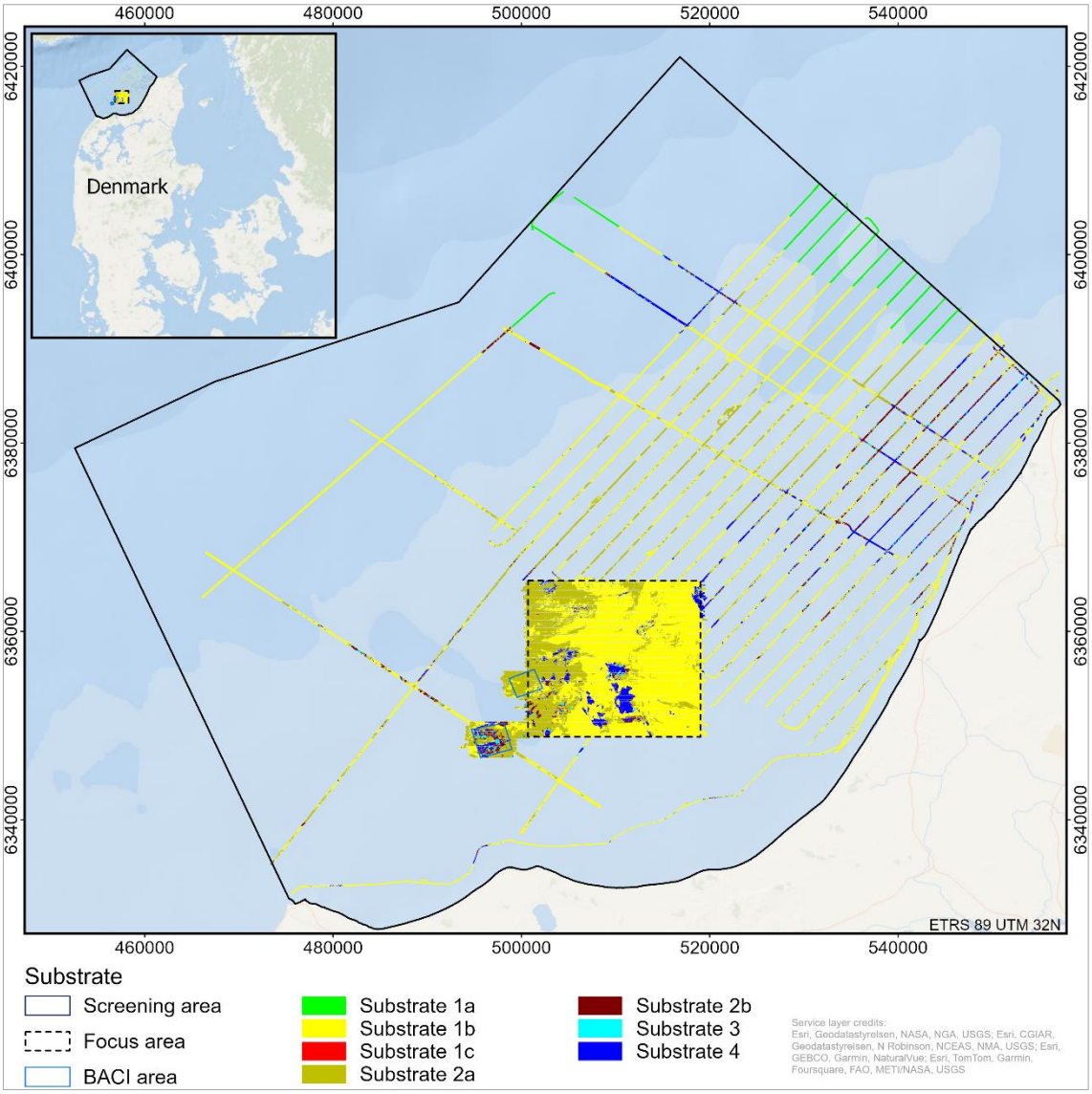

Figure 8.3: Mapped seabed substrates in the Screening area and Focus area.

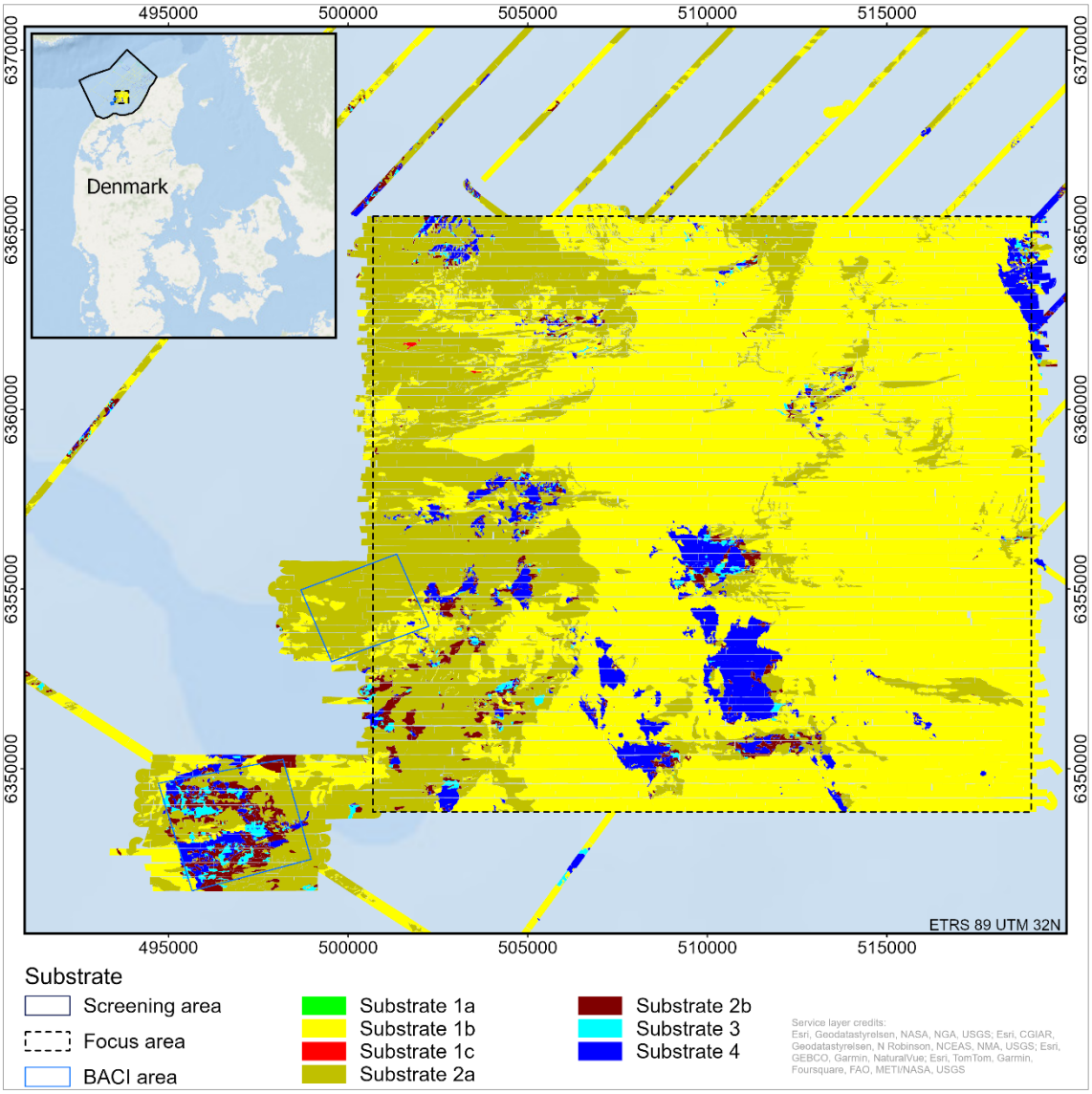

Figure 8.4: Zoom in on the mapped seabed substrates in the Focus area.

Table 8.2: Areal coverage of each of the mapped seabed substrate types.

	Area (m^2)	Area (km^2)	Area (%)
Substrate 1a	17,998,969	18.0	3.1
Substrate 1b	354,108,884	354.1	61.7
Substrate 1c	66,924	0.1	0.0
Substrate 2a	134,843,634	134.8	23.5
Substrate 2b	28,568,681	28.6	5.0
Substrate 3	6,661,256	6.7	1.2
Substrate 4	32,041,150	32.0	5.6

8.3.2 Human activity

Figure 8.5 shows the interpreted human activity in the Screening area and Focus area. Figure 8.6 shows a zoom-in of the Focus area.

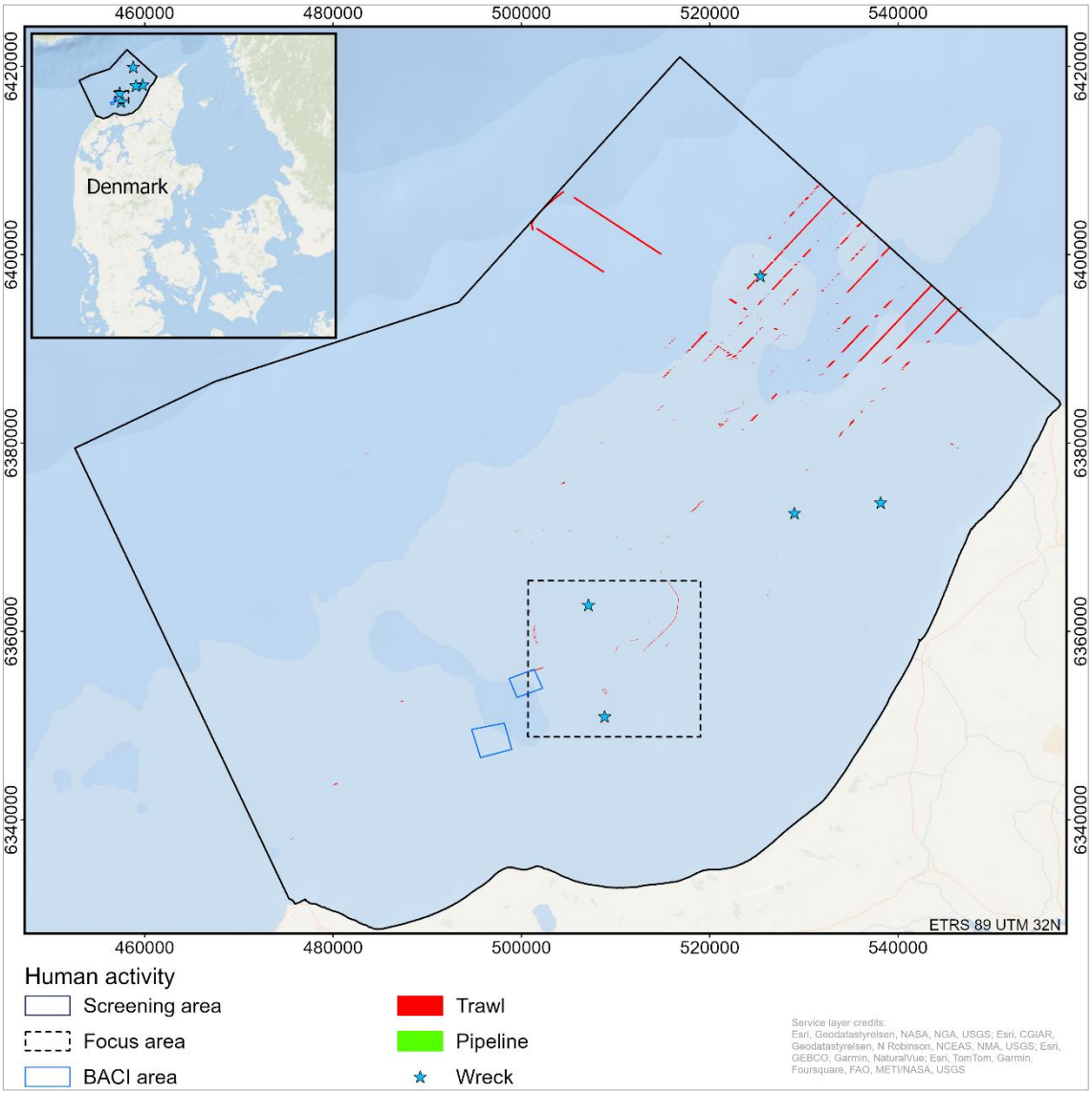

Figure 8.5: Mapped human activity in the Screening area and Focus area.

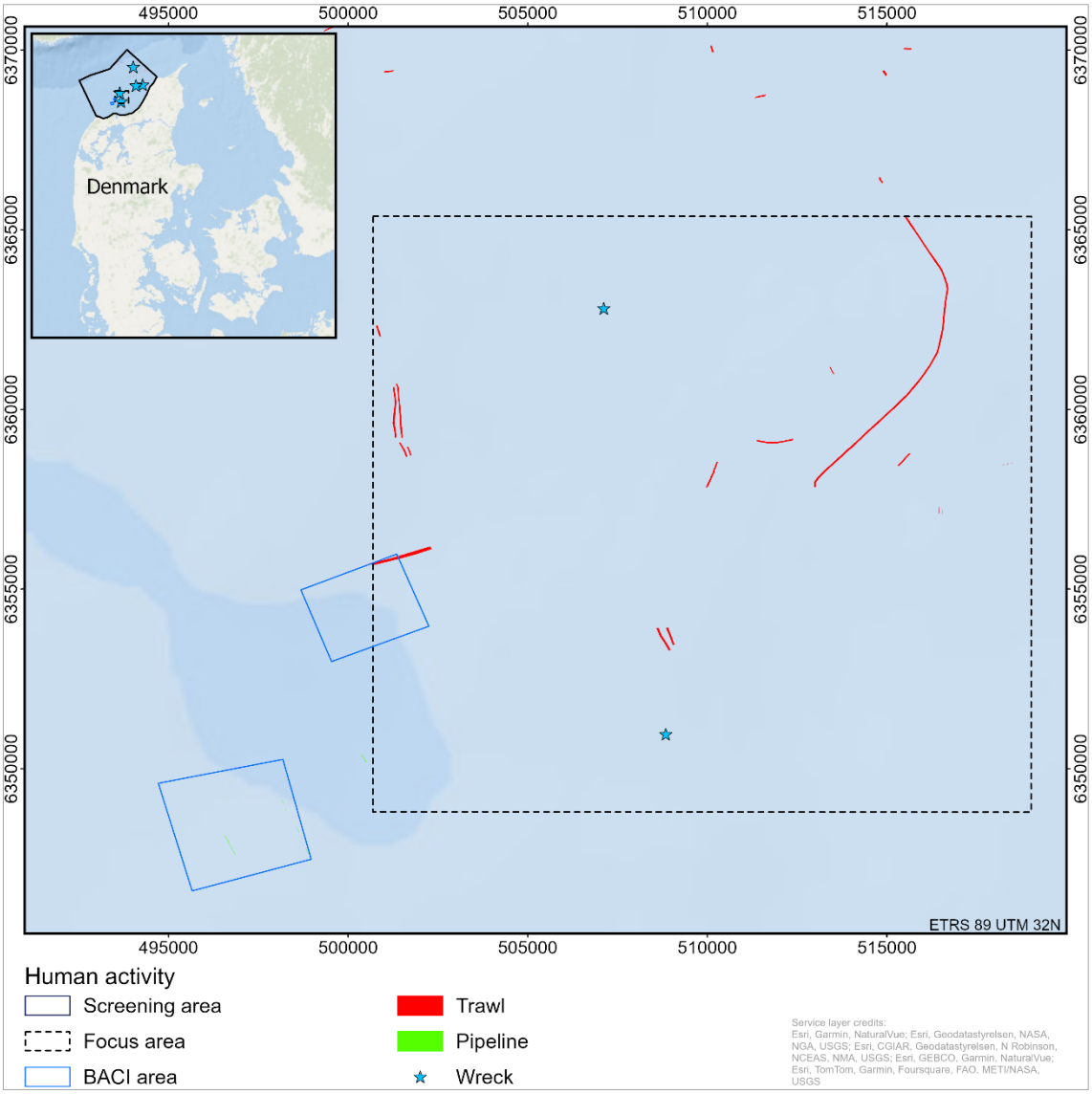

Figure 8.6: Zoom in on the mapped human activity in the Focus area.

An area of 22 km^2 was mapped as trawl marks, which are mostly found in the northern part of Jammer Bay in the Screening area. Only few trawl marks were found in the Focus area, even though a full coverage survey was conducted. Five wrecks have been observed in the data, 3 of them are found in the Screening area and 2 in the Focus area. Traces from pipelines are observed in the southern BACI area.

8.4 Discussion and perspectives

The seabed in the Jammer Bay consists of a diverse distribution of substrates, with complex patterns of hard and soft substrate types. It can be noticed from Figure 8.4 that the full coverage mapping in the Focus area has produced a high-resolution substrate distribution map within the area. Detailed information and position of different substrate types can be observed, and the boundaries of some of these substrates such as substrate 3 and 4 can be accurately traced. This will categorically enhance the Danish marine substrate map and provide highly confident and reliable information to be used in other applications. High-resolution substrate information

also exists in the Screening area but only along the survey lines. The current spatial distribution of the seabed substrates represents their status during data acquisition, i.e. a snapshot in time. This distribution may however change over time due to dynamic processes and/or human activities. Waves and currents are both dynamic processes that cause sediment transport, with the potential of removing the top soft sediment and thus exposing the hard underlaying layer. The reverse process is also possible where transported sediments will be deposited on top of a hard substrate seabed, thereby covering it and changing the seabed to a soft substrate type. This sediment transport and dynamics will have an impact on the substrate distribution as the instrument used for the mapping (the side scan sonar) will register or image the top surface layer only and not what is laying underneath. Such dynamic processes must be expected to cause changes, not least in an area as Jammer Bay on an open NW-oriented coast towards the North Sea, which is known for often high wind speeds and large waves. More changes caused by dynamic processes is expected to occur in shallow water where the impact of waves is higher, and less changes in deeper water. In this project, bedforms were observed in the side scan and bathymetry data, e.g. from the Focus area, indicating that wave and current induced sediment transport is occurring. At the same time, based on interpretation of the sub-bottom profiler data, it is shown that much of the Focus area is only covered by a thin layer of Holocene mobile sand (Figure 5.3).

The same argument can be applied to the identification of human activities where quite few trawl marks were identified and mapped; but in the Screening area for example, trawl marks can only be mapped along the survey lines, as mapping their spatial extent is not feasible due to line spacing. The seabed dynamics and sediment transport play an important role here, trawl marks can disappear quickly in dynamic areas where the sand is mobile and abundant.

As a future perspective it would be very interesting to come back for mapping the same area, especially in the Focus area, where the full coverage makes it an ideal dataset from which to measure 3-dimensional changes.

9. Seabed habitat maps (Task 1.8)

Mikkel S. Andersen, Zyad Al-Hamdani, Isak R. Larsen, Silas Clausen, Jakob R. Jørgensen, Lars Ø. Hansen, Niels Nørgaard-Pedersen, Nicklas Christensen, Jørgen O. Leth, Verner B. Ernstsen

9.1 Introduction and aim

The aim of Task 1.8 was to generate seabed habitat maps based on an integration of seabed substrate and morphology that was derived in previous tasks from multibeam echosounder, side scan sonar, and sub-bottom profiler data. Seabed habitats were classified according to the EU Habitats Directive following the European Commission Interpretation manual of habitats listed under Annex I (EC, 2013) and the associated translation and description by the Danish Environmental Protection Agency (DEPA) (Habitatdirektivets naturtyper in Danish) (Miljøstyrelsen 2016; Miljøstyrelsen 2021b).

The specific seabed habitats that will be mapped and spatially delineated are sandbank habitats (habitat code 1110) and stone reef habitats (habitat code 1170). The definition of the two habitats is almost similar in the two references. The sandbank was defined in the interpretation manual as “elevated, elongated, rounded or irregular topographic features, permanently submerged and predominantly surrounded by deeper water. They consist mainly of sandy sediments, but larger grain sizes, including boulders and cobbles, or smaller grain sizes including mud may also be present on a sandbank”. Both the national and the EU definition specified the depth of the sandbank to be less than 20m, although deeper sandbanks do exist. Reefs of either biogenic or geogenic origin was defined by the EU interpretation manual and the DEPA as “hard compact substrata on solid and soft bottoms, which arise from the sea floor in the sublittoral and littoral zone”.

In 2021, the DEPA upgraded the habitat definitions by adding another criterion for delineation where a minimum size of 2,500m² is required to be classified as sandbank, and a minimum size of 100 m^2 is required to be classified as stone reef (Miljøstyrelsen 2021b).

9.2 Materials and methods

Two principal input parameters were used in this work for defining the Habitats Directive seabed habitats, sandbank (1110) and stone reef (1170); they are the seabed substrate and bathymetry (morphology).

For sandbank habitats, the seabed substrate is 1b (sand) after DEPA definition, and it was interpreted from side scan images, sub-bottom profiler, multibeam bathymetry and the support of existing data as mentioned in Task 1.7.

The sandbanks in the area were identified according to the above-mentioned criteria by EU international manual and the DEPA definition using a semi-automated method in GIS. The method combines the seabed substrate 1b polygon with the morphology layer that exhibits an elevation above the general seabed level and a derived slope of the seabed. A slope threshold of 0.5° (1 m grid resolution) was used as support for delineating sandbank margins. Based on the overlay analysis and expert interpretation, the sandbanks were manually mapped.

Stone reef habitats were delineated with another semi-automatic method, where substrate 4 and substrate 3 were extracted as polygons in GIS, and stone reef habitats were identified and mapped where substrate 4 exist or where substrate 3 is attached and spatially connected to substrate 4.

9.3 Results

Figure 9.1 shows the spatial distribution of the mapped stone reef habitats (habitat 1170) in the Screening area and Focus area. Figure 9.2 shows a zoom in of the stone reefs in the Focus area. An area of 37 km^2 was mapped as stone reef.

The results show that both the Focus area and Screening area includes many stone reef habitats spatially scattered in the Jammer Bay.

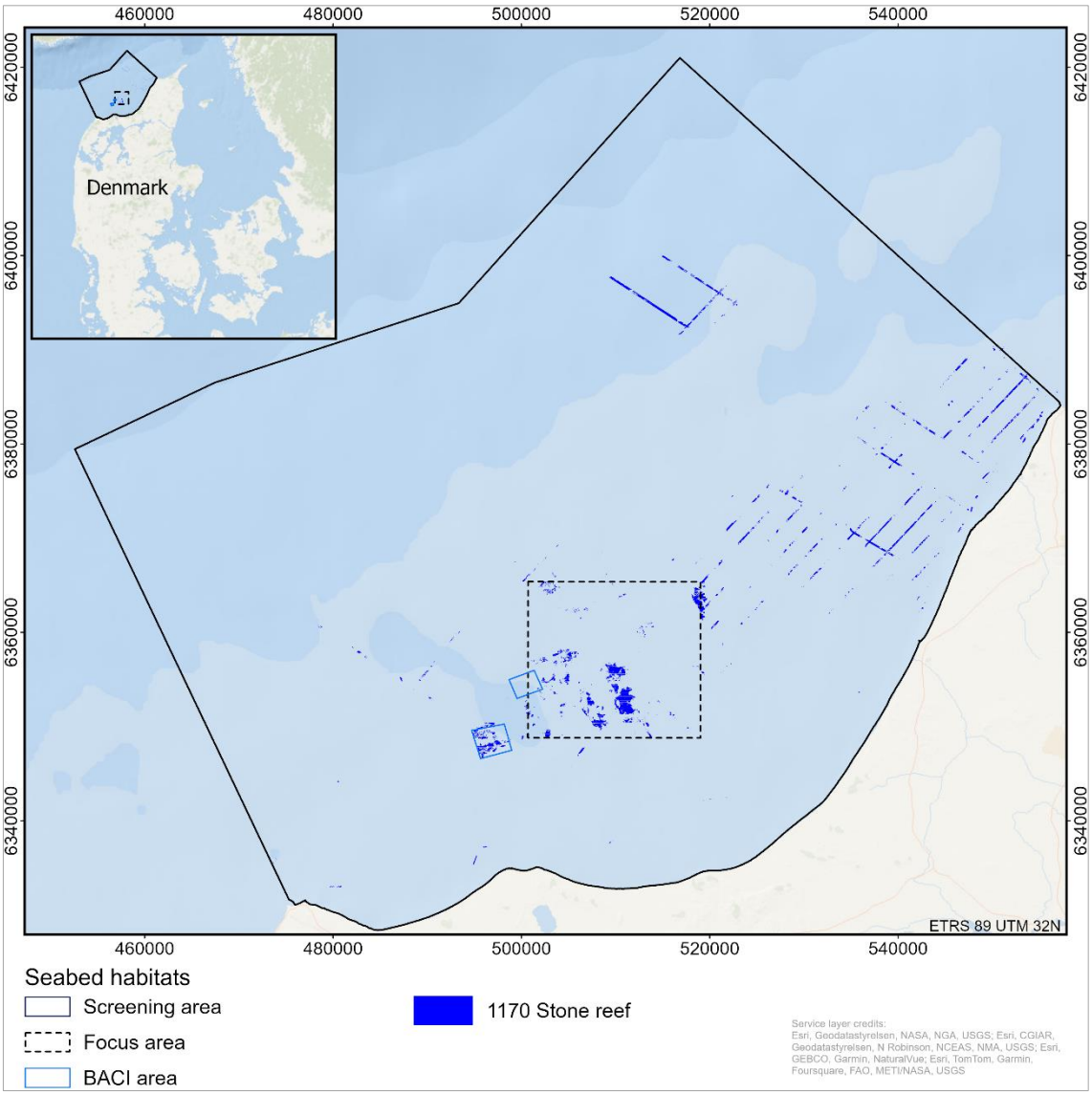

Figure 9.1: Mapped stone reef habitats (1170) in the Focus area and Screening area.

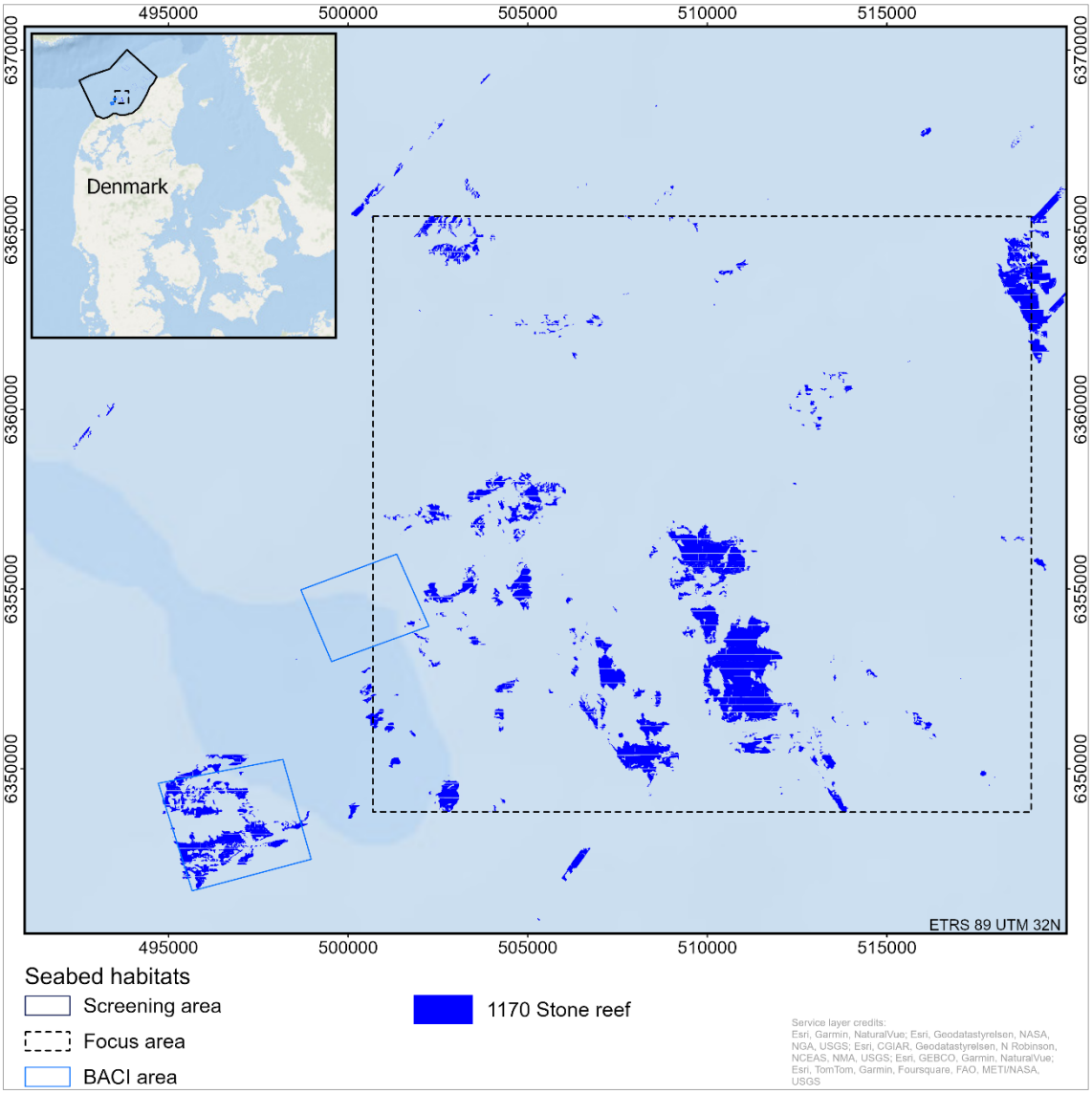

Figure 9.2: Zoom in of the mapped stone reef habitats (1170) in the Focus area.

Figure 9.3 shows the spatial distribution of the mapped sandbank habitats (habitat 1110) in the southern part of the Focus area. The mapping of sandbank habitats is still in progress in the northern part of the Focus area and in the Screening area.

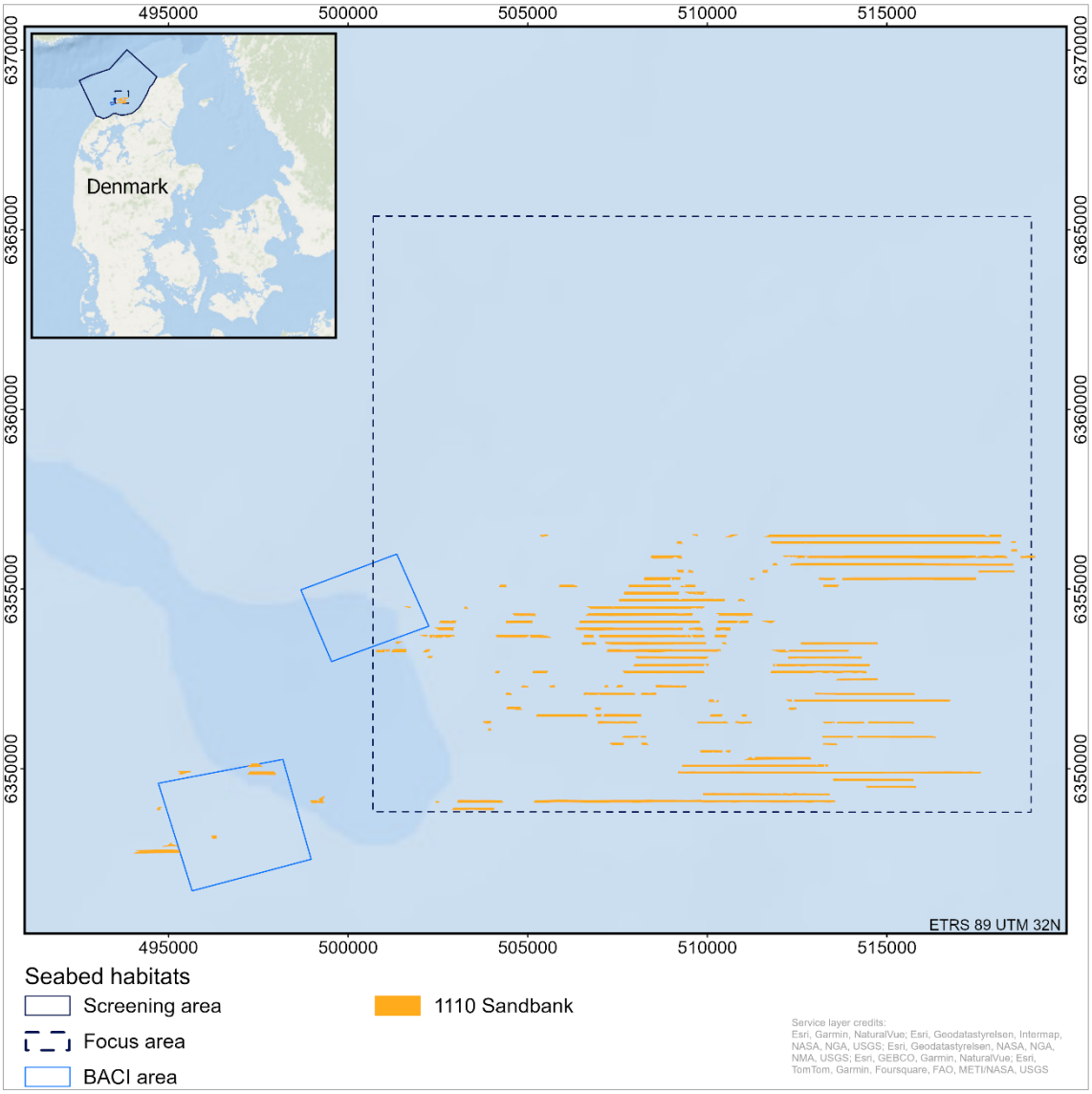

Figure 9.3: Zoom in of the mapped sandbank habitats (1110) in the southern part of the Focus area. The mapping of sandbank habitats is still in progress in the northern part of the Focus area and in the Screening area.

9.4 Discussion and perspectives

Jammer Bay has a high diversity in the spatial distribution and areal extent of stone reefs. Particularly in the Focus area (Figure 9.2). Due to the full coverage of the collected side scan sonar data, the actual extent can be seen of large coherent stone reefs as well as very small, isolated stone reefs. This information can play an important role in designing management plans for the area or in studying the ecological connectivity between these stone reef habitats. In comparison, there are also a lot of stone reefs in the Screening area (Figure 9.1). However, due to the large gap between the survey lines, interpolating the extent of stone reefs between these lines would yield low confidence and low reliability maps. Full coverage data is needed to; 1) map the actual spatial distribution and extent of stone reefs, and 2) monitor the changes of stone reefs caused by dynamic processes (e.g. burying or outcropping by sediment transport) or human impact (e.g. trawl).

The preliminary results regarding spatial distribution and areal extent of sandbanks in the Focus area, indicate the presence of both very large as well as smaller, isolated sandbanks.
The semi-automatic approach combining information of substrate and morphology provides quantitative support for the delineation of sandbanks; however, expert interpretation is still required. Furthermore, full coverage mapping of sandbanks in the Focus area is not achievable with 200 m line spacing due to swath coverage limitations of the MBES system. Sandbank interpolation between survey lines is potentially possible but will affect the confidence and reliability of the map.

All habitat data will contribute to the EMODnet Seabed Habitats database.

10. Offshore geophysical survey (Task 1.9)

Lars Ø. Hansen, Nicklas Christensen, Sigurd B. Andersen, Lars-Georg Rödel, Sofie Kousted, Silas Clausen, Jakob R. Jørgensen, Mikkel S. Andersen, Zyad Al-Hamdani, Verner B. Ernstsen

10.1 Introduction and aim

The aim of Task 1.9 was to plan and conduct a geophysical survey using vessel borne multibeam echosounder (MBES), side scan sonar (SSS) and sub-bottom profiler (SBP) systems.

New geophysical data were acquired in Jammer Bay in context of the JAMBAY project. Side scan sonar (SSS) and multibeam echosounder (MBES) data provides information on substrate and depth of the seabed surface, and sub-bottom profiler (SBP) data provides information on the shallow subsurface geology.

The aim of the geophysical survey was to map the seabed within the Jammer Bay offshore Screening area (5,230 km2, see Figure 10.1 for spatial extent) – covering the area along the EEZ border – in high spatial resolution and precision along the survey lines, with data gaps between survey lines. In addition, data were also collected nearshore due to poor weather conditions in the offshore area.

10.2 Materials and methods

10.2.1 Survey

Data were collected in the period between 5 December and 9 December 2023. The survey lines in the offshore Screening area were planned with 4,000 m line spacing. The nearshore survey lines had 400 m line spacing (Figure 10.1). The planned offshore survey lines, excluding planned transit lines, amounted to a total of 532 line-km.

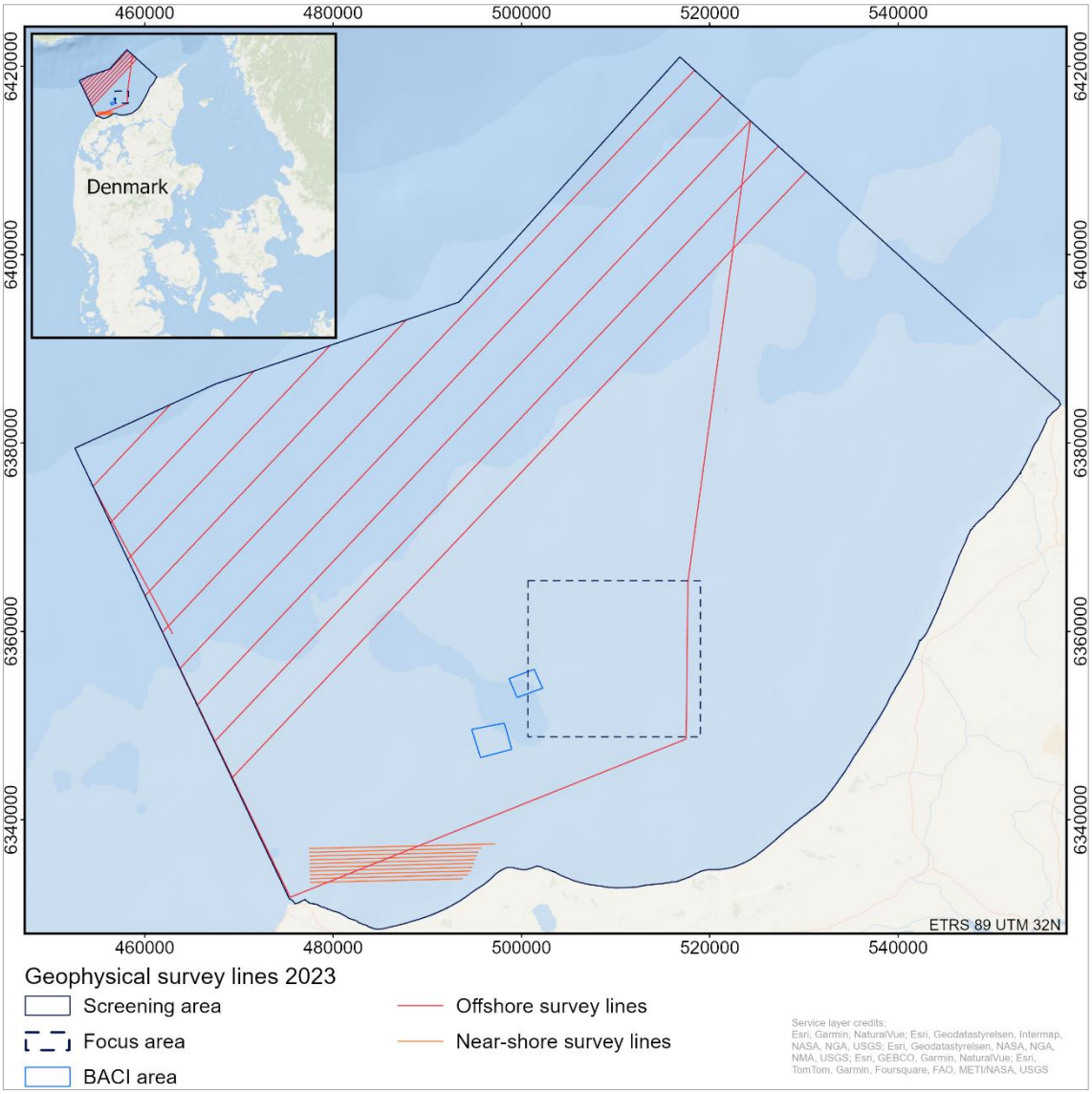

Figure 10.1: Planned offshore geophysical survey lines and nearshore backup lines.

MV Arctic Ocean was used as survey platform (Figure 2.2). The ship's length (LOA) and width (Beam) at the water line is 39.9 m and 9.45 m and the draught is 5.3 m. The ship is equipped with an A-frame and has a service speed of 10 kn, and an offshore endurance of 30+ days.

The team on MV Arctic Ocean constituted the ship's crew who operated the ship, and the scientific crew who operated the geophysical instruments and did the data collection.

10.2.2 Instruments

The instruments used for the geophysical survey comprised a towed Klein System 4900 side scan sonar, a pole-mounted Innomar SES-2000 medium sub-bottom profiler and, an R2Sonic 2024 multibeam echosounder. Primary position and motion were delivered by an SBG Navsight Ekinox GNSS/INS system. Motion input for the sub-bottom profiler was delivered by an SMC IMU-108. Sound velocity profiles were measured with a Valeport SWIFT SVP (Table 10.1).

Table 10.1: Instruments applied in the geophysical survey.

Instrument type	Instrument model	Mounting
Side scan sonar	Klein System 4900	Towed
Sub-bottom profiler	Innomar SES-2000 medium	Pole-mounted port
Multibeam sonar	R2Sonic 2024	Pole-mounted port
Sound velocity probe	Valeport SWIFT SVP	Hand-held
GNSS/INS	SBG Systems Navsight Ekinox	GNSS antennas on the ship INS pole-mounted port
IMU	SMC IMU-108	Pole-mounted port

The R2Sonic MBES was mounted on the port side pole on a custom-made bracket and the SBG IMU was mounted on the MBES. The sub-bottom profiler was mounted on the same bracket in a displaced position (forward and up) and the SMC IMU was mounted next to the pole on the railing. The Klein System 4900 side scan sonar was towed behind the ship in a tow cable connected to a tow cable winch. The sonar layback was accounted for using a cable counter (MacArtneys Cable Status Indicator MKII).

10.2.2.1 Positioning – SBG Navsight Ekinox

Navsight Ekinox consists of an Ekinox grade Inertial Measurement Unit connected to a Navsight processing unit embedding fusion intelligence and the GNSS receiver. Under optimal conditions the Ekinox provides accuracies as described in Table 10.2. The system delivered navigation solutions to the geophysical instruments.

Table 10.2: Navsight Ekinox Grade Marine Solution specifications (SBG Systems, 2022). *Baseline, dual antenna.

Parameter	RTK	PPK	RTK outage (30 s)	PPK outage (30 s)
Roll, Pitch	0.015°	0.01°	0.05°	0.04°
Heading* - 2 m / 4 m	0.03° / 0.02°	0.02° / 0.02°	0.12° / 0.1°	0.05° / 0.05°
Position (XY)	0.01 m + 0.5 ppm	0.01 m + 0.5 ppm	3 m	1 m
Altitude (z)	0.015 m + 1 ppm	0.015 m + 1 ppm	0.75 m	0.3 m
	Heave	**Wave period**		
Real-time heave	5 cm	Up to 20 s		
Delayed heave	2 cm	Up to 40 s		

10.2.2.2 Side scan sonar – Klein System 4900

The towed Klein System 4900 side scan sonar was used to obtain higher resolution side scan data in the deep parts of the survey area. The Klein System 4900 side scan sonar was towed behind the ship in a tow cable connected to a tow cable winch. The sonar layback was accounted for using a cable counter (MacArtneys Cable Status Indicator MKII). The height of the sonar above the seabed was generally kept around 20 m. The sonar is a dual frequency system applying a low frequency of 455 kHz and a high frequency of 900 kHz. The side scan sonar recording ranges were 100-150 m (Table 10.3). Data was recorded with SonarPro acquisition software.

Table 10.3: Klein System 4900 side scan sonar frequencies and recording range.

KLEIN SYSTEM 4900	Low frequency	High frequency
Centre frequency	455 kHz	900 kHz
Recording range (per side)	100 m – 150 m	100 m

10.2.2.3 Sub-bottom profiler – Innomar SES-2000 Medium

The sub-bottom profiler mounted on the port side pole delivered shallow subsurface seismics for interpretation of the shallow subsurface geology. Select system settings are described in Table 10.4. Data was recorded in Innomar SES-Win acquisition software. The system was roll and heave compensated by the SMC IMU-108 motion sensor.

Table 10.4: Innomar SES-2000 Medium frequencies and ping rate setting.

Innomar SES-2000 Medium	Setting
Primary high frequency (PHF)	85-115 kHz
Secondary low frequency (SLF)	6-12 kHz
Ping rate	Variable – slave of R2Sonic MBES

10.2.2.4 Multibeam echosounder – R2Sonic 2024

The R2Sonic MBES has a long range of adjustable settings to optimize data collection for any specific objective. The settings applied during this survey are listed in Table 10.5. The Ultra High Density (UHD) bottom sampling mode searches across each beam footprint for additional soundings providing up to 1024 real bottom soundings (R2Sonic, 2022). The swath width was controlled manually during the survey to ensure that outer beam outliers were reduced to a minimum, while at the same time increasing the ping rate because of lowered swath width. Swath width was typically between 90°-140°. The pulse length determines the transmit pulse duration time. The pulse length was manually adjusted during survey to maintain optimal bottom detection resolution. Generally, the deeper the water depth the longer the pulse length must be to maintain adequate power in the water. The pulse length was typically kept between 20 - 35 µs. The power of the transmit pulse (191 - 221dB) was kept as high as possible while the receiver gain was kept as low as possible aiming to maintain a good balance between source level power and receiver gain and thus a good receive saturation curve. The ocean settings, i.e. spreading loss and absorption are the main components of the Time Varied Gain (TVG). The spreading loss and absorption were determined from a calculator inside the sonar GUI which required input of frequency, mean depth, temperature, and salinity.

The MBES data were recorded using QINSY acquisition software and stored in QPS db-file format.

Table 10.5: R2Sonic MBES specifications and settings.

R2Sonic 2024	Setting
Frequency	450 kHz
Beam pattern	Equidistant - Ultra High Density (UHD)
Number of soundings	Up to 1024
Beam width (across x along)	0.45° x 0.9°
Swath width	100° - 140°
Roll stabilized beams	Yes
Pulse length	Variable
Pulse type	Shaped CW
Ping rate	Up to 60 Hz
Bandwidth	Up to 60 kHz
Bottom detect resolution	3 mm

10.2.2.5 Sound velocity profiler

The speed of sound in water depends on temperature, salinity, and pressure. Information on water column sound velocity is required to properly correct the bathymetric measurements in the MBES data.

The SVP strategy for this survey was to take an SVP measurement at the end of each survey line.

10.3 Results

10.3.1 Survey track line

The vessel track lines exported from the MBES data (Figure 10.2), including instrument test, turns, and recorded transit lines sum up to a total of 687 line-km.

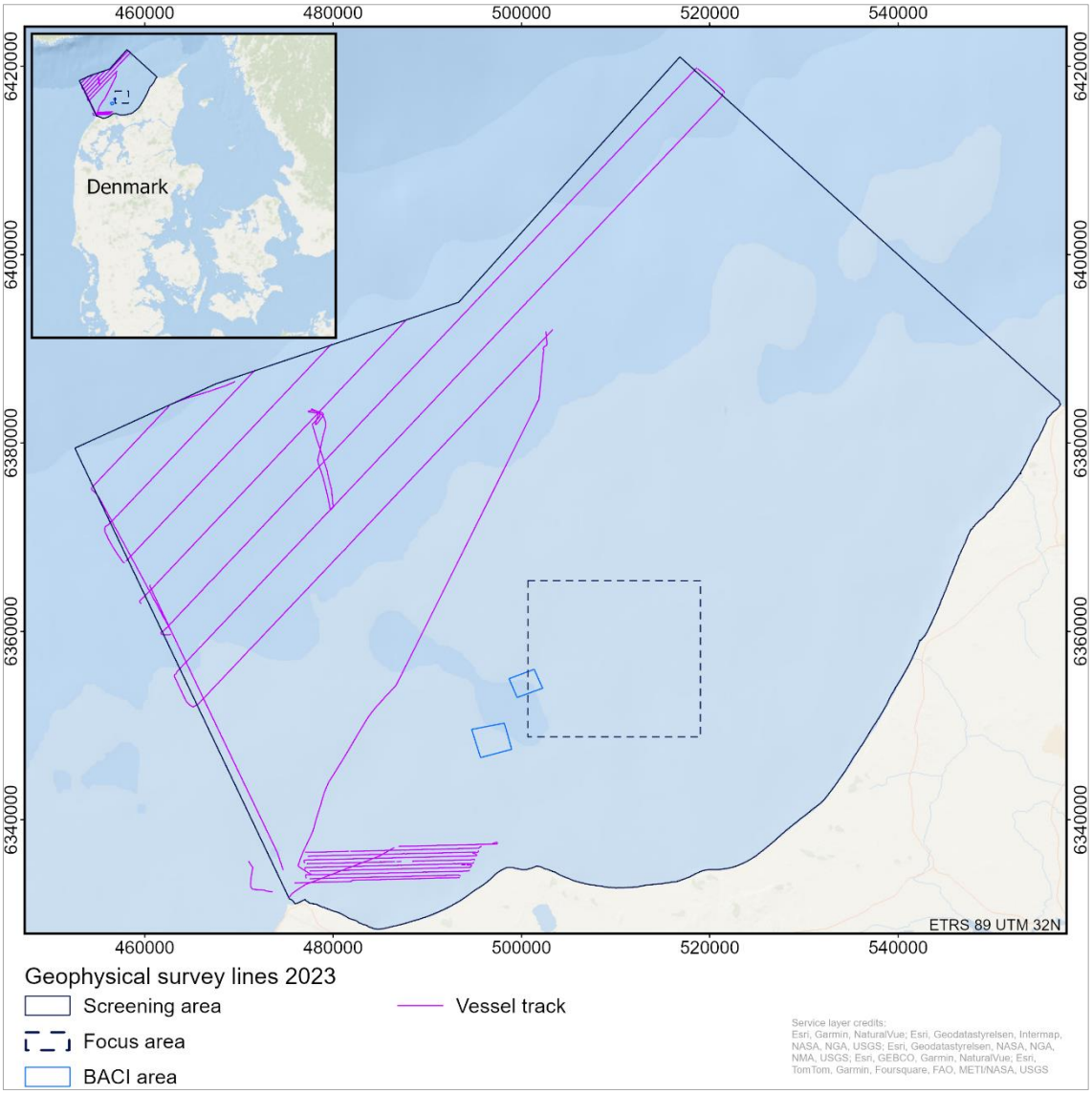

Figure 10.2: Vessel track line exported from the MBES. Screening area survey, December 2023.

10.4 Discussion and perspectives

Despite poor weather conditions and the limited survey duration, most of the planned survey lines were completed. Unfortunately, the side scan sonar and tow cable were lost. However, the MBES system recorded backscatter which also provides information that is applicable for interpretation of seabed substrate.

Due to the poor weather conditions in the offshore area, nearshore survey lines were added to the survey. These data provide valuable information in relation to the complex geology and the diverse spatial distribution of substrate types off the coast of Hanstholm.

11. Topobathymetric airborne laser scanning survey (Task 1.10)

Mikkel S. Andersen, Lars Ø. Hansen, Zyad Al-Hamdani, Verner B. Ernstsen

11.1 Introduction and aim

The aim of Task 1.10 was to plan and conduct a topobathymetric airborne laser scanning (ALS) survey in the shallow water coastal zone of Jammer Bay and process and analyse the acquired ALS data.

Topobathymetric ALS, also commonly known as green lidar (light detection and ranging), utilises short green laser pulses for high resolution mapping of bathymetry in very shallow waters. It is an active remote sensing technique that is used to create accurate and precise 3D models and visualisations of landscapes and surfaces whether above or below water. Topobathymetric ALS data were recorded from the coastline towards the 10 m water depth curve in the southern part of the Jammer Bay. Simultaneously, high-resolution RGB-images were recorded. The topobathymetric ALS data were processed to deliver fully processed and classified point clouds as well as digital surface models (DSM) of the water surface and the seabed and digital terrain models (DTM) of the seabed.

11.2 Materials and methods

Topobathymetric ALS data were collected by Airborne Hydro Mapping GmbH (AHM). A twin-engine plane (Tecnam P2006T) was used as flight deck with a laser scanner (RIEGL VQ-880-G) integrated in the frontal part of the aircraft. The laser scanner emits a green laser pulse with a wavelength of 532 nm with a laser pulse repetition rate of up to 550 kHz. The flight altitude was 500 m, which combined with a laser beam divergence of 1.1 mrad, yields a laser beam footprint of ~0.5 m. The laser scan pattern is circular with an incidence angle of 20°, generating a scan pattern of curved parallel lines with a swath width of ~500 m at a flight altitude of 500 m. The point density is ~20 points/m^2 at a flight altitude of 500 m and a flight speed of ~80 kn (~150 km/h). According to RIEGL, the typical water depth measuring range is 1.5 Secchi depth. The laser scanner system records full waveform data. Intensity information is provided for each returned signal.

Aerial RGB images were recorded by an aerial camera (Hasselblad H3D-39 with a focal length of 35 mm) integrated in the back of the aircraft. The ground sampling distance (GSD) of the RGB images is ~10 cm at a flight altitude of 500 m. The RGB images serve also as ground truth data due to this high image resolution.

Aircraft position and attitude were recorded by a GNSS/IMU navigation system at a rate of 256 Hz consisting of a compact GNSS antenna (NovAtel 42G1215A-XT-1-1-CERT) mounted outside of the aircraft and an IMU (IGI AEROcontrol-IIe) mounted on top of the laser scanner.

The processing of the raw ALS data for producing a point cloud and subsequently a digital elevation model (DEM) followed the processing procedure outlined by Andersen et al. (2017). The

processing pipeline contained the overall steps of determining the flight trajectory; georeferencing the point cloud; aligning the swaths (i.e. strip adjustment) to minimize the bias between individual swaths; filtering (or classifying) the point cloud to remove noise; detecting the water surface (i.e. water surface modelling); correcting all points below the water surface for refraction of the laser beam; and producing a DEM from the filtered and corrected point cloud (see Andersen et al. (2017) for a detailed description of each step).

11.3 Results

The spatial coverage of the topobathymetric ALS data in the coastal zone in the southern part of Jammer Bay is shown in Figure 11.1. Processing and analyses of the ALS data are ongoing.

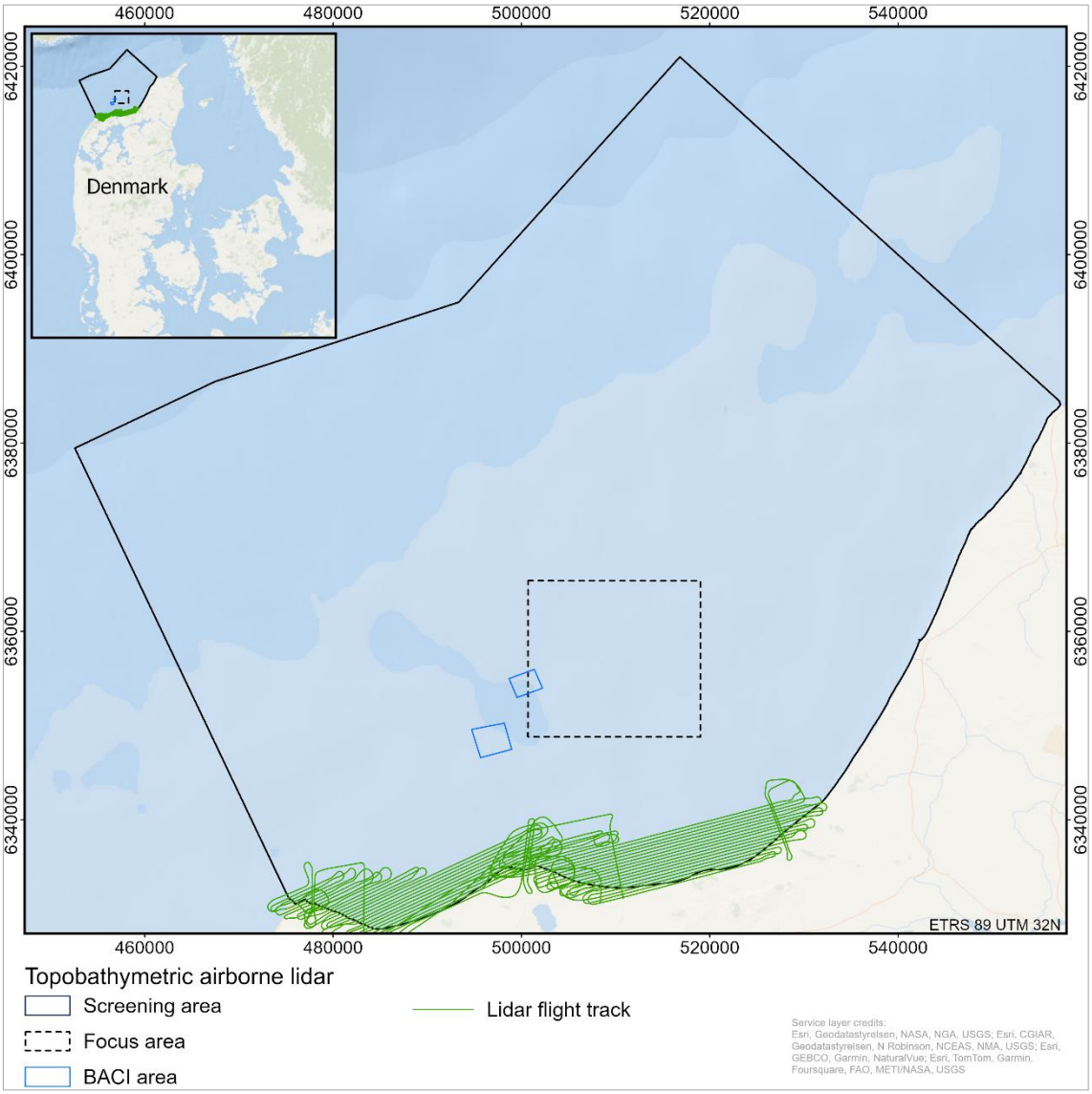

Figure 11.1: Spatial coverage of the topobathymetric ALS data in the coastal zone in the southern part of Jammer Bay.

11.4 Discussion and perspectives

The processing pipeline, specifically the filtering/classification step and the water surface modelling step, was further developed and optimised to improve the quality of the filtering/classification and to reduce the processing time, which is essential when working with large datasets (i.e. millions of points with multiple attributes).

Topobathymetric ALS provides the potential of extending detailed seabed mapping into the shallow water zone towards the coastline and across the land-water transition zone. Full-coverage seabed mapping by vessel borne MBES in very shallow water is very time consuming and therefore also expensive, which makes it practically inapplicable for large scale coastal zone mapping in very shallow water at regional and national level.

From a future application-perspective, high-resolution and full-coverage seabed mapping in shallow water coastal zones is feasible using topobathymetric ALS, and it has an enormous potential for mapping and monitoring geodiversity and benthic habitats in such shallow waters. Hence, topobathymetric ALS enables seamless mapping of geodiversity and habitats in the shallow water coastal zone and across the land-water transition. However, the lidar data processing time is still considerable despite continuous optimisation of the processing pipeline. Hence, further automatisation of ALS data processing is still required.

12. Sediment and carbon analyses (Task 1.11)

Lars Ø. Hansen, Henrik I. Petersen, Pernille Stockmarr, Mikkel S. Andersen, Zyad Al-Hamdani, Verner B. Ernstsen

12.1 Introduction and aim

The aim of Task 1.11 was to perform sediment and carbon analyses to determine seabed sediment and carbon composition.

An ROV video and HAPS sampler survey was conducted to provide additional information on seabed substrates and grain size distributions. HAPS cores were collected at 71 locations in autumn 2023 by WSP (cf. Appendix 1.1). Subsamples were taken from the upper 2 cm and analysed in GEUS' Sediment Lab to determine water content, organic matter content and grain size distributions by both sieving and laser diffraction that includes the finer fractions <63µm. Furthermore, 60 sediment samples collected by a grab sampler in spring 2023 by DTU Aqua were analysed in GEUS' Sediment Lab to determine organic matter content and grain size distributions by sieving, i.e. only the coarser fractions >63µm. The 60 sediment samples collected in spring 2023 as well as the 71 sediment samples collected in autumn 2023 were analysed in GEUS' Carbon Lab to determine total carbon (TC) and total sulfur (TS) as well as total organic carbon (TOC).

12.2 Materials and methods

Sample positions and ID of the 71 HAPS-samples collected in the Screening area and the Focus area as well as the 60 grab samples collected inside the BACI area are shown in Figure 12.1, Figure 12.2., and Figure 12.3.

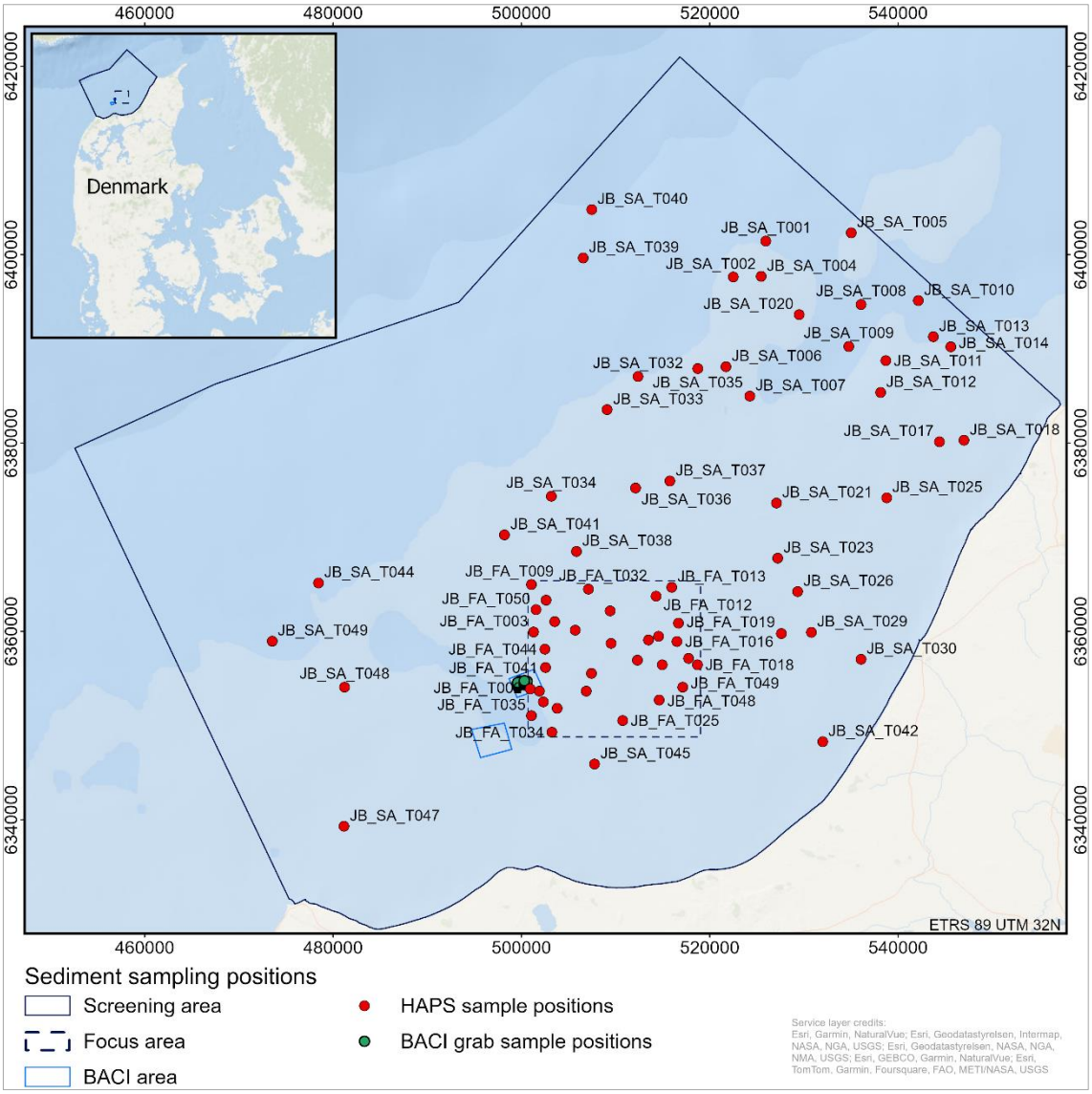

Figure 12.1: HAPS sample positions and ID of the 71 samples collected from the upper 2 cm of the seabed. For analysis results see appendix 1.2.

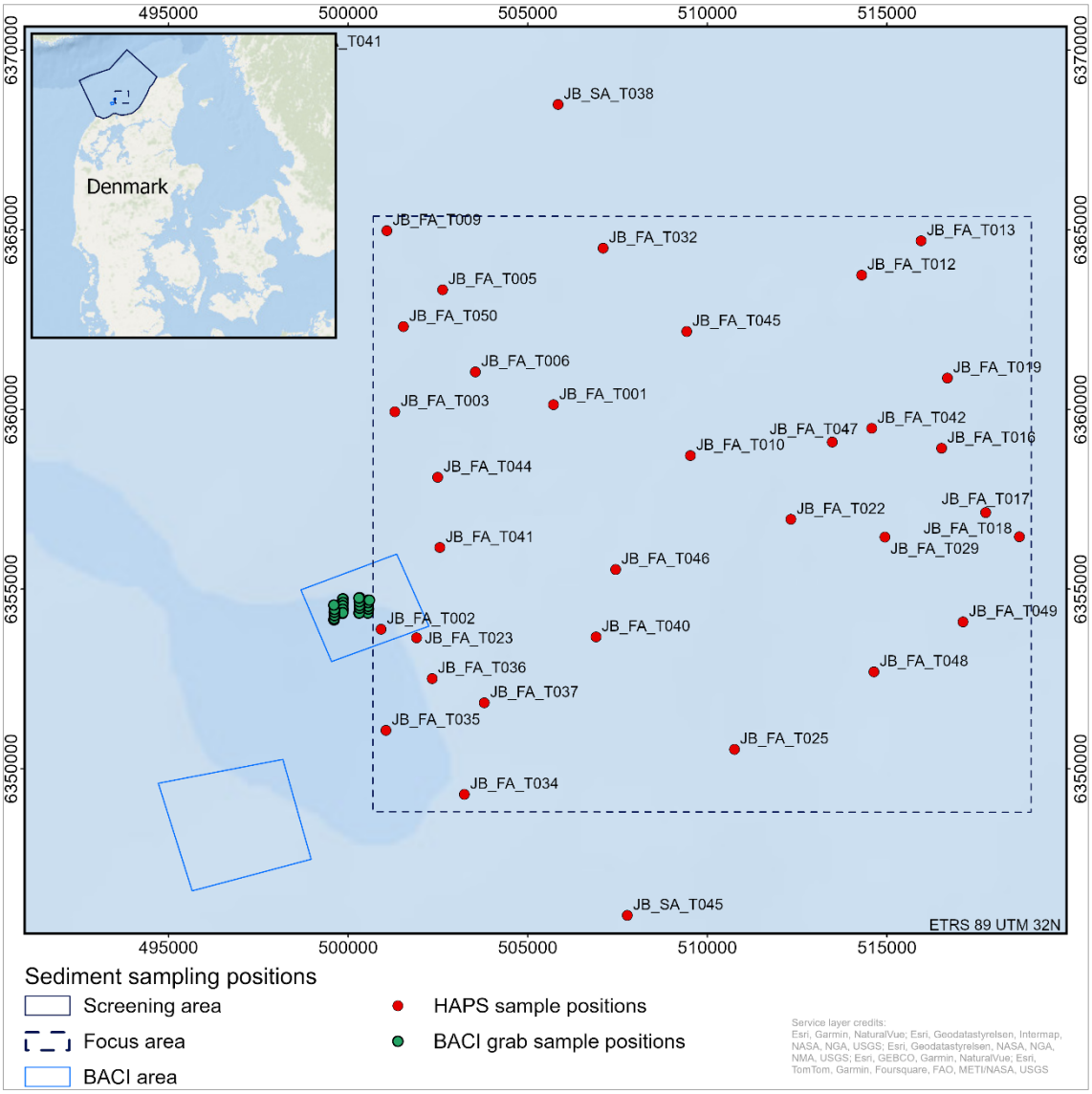

Figure 12.2: HAPS sample positions and ID of the samples collected from the upper 2 cm of the seabed inside the Focus area. For analysis results see appendix 1.2.

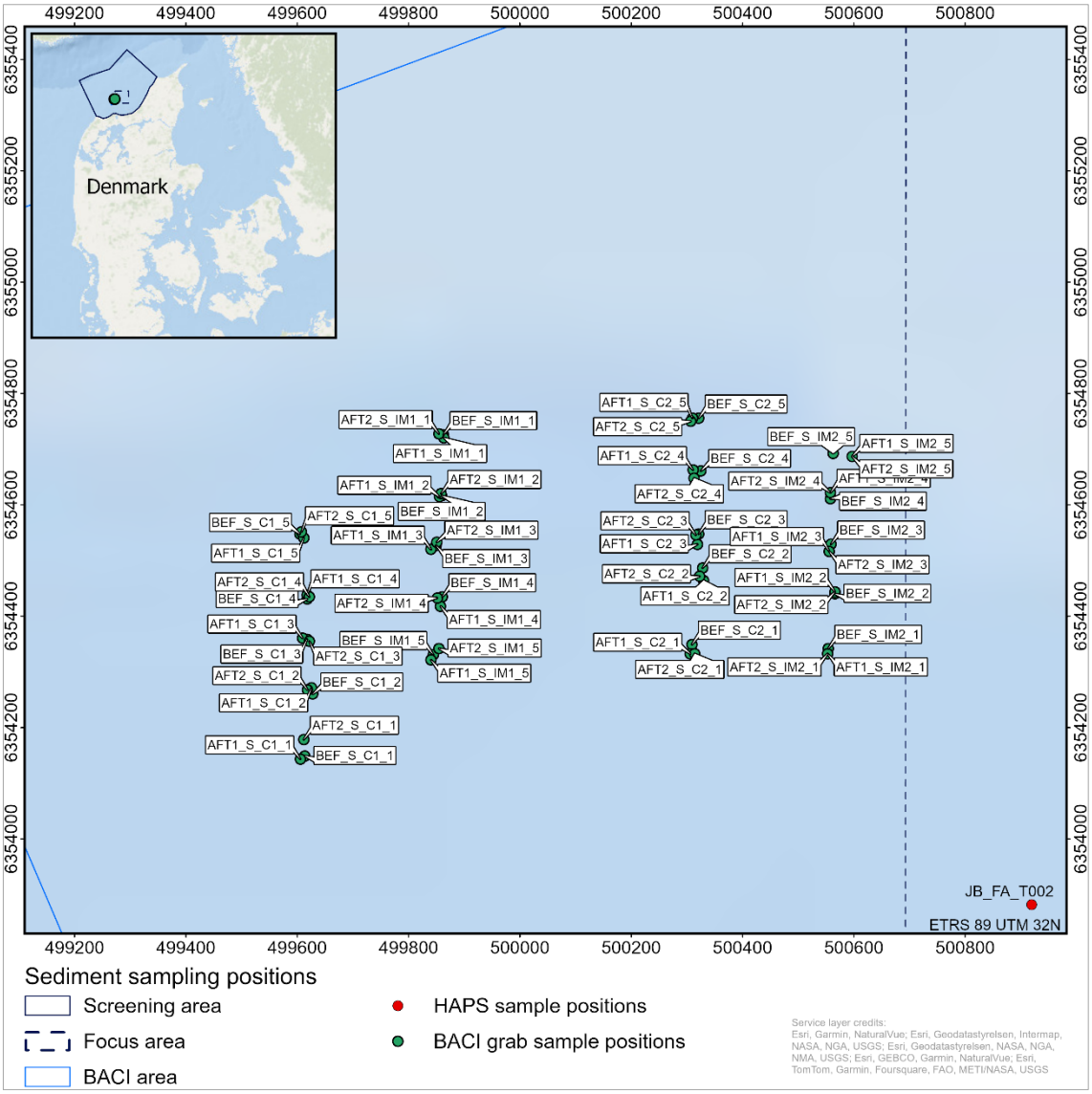

Figure 12.3: Grab sample positions and ID inside the BACI area. For analysis results see appendix 1.3.

Grain size distributions and organic matter content were determined in GEUS' Sediment Lab and carried out as illustrated in Figure 12.4.

Each of the three analyses was based on subsamples. Water content and organic matter content were determined according to the DS 405.11 and DS 204 standards. First the wet sample weight was determined whereafter the sample was oven dried at 105°C to obtain the dry sample weight. The water content was obtained by subtracting the dry sample weight from wet sample weight. To determine the organic matter content by Loss on Ignition (LOI) the dry sample was burned at 550°C. The weight of the burned sample was subtracted from the dry sample weight to obtain LOI.

Grain size distributions of the coarse fraction (>63µm) was determined by dry sieving according to the DS 405.9 standard extended to ½ phi scale with the following sieve sizes (µm): 32,000; 16,000; 8,000; 4,000; 2,800; 2,000; 1,400; 1,000; 710; 500; 355; 250; 180; 125; 90; 75 and 63.

The sediment retained in each of the sieves was weighed to obtain the sample distribution in relation to the total dry sample weight.

Grain size distributions of the fine fraction (<63µm) were determined by laser diffraction using a Malvern MasterSizer 2000. Based on the dry sieving results, samples for laser diffraction were selected based on weight-% of fine grains, i.e. samples containing >5% fines were analysed with laser diffraction. The subsamples were initially wet sieved to isolate the fine fraction for the grain size analysis.

Grain size statistics were computed in GRADISTAT v.9.1 (Blott and Pye 2001).

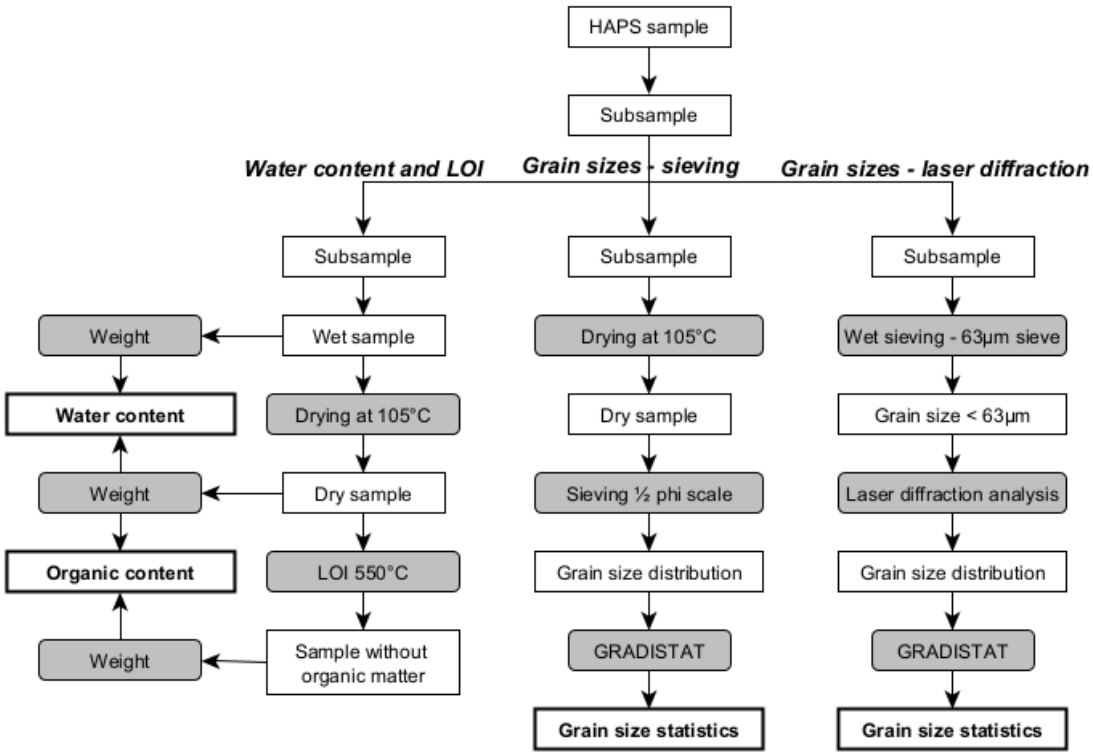

Figure 12.4: Flowchart illustrating the analysis steps to determine water content and organic matter content by Loss on Ignition (LOI), and grain size distribution of the coarse fraction (>63µm) by sieving and of the fine fraction (<63µm) by laser diffraction.

A LECO CS-200 induction furnace was used to determine the contents of Total Organic Carbon (TOC, wt%), Total Carbon (TC, wt%), and Total Sulfur (TS, wt%). The samples were crushed to powder and 50 mg was used for TC/TS determination. TOC was determined after removal of carbonate-bonded carbon by HCl. A total of 300 mg was pyrolyzed. The content of inorganic carbon was determined by subtracting TOC from TC.

The analysis results were merged in an Excel spread sheet and converted to a shape file in ArcGIS Pro for visualization purposes.

12.3 Results

Figure 12.5 shows the sediment size class distributions of the upper 2 cm of the seabed superimposed on the interpreted substrate types. The results show a diverse distribution of the sediment size classes, many samples are dominated by fine and medium sized sand.

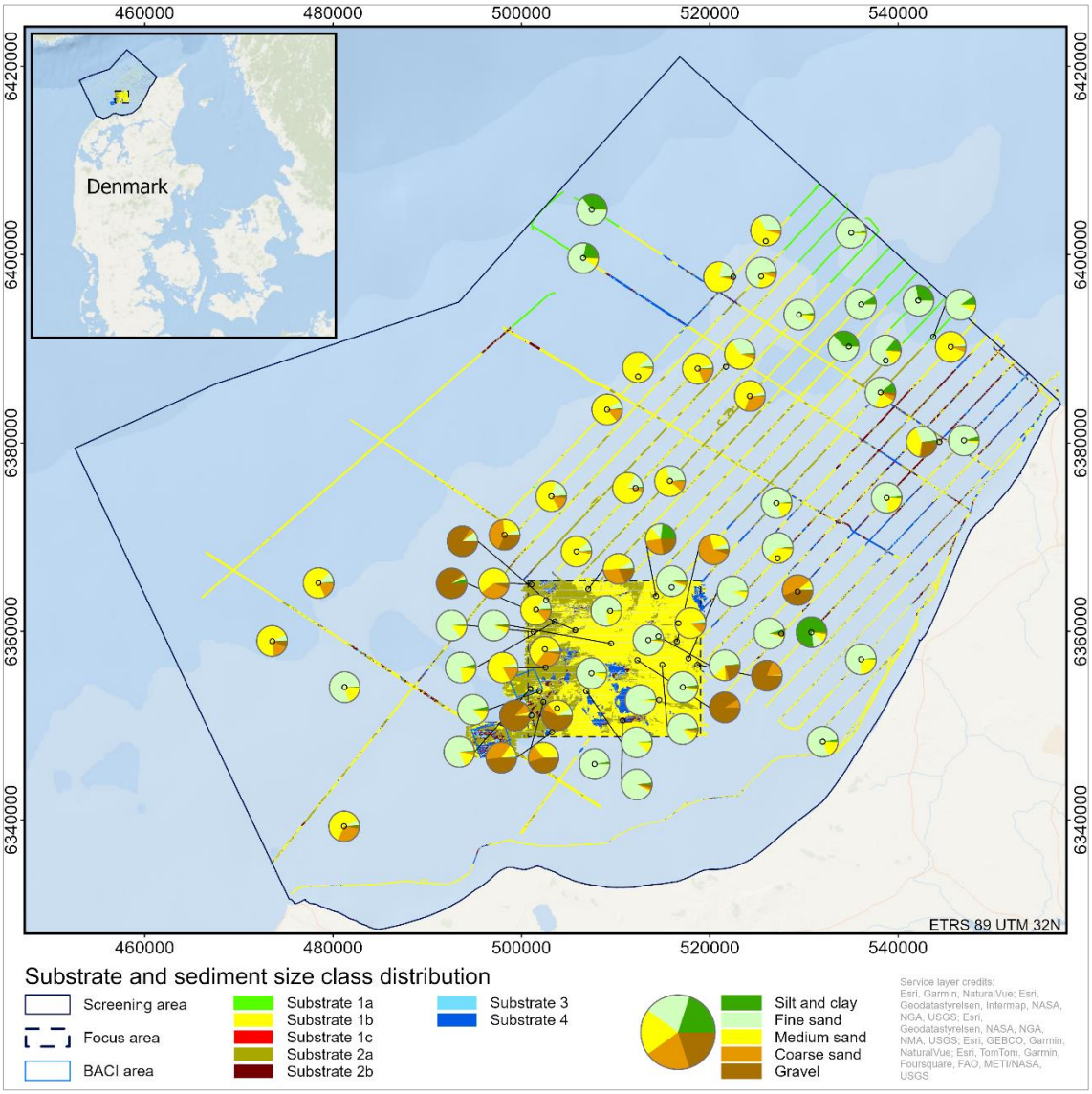

Figure 12.5: Pie charts of the sediment size class distributions in each of the analysed samples superimposed on the substrate types.

The mean grain size of the sand and gravel fractions (> 63 µm) labelled according to the descriptive terms of Folk & Ward (1957) is shown in Figure 12.6 superimposed on the interpreted substrate types. The spatial distribution of the mean grain size analysis shows that most samples, characterized by a coarse mean grain size, are found in and around the Focus area.

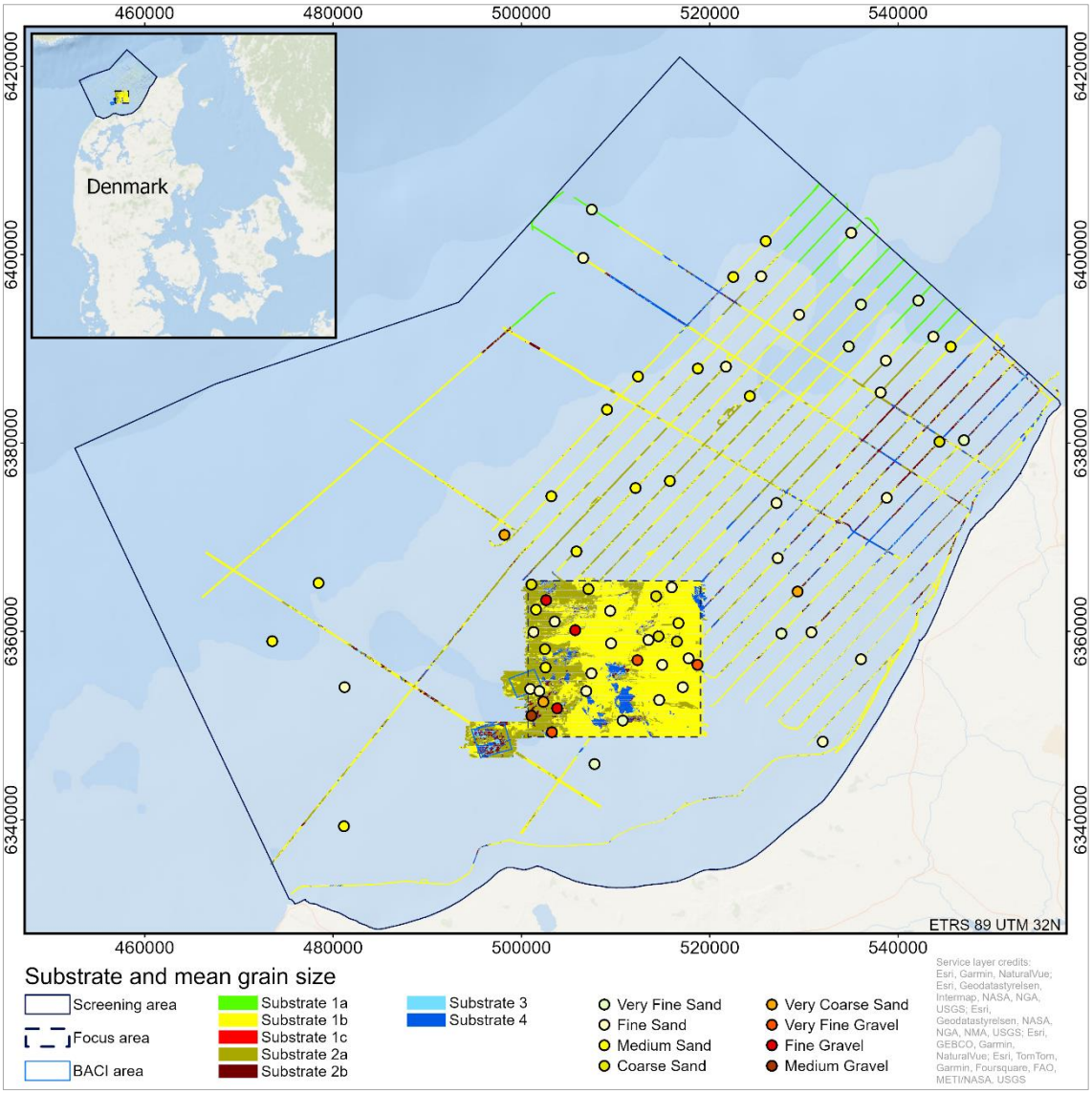

Figure 12.6: Description of mean grain size (after Folk and Ward, 1957) in each of the analysed samples superimposed on the substrate types.

For detailed results of the sediment and carbon analyses see appendix 1.2 and 1.3.

12.4 Discussion and perspectives

The sediment grain size analyses and grain size statistics will be used to verify the geophysical interpretations in relation to seabed substrate types and seabed habitat types to generate maps that combine spatial geophysical data and point ground truth data to achieve optimal mapping results – which was beyond the tasks of the JAMBAY project due to time constraints. This verification is specifically important in areas with diffuse gradients from finer to coarser sediments or vice versa.

In addition, the sediment grain size analyses and grain size statistics form the basis for estimating thresholds of sediment mobilisation and/or resuspension. Hence, the grain size characteristics are fundamental to assess the stability/dynamics of the seabed. Finally, the combination of

seabed morphology (Chapter 7) and seabed substrates and sediments (Chapters 8 and 12) are key components to develop conceptual geomorphological models for the Jammer Bay. This is important to understand the current and prevailing seabed dynamics, and to be able to assess potential changes in the future.

The carbon analyses will be a first step towards a large-scale estimation of carbon content in seabed surface sediments across different substrate types, water depths and other environmental conditions in Danish waters. The carbon analyses will enable further investigations of the impact of bottom trawling on the release of carbon from seabed surface sediments and the subsequent ability of the seabed surface sediments to store carbon. Hence, the data and information will also contribute to shed light on the ongoing discussion on the role of bottom trawling in releasing carbon and specifically carbon dioxide from seabed sediments to the atmosphere, and thereby on the degree of impact of bottom trawling on climate (cf. Sala et al. 2021; Hiddink et al. 2023; Atwood et al. 2024).

13. Acknowledgements

We wish to thank the Danish Environmental Protection Agency, the Danish Coastal Authority, and the Danish Energy Agency for providing supplementary survey data from the Jammer Bay area. In addition, we thank the captain and crew onboard MV Arctic Ocean for their efforts during the JAMBAY surveys in June and December 2023.

This project was funded by the project 'Mapping of seabed habitats and impacts of beam trawling and other demersal fisheries for spatial ecosystem-based management of the Jammer Bay (JAMBAY)' (Grant Agreement No 33113-B-23-189) by the European Maritime and Fisheries Fund (EMFF) and the Ministry of Food, Agriculture and Fisheries of Denmark.

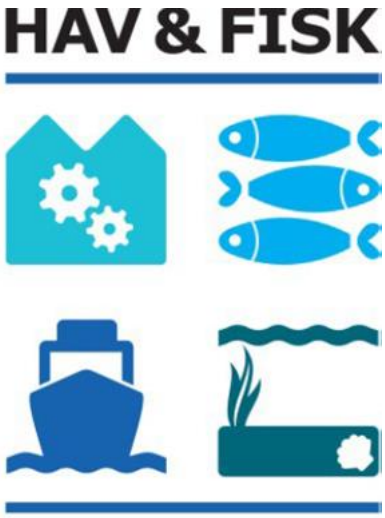

14. References

Andersen MS, Gergely A, Al-Hamdani Z, Steinbacher F, Larsen LR, Ernstsen VB (2017). Processing and performance of topobathymetric lidar data for geomorphometric and morphological classification in a high-energy tidal environment (2017). *Hydrology and Earth System Sciences*, 21: 43-63.

Andersen, T.S., Huuse, M., Jørgensen, F. and Christensen, S. (2012). Seismic investigations of buried tunnel valleys on- and offshore Denmark. Geol. Soc. London. Special publication. Vol. 368, pp. 129-144. DOI: 10.1144/SP368.14.

Astrup, P.M. (2023). North Sea OWF Zone Maritime archaeology Geo-archaeological analysis, report for Energistyrelsen. Nordjyllands Kystmuseum, Moesgaard Museum og De kulturhistoriske Museer, Holstebro Kommune, 2023.

Atwood, T. B., Romanou, A., DeVries, T., Lerner, P. E., Mayorga, J. S., Bradley, D., … Sala, E. (2024). Atmospheric CO2 emissions and ocean acidification from bottom-trawling. *Frontiers in Marine Science*, *10*. doi:10.3389/fmars.2023.1125137

Bennike, O., Nørgaard-Pedersen, N., Jensen, J.B., Andresen, K.J. & Seidenkrantz, M.-S. (2019). Development of the western Limfjord, Denmark, after the last deglaciation: a review with new data. Bulletin of the Geological Society of Denmark, Vol. 67, pp. 53–73, ISSN 2245-7070. (www.2dgf. dk/publikationer/bulletin).

Blott, S.J., Pye, K. (2001). GRADISTAT: a grain size distribution and statistics package for the analysis of unconsolidated sediments. Earth Surf. Process. Landf. 26 (11), 1237–1248. https://doi.org/10.1002/esp.261.

Brandes, C., Steffen, H., Sandersen, P.B.E, Wu, P., Winsemann, J. (2018). Glacially induced faulting along the NW segment of the Sorgenfrei-Tornquist Zone, northern Denmark: Implications for neotectonics and Late glacial fault-bound basin formation. Quaternary Science Reviews 189, 149-168. https://doi.org/10.1016/j.quascirev.2018.03.036.

Council Directive 92/43/EEC of 21 May 1992 on the conservation of natural habitats and of wild fauna and flora, O.J. L206, 22.07.92

EC (European Commission) (2013). Interpretation Manual of European Union habitats. EUR 28: 1–144. http://ec.europa.eu/environment/nature/legislation/habitatsdirective/docs/Int_Manual_EU28.pdf

Folk, R.L., Ward, W.C. (1957). Brazos River bar: a study in the significance of grain size parameters. Journal of Sedimentary Petrology, 27, 3-26.

Funck, T., Ehrhardt, A., Andreasen, N. R., Behrens, T., Christensen, N., Demir, Ü., Ebert, T., Nielsen, T. B., Nørmark, E., Pedersen, H., Schramm, B., Smith, L., Steinborn, P., & Trinhammer, P. (2023). *Acquisition of marine seismic data in Jammerbugt in 2023. CCS2022-2024*

WP1: Seismic data acquisition across the Jammerbugt structure on research vessel Jákup Sverri. GEUS. Danmarks og Grønlands Geologiske Undersøgelse Rapport Bind 2023 Nr. 39 https://doi.org/10.22008/gpub/34706

Helmig, S.A., Nielsen, M.M. & Petersen, J.K. (2020). Andre presfaktorer end næringsstoffer og klimaforandringer – vurdering af omfanget af stenfiskeri i kystnære marine områder. DTU Aqua-rapport nr. 360-2020. Institut for Akvatiske Ressourcer, Danmarks Tekniske Universitet. 24 pp

Hiddink, J. G., Van de Velde, S. J., McConnaughey, R. A., De Borger, E., Tiano, J., Kaiser, M. J., … Sciberras, M. (2023). Quantifying the carbon benefits of ending bottom trawling. *Nature*, 617(7960), E1-E2. doi:10.1038/s41586-023-06014-7

Hughes-Clarke, J. E., Mayer, L. A., & Wells, D. E. (1996). Shallow-Water Imaging Multibeam Sonars: A New Tool for Investigating Seafloor Processes in the Coastal Zone and on the Continental Shelf. Marine Geophysical Researches, 18, 607-629.

Hughes-Clarke, J. E. (2018). The impact of acoustic imaging geometry on the fidelity of seabed bathymetric models. *Geosciences* 2018, 8, 109; doi:10.3390/geosciences8040109.

Jasiewicz, J., Stepinski, T. J. (2013). Geomorphons – a pattern recognition approach to classification and mapping of landforms, Geomorphology, 182, January 15, 2013: 147-56. https://doi.org/10.1016/j.geomorph.2012.11.005

Jensen, J.B., Leth, J.O., Borre, S. & Nørgaard-Pedersen, N. (2010). Model for potentielle sand- og grusforekomster for de danske farvande. Delområdet Jyske Rev - Lille Fisker Banke. GEUS Report 2010 (23).

Larsen, N. K., Knudsen, K. L., Krohn, C. F., Kronborg, C., Murray, A. S. & Nielsen, O. B. (2009). Late Quaternary ice sheet, lake and sea history of southwest Scandinavia– a synthesis. Boreas, Vol. 38, pp. 732–761. 10.1111/j.1502-3885.2009.00101.x. ISSN 0300-9483.

Leth, J. O. (1996). Late Quaternary geological development of the Jutland Bank and the initiation of the Jutland Current, NE North Sea. Norges geologiske undersøgelse Bulletin 430, 25–34.

Michelsen, O. & Nielsen, L.H. (1993). Structural development of the Fennoscandian Border Zone, offshore Denmark. Marine and Petroleum Geology, Vol. 10(2), p.124-134. https://doi.org/10.1016/0264-8172(93)90017-M.

Miljøstyrelsen (2021a). Marin habitatkortlægning i Nordsøen 2019-2020. Udført af GEUS og WSP Danmark for Miljøstyrelsen.

Miljøstyrelsen (2021b). Faglige kriterier for opdatering af habitatområdernes udpegningsgrundlag for habitatnaturtyper – 2021. Miljøstyrelsen, J.nr. MST-821-00515, 3 pp.

Miljøstyrelsen (2018). Kortlægning af Natura 2000-områder Marin habitatkortlægning i Skagerrak og Nordsøen 2017-2018. Udført af GEUS og Orbicon for Miljøstyrelsen.

Miljøstyrelsen (2016). Habitatbeskrivelser, årgang 2016 – Beskrivelse af danske naturtyper omfattet af habitatdirektivet (NATURA 2000 typer). Miljøstyrelsen, Habitatbeskrivelser, ver. 1.05, maj 2016, 38 pp.

Morén, B. M., Sejrup, H. P., Hjelstuen, B. O., Borge, M. V. & Schäuble, C. (2018). The last deglaciation of the Norwegian Channel– geomorphology, stratigraphy and radiocarbon dating. Boreas, Vol. 47, pp. 347–366. https://doi.org/10.1111/bor.12272. ISSN 0300-9483.

Naturstyrelsen (2011). Marin råstof- og naturtypekortlægning i Nordsøen 2010. Udført af GEUS og Orbicon for Naturstyrelsen.

Nielsen, T., Mathiesen, A., Bryde-Auken, M. (2008). Base Quaternary in the Danish parts of the North Sea and Skagerak. Gological Survey of Denmark and Greenland Bulletin 15. DOI:10.34194/GEUSB.V15.5038.

Pedersen, S.A.S. (2006). Strukturer og dynamisk udvikling af Rugbjerg Knude Glacialtektoniske Kompleks, Vendsyssel, Danmark. Geologisk Tidsskrift, hæfte 1, 46 pp.

Pike, R. J., Evans, I. S., & Hengl, T. (2009). Geomorphometry: A Brief Guide. In H. Tomislav & I. R. Hannes (Eds.), Geomorphometry: Concepts, Software, Applications. Developments in soil science (Vol. 33, pp. 3-30). Amsterdam: Elsevier.

Påsse, T. & Andersson, L., (2005). Shore-level displacement in Fennoscandia calculated from empirical data. Geologiska Föreningens i Stockholm Förhandlingar 127, 253–268.

QPS (2023). Qimera 2.5 Documentation, 10 July 2023. QPS B.V.

R2Sonic (2022). Sonic 2026/2024/2022 Broadband multibeam echosounders – operation manual v6.3, rev. 012. R2Sonic LLC, Austin, Texas, USA, 2021.

Sala, E., Mayorga, J., Bradley, D., Cabral, R. B., Atwood, T. B., Auber, A., … Lubchenco, J. (2021). Protecting the global ocean for biodiversity, food and climate. *Nature, 592,* 397-402. doi:10.1038/s41586-021-03371-z

Sandersen, P. B. E., Jørgensen, F., Larsen, N. K., Westergaard, J. H., & Auken, E. (2009). Rapid tunnel-valley formation beneath the receding Late Weichselian ice sheet in Vendsyssel, Denmark. BOREAS, Vol. 38, Issue 4, pp. 834-851

SBG Systems (2022). Navsight Marine Solution. Leaflet MK011EN v2.4 2022.11. SBG Systems.

Wilson, M. F. J., O'Connell, B., Brown, C., Guinan, J. C., & Grehan, A. J. (2007). Multiscale Terrain Analysis of Multibeam Bathymetry Data for Habitat Mapping on the Continental Slope. Marine Geodesy, 30, 3-35.

Appendix 1.1: Marine ROV and HAPS sampling survey in Jammer Bay 2023 by WSP

Report by WSP

As part of the JAMBAY project 2023, WSP has performed two types of surveys – A ROV/HAPS survey regarding visual verification of the seabed sediment characteristics, and sediment sampling for grain size analysis. The results from the survey were primarily used by GEUS for further analyses.
The other survey was conducted as an in-fauna HAPS survey for in-fauna analysis and statistics. The results from the survey were primarily used by DTU Aqua for further analyses.

ROV sampling
As part of the visual verification survey – app. 100 target positions were pointed out by GEUS for further investigation. All positions were visually inspected as part of the survey.
A ROV was used for visual inspection of the seabed and quantification of seabed type and characteristics, benthic flora and fauna including species/taxa number and coverage (%) and the number of fish species and coverage (%). The first activity on each station was a ROV inspection showing the seabed characteristics, flora and fauna live on deck. Visual inspection of the seabed with ROV is always done before HAPS sampling to ensure sampling on loose sediment. A BlueROV2 (Fig. 1) was used, with an exact position of the crane, which gives information of the position of the ROV as well as showing the position in each frame/photography. A complete Digital Video System was used, including all equipment, laptops, cabling, connections, screens, spares etc. The equipment is set up so both the helmsman and the camera operator can see the image/video in real time. A voiceover for the video was recorded as well as filling out a field log (logbook) for each station. The logbooks include position, depth, seabed sediment types/composition, habitat types and determination of species (flora and fauna) and coverage of species and biogenic structures observed on the seabed surface (e.g., sandworms, fish foraging holes in the seabed, mysids/shrimps etc.). Other parameter targets, at the same station were included in the logbook. Sufficient storage media was ensured, and back-up of all data was performed at least twice a day on two hard discs.

Figure 1. ROV being pulled out of the water.

HAPS sampling

A HAPS core sampler (Fig. 2) was used for sampling of sediment characteristics, chemical analyses, and infauna quantification. The HAPS core sampler samples a seabed area of 0.0145 m². This instrument complies with the technical requirements for soft bottom fauna sampling in the NOVANA program. Three attempts were made before moving to the next location including the use of a vibrating unit used to force the HAPS into the sediment.

Figure 2. HAPS core sampler.

The first activity at each station was a ROV inspection of the seabed showing the seabed characteristics, flora and fauna live on deck. If e.g., the ROV-video at a station showed, that it was not possible to take HAPS samples due to presence of hard sediment, the position was moved a maximum of three times = three attempts before sampling was abandoned. All in all, 100 HAPS samples were collected for later grain size analysis.

Sediment characteristics

On deck, each successful HAPS-core sediment sample was visually described together with descriptions of sediment composition, colour, smell, and visible fauna. This was logged in the logbooks. Hereafter each sample was stored for later analysis in GEUS laboratory.

Appendix 1.2: Sediment and carbon analyses

Table showing coordinates and results of the sediment and carbon analyses of the 71 HAPS samples collected in the Focus area and Screening area. Grain size statistics are computed from dry sieving results of the size fraction >63 µm. * indicates ROV deployment position.

	Coordinates (DD)		Organic content (wt%)	Grain size classes (wt%)					Folk & Ward descriptive grain size statistics (size in mm)		Carbon (wt%)		Sulfur (wt%)
Sample ID	Long	Lat	Loss on ignition	Silt & Clay	Fine sand	Medium sand	Coarse sand	Gravel	Mean	Sorting	TOC	TC	TS
FA_T001	9.09510	57.38392	1.0	4.84	3.28	0.50	2.20	89.18	Fine Gravel (6.54)	Moderately Sorted	0.03	0.14	0.03
FA_T002	9.01527	57.32785	0.5	1.46	79.99	15.75	2.63	0.17	Fine Sand (0.17)	Moderately Well Sorted	0.02	0.19	0.04
FA_T003	9.02170	57.38225	0.5	1.31	83.90	13.54	1.08	0.18	Fine Sand (0.15)	Well Sorted	0.04	0.18	0.04
FA_T005	9.04377	57.41270	0.4	0.27	9.22	1.10	5.09	84.32	Fine Gravel (4.55)	Poorly Sorted	0.13	0.35	0.05
FA_T006	9.05900	57.39220	0.6	3.79	73.19	21.34	1.39	0.28	Fine Sand (0.17)	Moderately Well Sorted	0.03	0.36	0.04
FA_T009	9.01795	57.42750	0.3	0.61	0.92	58.67	34.22	5.58	Coarse Sand (0.56)	Moderately Sorted	0.01	0.15	0.01
FA_T010	9.15850	57.37117	0.8	1.86	89.12	6.30	0.68	2.05	Fine Sand (0.14)	Well Sorted	0.00	0.28	0.05
FA_T012	*9.23797	*57.41615	2.6	22.93	13.24	16.09	25.60	22.13	Coarse Sand (0.77)	Very Poorly Sorted	0.39	0.97	0.15
FA_T013	9.26562	57.42467	0.5	1.42	91.12	2.57	3.51	1.38	Fine Sand (0.14)	Moderately Well Sorted	0.10	0.22	0.04
FA_T016	9.27472	57.37280	0.3	0.59	6.01	23.25	64.53	5.61	Coarse Sand (0.83)	Poorly Sorted	0.02	0.30	0.02
FA_T017	9.29500	57.35667	0.5	1.11	91.24	7.28	0.34	0.02	Fine Sand (0.13)	Well Sorted	0.02	0.17	0.04
FA_T018	9.31052	57.35062	0.5	0.10	0.17	0.89	17.80	81.04	Very Fine Gravel (3.33)	Moderately Sorted	0.01	0.32	0.03
FA_T019	9.27752	57.39032	0.3	0.93	3.86	83.40	10.02	1.80	Medium Sand (0.44)	Well Sorted	0.02	0.20	0.02
FA_T022	9.20490	57.35513	0.3	0.03	0.04	0.08	8.53	91.31	Very Fine Gravel (3.30)	Moderately Well Sorted	0.02	0.23	0.02
FA_T023	9.03170	57.32568	0.8	3.61	83.01	10.74	2.23	0.41	Fine Sand (0.14)	Moderately Well Sorted	0.06	0.34	0.05
FA_T025	9.17843	57.29770	0.7	1.80	89.66	2.03	2.63	3.87	Very Fine Sand (0.12)	Moderately Sorted	0.05	0.29	0.03
FA_T029	*9.24827	*57.35062	0.7	1.81	84.25	9.97	2.43	1.54	Fine Sand (0.13)	Moderately Well Sorted	0.06	0.38	0.05
FA_T032	9.11827	57.42307	0.4	0.76	7.38	43.13	30.71	18.01	Coarse Sand (0.72)	Poorly Sorted	0.02	0.61	0.04
FA_T034	9.05373	57.28655	0.4	0.72	2.76	11.48	36.85	48.19	Very Fine Gravel (2.02)	Poorly Sorted	0.03	0.26	0.02
FA_T035	9.01752	57.30257	0.6	0.12	0.19	3.18	10.05	86.46	Medium Gravel (10.1)	Poorly Sorted	0.02	0.28	0.03
FA_T036	9.03885	57.31553	0.5	0.42	1.41	33.79	18.89	45.49	Very Coarse Sand (1.68)	Poorly Sorted	0.09	0.26	0.03
FA_T037	9.06297	57.30945	0.8	0.51	7.77	27.42	7.53	56.76	Fine Gravel (4.35)	Very Poorly Sorted	0.01	0.24	0.03
FA_T040	9.11460	57.32588	0.5	1.26	87.06	11.57	0.11	0.00	Fine Sand (0.15)	Well Sorted	0.02	0.13	0.04
FA_T041	9.04243	57.34825	0.3	1.09	4.13	77.70	16.68	0.40	Medium Sand (0.41)	Moderately Well Sorted	0.01	0.09	0.02
FA_T042	9.24237	57.37782	0.6	1.45	61.41	13.37	3.41	20.36	Coarse Sand (0.53)	Very Poorly Sorted	0.11	0.29	0.04
FA_T044	9.04153	57.36583	0.4	0.71	4.05	60.05	32.34	2.85	Coarse Sand (0.51)	Moderately Sorted	0.01	0.24	0.02
FA_T045	9.15680	57.40218	0.6	1.07	76.48	22.05	0.37	0.04	Fine Sand (0.16)	Well Sorted	0.03	0.22	0.04
FA_T046	9.12372	57.34275	0.6	1.47	91.30	6.78	0.41	0.04	Fine Sand (0.13)	Well Sorted	0.03	0.26	0.04
FA_T047	9.22417	57.37442	0.6	1.43	94.88	2.20	1.09	0.40	Fine Sand (0.13)	Very Well Sorted	0.04	0.33	0.05
FA_T048	9.24307	57.31695	0.6	1.25	96.14	2.42	0.17	0.01	Fine Sand (0.13)	Very Well Sorted	0.03	0.21	0.04
FA_T049	9.28437	57.32937	0.9	2.37	92.58	3.12	0.55	1.38	Fine Sand (0.13)	Well Sorted	0.06	0.30	0.04
FA_T050	9.02562	57.40348	0.4	1.35	12.70	72.01	13.06	0.87	Medium Sand (0.34)	Moderately Sorted	0.00	0.16	0.02
SA_T001	9.43622	57.75423	0.5	1.12	31.91	62.73	3.79	0.44	Medium Sand (0.25)	Moderately Well Sorted	0.03	0.40	0.05
SA_T002	9.37770	57.72022	0.3	1.26	19.44	75.76	2.37	1.18	Medium Sand (0.25)	Well Sorted	0.02	0.51	0.04
SA_T004	9.42720	57.72057	0.6	1.70	70.29	21.96	5.01	1.04	Fine Sand (0.19)	Moderately Sorted	0.04	0.29	0.05
SA_T005	9.58862	57.76153	0.9	2.03	95.58	2.01	0.27	0.11	Fine Sand (0.13)	Very Well Sorted	0.08	0.27	0.06
SA_T006	9.36385	57.63470	0.4	1.32	32.80	60.71	4.22	0.95	Fine Sand (0.25)	Moderately Well Sorted	0.02	0.06	0.03

	Coordinates (DD)		Organic content (wt%)	Grain size classes (wt%)					Folk & Ward descriptive grain size statistics (size in mm)		Carbon (wt%)		Sulfur (wt%)
Sample ID	Long	Lat	Loss on ignition	Silt & Clay	Fine sand	Medium sand	Coarse sand	Gravel	Mean	Sorting	TOC	TC	TS
SA_T007	9.40602	57.60662	0.3	0.87	3.58	64.87	30.41	0.27	Medium Sand (0.48)	Moderately Well Sorted	0.02	0.08	0.03
SA_T008	9.60488	57.69300	1.1	8.80	90.32	0.72	0.14	0.02	Very Fine Sand (0.12)	Well Sorted	0.12	0.44	0.05
SA_T009	9.58223	57.65323	2.5	36.63	62.50	0.55	0.31	0.01	Very Fine Sand (0.09)	Very Well Sorted	0.32	1.00	0.09
SA_T010	9.70728	57.69622	1.9	27.94	71.63	0.37	0.06	0.00	Very Fine Sand (0.09)	Very Well Sorted	0.28	0.71	0.08
SA_T011	9.64798	57.63937	1.6	13.88	67.90	16.46	0.88	0.88	Fine Sand (0.14)	Moderately Well Sorted	0.16	0.78	0.09
SA_T012	9.63812	57.60895	1.3	11.05	58.20	21.58	5.49	3.69	Fine Sand (0.18)	Poorly Sorted	0.19	0.61	0.07
SA_T013	9.73313	57.66162	1.2	9.28	82.71	7.66	0.19	0.15	Fine Sand (0.13)	Well Sorted	0.14	0.54	0.08
SA_T014	9.76385	57.65183	0.3	0.88	2.38	90.82	5.27	0.66	Medium Sand (0.35)	Well Sorted	0.02	0.18	0.03
SA_T017	9.74192	57.56147	0.7	1.92	29.65	40.82	1.28	26.34	Coarse Sand (0.95)	Very Poorly Sorted	0.06	0.37	0.04
SA_T018	9.78535	57.56252	0.7	4.51	92.21	2.37	0.41	0.49	Very Fine Sand (0.11)	Very Well Sorted	0.05	0.31	0.04
SA_T020	9.49462	57.68383	0.7	2.05	89.02	8.10	0.25	0.57	Fine Sand (0.14)	Well Sorted	0.07	0.21	0.04
SA_T021	9.45212	57.50447	0.3	1.26	79.44	18.58	0.62	0.10	Fine Sand (0.15)	Moderately Well Sorted	0.02	0.17	0.04
SA_T023	9.45353	57.45170	0.4	1.23	61.17	35.69	1.91	0.00	Fine Sand (0.18)	Moderately Sorted	0.07	0.11	0.04
SA_T025	9.64722	57.50858	0.5	2.01	74.53	22.73	0.67	0.06	Fine Sand (0.15)	Moderately Well Sorted	0.03	0.19	0.03
SA_T026	9.48838	57.41992	0.6	0.65	2.70	7.13	45.10	44.42	Very Coarse Sand (1.79)	Poorly Sorted	0.03	0.93	0.05
SA_T028	9.45913	57.37990	0.9	4.94	89.30	2.75	1.70	1.31	Very Fine Sand (0.11)	Well Sorted	0.08	0.44	0.06
SA_T029	*9.51235	*57.38100	4.2	77.14	12.18	8.27	1.72	0.68	Fine Sand (0.20)	Poorly Sorted	0.37	2.63	0.24
SA_T030	9.59917	57.35472	0.4	1.53	73.44	24.67	0.36	0.01	Fine Sand (0.15)	Moderately Well Sorted	0.02	0.11	0.03
SA_T032	9.20723	57.62557	0.5	1.12	9.79	87.10	1.91	0.08	Medium Sand (0.31)	Well Sorted	0.03	0.12	0.04
SA_T033	9.15225	57.59435	0.4	1.33	7.47	77.13	13.87	0.19	Medium Sand (0.36)	Moderately Well Sorted	0.02	0.08	0.02
SA_T034	9.05290	57.51165	0.4	1.19	18.49	64.10	13.92	2.29	Medium Sand (0.33)	Moderately Sorted	0.02	0.12	0.02
SA_T035	9.31368	57.63297	0.3	1.01	3.43	76.96	18.12	0.49	Medium Sand (0.43)	Moderately Well Sorted	0.01	0.10	0.03
SA_T036	9.20255	57.51947	0.3	1.14	15.80	78.59	4.17	0.30	Medium Sand (0.28)	Moderately Well Sorted	0.01	0.11	0.03
SA_T037	9.26345	57.52585	0.4	1.27	28.42	58.75	11.26	0.30	Medium Sand (0.29)	Moderately Sorted	0.02	0.09	0.02
SA_T038	9.09737	57.45898	0.4	1.14	9.32	86.67	2.69	0.18	Medium Sand (0.30)	Well Sorted	0.01	0.11	0.03
SA_T039	9.11005	57.73882	0.3	21.71	68.74	8.93	0.52	0.10	Fine Sand (0.14)	Well Sorted	0.25	0.76	0.07
SA_T040	9.12562	57.78495	1.9	35.87	63.52	0.40	0.21	0.00	Very Fine Sand (0.10)	Well Sorted	0.40	1.04	0.09
SA_T041	8.97018	57.47492	2.9	0.60	4.93	21.10	41.86	31.52	Very Coarse Sand (1.22)	Poorly Sorted	0.02	0.25	0.02
SA_T042	9.53048	57.27648	0.6	2.45	78.88	17.88	0.78	0.01	Fine Sand (0.14)	Moderately Well Sorted	0.04	0.20	0.03
SA_T044	8.64125	57.42847	0.5	1.08	10.85	69.89	17.82	0.35	Medium Sand (0.37)	Moderately Sorted	0.02	0.52	0.04
SA_T045	9.12890	57.25625	0.6	2.57	96.79	0.43	0.18	0.02	Very Fine Sand (0.11)	Very Well Sorted	0.03	0.26	0.04
SA_T047	8.68840	57.19643	0.3	1.35	4.97	61.72	29.20	2.77	Medium Sand (0.48)	Moderately Sorted	0.02	0.19	0.03
SA_T048	8.68818	57.32913	0.3	0.76	78.54	20.53	0.17	0.00	Fine Sand (0.17)	Very Well Sorted	0.00	0.07	0.03
SA_T049	8.55985	57.37280	0.3	0.88	5.77	70.19	16.45	6.70	Medium Sand (0.41)	Poorly Sorted	0.01	0.16	0.02

Appendix 1.3: Sediment and carbon analyses in BACI areas

Table showing coordinates and results of the sediment and carbon analyses of the 60 grab samples collected in the two BACI areas. Grain size statistics are computed from dry sieving results of the size fraction >63 µm.

	Coordinates (DD)		Organic content (wt%)	Grain size classes (wt%)					Folk & Ward descriptive grain size statistics (size in mm)		Carbon (wt%)		Sulfur (wt%)
Sample ID	Long	Lat	Loss on ignition	Silt & Clay	Fine sand	Medium sand	Coarse sand	Gravel	Mean	Sorting	TOC	TC	TS
BEF_S_C1_1	8.99358	57.33025	0.3	1.64	4.02	76.24	17.20	0.90	Medium Sand (0.42)	Moderately Well Sorted	0.01	0.12	0.03
BEF_S_C1_2	8.99382	57.33125	0.3	0.97	7.91	80.60	10.41	0.10	Medium Sand (0.36)	Moderately Well Sorted	0.01	0.15	0.03
BEF_S_C1_3	8.99365	57.33213	0.4	1.21	12.38	77.40	8.57	0.44	Medium Sand (0.34)	Moderately Well Sorted	0.00	0.14	0.04
BEF_S_C1_4	8.99365	57.33278	0.4	0.98	16.17	73.53	9.09	0.23	Medium Sand (0.31)	Moderately Well Sorted	0.01	0.13	0.02
BEF_S_C1_5	8.99343	57.33383	0.5	2.00	80.18	16.42	1.23	0.17	Fine Sand (0.15)	Well Sorted	0.02	0.19	0.03
BEF_S_C2_1	9.00513	57.33205	0.4	1.05	4.01	73.89	19.36	1.70	Medium Sand (0.43)	Moderately Well Sorted	0.00	0.13	0.03
BEF_S_C2_2	9.00545	57.33328	0.3	1.13	11.64	80.19	6.95	0.09	Medium Sand (0.33)	Moderately Well Sorted	0.01	0.11	0.03
BEF_S_C2_3	9.00533	57.33383	0.3	1.11	8.88	79.99	9.83	0.20	Medium Sand (0.37)	Moderately Well Sorted	0.04	0.09	0.02
BEF_S_C2_4	9.00540	57.33485	0.4	0.91	8.03	73.87	16.69	0.49	Medium Sand (0.40)	Moderately Well Sorted	0.00	0.13	0.02
BEF_S_C2_5	9.00533	57.33570	0.4	0.64	3.06	60.74	31.80	3.75	Coarse Sand (0.52)	Moderately Sorted	0.00	0.25	0.03
BEF_S_IM1_1	8.99772	57.33543	0.4	1.83	71.29	26.15	0.67	0.05	Fine Sand (0.17)	Moderately Well Sorted	0.01	0.14	0.34
BEF_S_IM1_2	8.99767	57.33445	0.5	1.28	60.90	33.17	3.92	0.73	Fine Sand (0.20)	Moderately Sorted	0.01	0.13	0.03
BEF_S_IM1_3	8.99750	57.33365	0.4	1.18	46.17	51.42	1.23	0.00	Fine Sand (0.21)	Moderately Well Sorted	0.02	0.14	0.05
BEF_S_IM1_4	8.99768	57.33282	0.2	0.69	3.41	67.85	25.02	3.03	Medium Sand (0.47)	Moderately Sorted	0.01	0.12	0.03
BEF_S_IM1_5	8.99742	57.33188	0.3	1.04	7.16	77.03	14.15	0.62	Medium Sand (0.39)	Moderately Well Sorted	0.00	0.11	0.02
BEF_S_IM2_1	9.00920	57.33198	0.3	0.63	14.14	81.93	3.24	0.06	Medium Sand (0.30)	Moderately Well Sorted	0.01	0.09	0.01
BEF_S_IM2_2	9.00940	57.33287	0.5	0.91	3.30	58.08	28.31	9.40	Coarse Sand (0.56)	Poorly Sorted	0.00	0.14	0.01
BEF_S_IM2_3	9.00928	57.33367	0.4	0.85	4.59	67.66	21.98	4.92	Medium Sand (0.45)	Moderately Sorted	0.04	0.10	0.02
BEF_S_IM2_4	9.00927	57.33440	0.4	1.12	3.41	64.97	27.55	2.96	Medium Sand (0.48)	Moderately Sorted	0.08	0.21	0.03
BEF_S_IM2_5	9.00935	57.33513	0.3	0.87	4.43	63.88	22.67	8.15	Medium Sand (0.49)	Poorly Sorted	0.03	0.17	0.03
AFT1_S_IM1_1	8.99773	57.33538	0.3	1.70	47.60	49.29	1.38	0.02	Fine Sand (0.21)	Moderately Well Sorted	0.07	0.11	0.04
AFT1_S_IM1_2	8.99760	57.33443	0.5	1.40	67.85	26.83	3.54	0.38	Fine Sand (0.18)	Moderately Sorted	0.01	0.16	0.04
AFT1_S_IM1_3	8.99735	57.33358	0.5	1.81	81.65	14.42	2.04	0.08	Fine Sand (0.16)	Well Sorted	0.07	0.25	0.03
AFT1_S_IM1_4	8.99763	57.33267	0.3	1.02	5.40	77.63	15.42	0.53	Medium Sand (0.40)	Moderately Well Sorted	0.07	0.13	0.03
AFT1_S_IM1_5	8.99735	57.33180	0.3	0.98	9.94	76.51	10.95	1.62	Medium Sand (0.36)	Moderately Well Sorted	0.11	0.19	0.03
AFT1_S_IM2_1	9.00918	57.33190	0.3	0.69	6.75	74.69	16.43	1.44	Medium Sand (0.39)	Moderately Well Sorted	0.00	0.10	0.02
AFT1_S_IM2_2	9.00940	57.33290	0.4	0.97	5.07	63.61	26.94	3.42	Medium Sand (0.48)	Moderately Sorted	0.01	0.16	0.02
AFT1_S_IM2_3	9.00923	57.33355	0.4	0.84	2.47	59.11	32.97	4.61	Coarse Sand (0.54)	Moderately Sorted	0.01	0.19	0.02
AFT1_S_IM2_4	9.00927	57.33450	0.4	0.51	3.04	62.17	27.61	6.67	Coarse Sand (0.52)	Moderately Sorted	0.00	0.16	0.03
AFT1_S_IM2_5	9.00992	57.33508	0.3	1.08	5.22	67.68	21.04	4.99	Medium Sand (0.45)	Moderately Sorted	0.03	0.12	0.02
AFT1_S_C1_1	8.99345	57.33020	0.3	0.87	5.71	77.22	15.75	0.45	Medium Sand (0.41)	Moderately Well Sorted	0.01	0.11	0.02
AFT1_S_C1_2	8.99378	57.33135	0.3	0.89	7.09	80.67	11.07	0.27	Medium Sand (0.38)	Moderately Well Sorted	0.01	0.19	0.02
AFT1_S_C1_3	8.99352	57.33215	0.4	1.20	11.00	76.42	11.16	0.23	Medium Sand (0.35)	Moderately Well Sorted	0.01	0.17	0.02
AFT1_S_C1_4	8.99365	57.33285	0.4	1.29	31.94	61.86	4.54	0.37	Medium Sand (0.26	Moderately Sorted	0.02	0.12	0.02
AFT1_S_C1_5	8.99355	57.33377	0.4	2.26	80.53	14.19	1.27	1.75	Fine Sand (0.15)	Moderately Well Sorted	0.05	0.19	0.02

	Coordinates (DD)		Organic content (wt%)	Grain size classes (wt%)					Folk & Ward descriptive grain size statistics (size in mm)		Carbon (wt%)		Sulfur (wt%)
Sample ID	Long	Lat	Loss on ignition	Silt & Clay	Fine sand	Medium sand	Coarse sand	Gravel	Mean	Sorting	TOC	TC	TS
AFT1_S_C2_1	9.00508	57.33190	0.3	1.11	8.59	75.69	13.90	0.72	Medium Sand (0.39)	Moderately Well Sorted	0.02	0.07	0.01
AFT1_S_C2_2	9.00548	57.33308	0.3	1.45	7.81	80.89	9.81	0.04	Medium Sand (0.37)	Moderately Well Sorted	0.01	0.07	0.02
AFT1_S_C2_3	9.00530	57.33367	0.3	0.96	9.73	80.50	8.81	0.00	Medium Sand (0.36)	Moderately Well Sorted	0.01	0.06	0.02
AFT1_S_C2_4	9.00517	57.33487	0.4	1.23	8.59	79.51	10.54	0.13	Medium Sand (0.37)	Moderately Well Sorted	0.02	0.08	0.02
AFT1_S_C2_5	9.00515	57.33570	0.3	0.71	4.23	64.13	25.85	5.08	Medium Sand (0.49)	Moderately Sorted	0.00	0.14	0.02
AFT2_S_IM1_1	8.99758	57.33545	0.3	1.43	71.31	26.44	0.82	0.00	Fine Sand (0.17)	Moderately Well Sorted	0.01	0.09	0.02
AFT2_S_IM1_2	8.99765	57.33448	0.5	2.05	64.82	27.03	4.14	1.97	Fine Sand (0.19)	Moderately Sorted	0.02	0.15	0.02
AFT2_S_IM1_3	8.99752	57.33370	0.5	2.40	79.37	16.28	1.69	0.26	Fine Sand (0.16)	Moderately Well Sorted	0.02	0.13	0.02
AFT2_S_IM1_4	8.99753	57.33280	0.3	0.99	5.19	78.50	14.89	0.42	Medium Sand (0.40)	Moderately Well Sorted	0.01	0.11	0.01
AFT2_S_IM1_5	8.99758	57.33198	0.3	1.08	5.67	72.57	19.85	0.83	Medium Sand (0.41)	Moderately Well Sorted	0.01	0.11	0.01
AFT2_S_IM2_1	9.00918	57.33190	0.3	1.29	12.93	76.06	7.51	2.22	Medium Sand (0.32)	Moderately Well Sorted	0.01	0.07	0.01
AFT2_S_IM2_2	9.00940	57.33290	0.4	0.80	6.28	55.23	31.13	6.56	Coarse Sand (0.52)	Poorly Sorted	0.02	0.11	0.01
AFT2_S_IM2_3	9.00923	57.33355	0.4	0.85	4.21	59.22	26.01	9.71	Coarse Sand (0.54)	Poorly Sorted	0.01	0.43	0.01
AFT2_S_IM2_4	9.00927	57.33450	0.3	0.85	4.57	70.75	21.36	2.47	Medium Sand (0.44)	Moderately Sorted	0.02	0.07	0.01
AFT2_S_IM2_5	9.00992	57.33508	0.3	0.98	3.96	61.43	28.15	5.48	Coarse Sand (0.51)	Moderately Sorted	0.01	0.07	0.01
AFT2_S_C1_1	8.99355	57.33052	0.3	1.28	4.10	78.70	15.83	0.09	Medium Sand (0.41)	Moderately Well Sorted	0.00	0.09	0.01
AFT2_S_C1_2	8.99367	57.33132	0.3	1.08	6.12	79.70	12.96	0.14	Medium Sand (0.39)	Moderately Well Sorted	0.01	0.08	0.01
AFT2_S_C1_3	8.99372	57.33210	0.3	1.05	9.17	80.81	8.66	0.31	Medium Sand (0.35)	Moderately Well Sorted	0.01	0.08	0.01
AFT2_S_C1_4	8.99372	57.33282	0.4	1.26	26.91	67.43	4.25	0.15	Medium Sand (0.26)	Moderately Well Sorted	0.02	0.12	0.01
AFT2_S_C1_5	8.99348	57.33387	0.4	1.54	82.29	14.18	1.48	0.50	Fine Sand (0.15)	Moderately Well Sorted	0.02	0.16	0.01
AFT2_S_C2_1	9.00522	57.33190	0.3	0.76	6.61	77.97	14.00	0.67	Medium Sand (0.39)	Moderately Well Sorted	0.02	0.08	0.01
AFT2_S_C2_2	9.00537	57.33315	0.3	1.10	6.81	80.61	11.28	0.21	Medium Sand (0.38)	Moderately Well Sorted	0.01	0.07	0.01
AFT2_S_C2_3	9.00525	57.33382	0.3	1.16	8.60	79.82	10.32	0.10	Medium Sand (0.37)	Moderately Well Sorted	0.01	0.06	0.03
AFT2_S_C2_4	9.00520	57.33473	0.3	1.22	13.38	79.74	5.54	0.13	Medium Sand (0.32)	Moderately Well Sorted	0.01	0.06	0.02
AFT2_S_C2_5	9.00510	57.33565	0.3	0.85	3.68	63.12	29.32	3.03	Medium Sand (0.49)	Moderately Sorted	0.01	0.12	0.01